UNIVERSITÀ POLITECNICA DELLE MARCHE

FACOLTÀ DI INGEGNERIA

Department of Information Engineering

Master's Degree in Biomedical Engineering

GALVANIC SKIN RESPONSE MEASUREMENT DATA PROCESSING FOR USER-RELATED INFORMATION EXTRACTION

Supervisor:

Prof. Susanna Spinsante

Co-Supervisor:

Prof. Stefania Cecchi

Author:

Anna Brocanelli

Academic Year 2018/2019

Abstract

Emotions play a key role in everyday life of human beings. For this reason, in the last years, researchers have exploited physiological changes caused by emotional stimuli in order to develop methods to automatically recognize the emotional involvement of individuals. Among physiological signals, the Galvanic Skin Response (GSR) is one of the most interesting in emotion research.

In this work, the whole process of acquisition, elaboration, and analysis of the GSR signal is described in detail. GSR data were measured by using a wearable wrist-worn device. Participants were enrolled and contributed to two experimental tests, where they were submitted to physical and auditory stimuli. The collected data were analyzed in the time domain by computing the number of GSR peaks for each signal, and in the frequency domain by calculating the amount of spectral content within specific frequency sub-bands.

GSR signals acquired after physical efforts of different intensities were analyzed in both the time and frequency domain. The results of the time domain analysis show a growth of the GSR peaks number as the intensity of physical efforts increases. While the analysis in the frequency domain shows a shift of the GSR spectral content towards higher frequencies when subjects perform physical exercises of increasing intensities.

GSR data recorded during the listening of acoustic stimuli of different pleasure levels were examined in the time domain only. The analysis of the results shows that pleasant and neutral sounds do not produce evident effects on the number of GSR peaks, while the listening of an unpleasant sound elicits a slight increase in the GSR peaks rate. Such an increase is higher when the sound is shorter, probably due to the expectation phenomenon.

Table of Contents

Introduction 4

Chapter 1 **Galvanic Skin Response Signal** 6

1.1 **Skin and Sweat Glands Anatomy and Physiology** 6

1.2 **Emotion Recognition using GSR Analysis** 10

1.3 **GSR Signal Analysis** 12

1.3.1 **GSR Signal** 13

1.3.2 **GSR Signal Acquisition** 16

1.3.3 **GSR Signal Processing** 17

Chapter 2 **Materials and Methods** 20

2.1 **Tools** 20

2.1.1 **Empatica E4 Wristband** 20

2.1.2 **Ledalab Toolbox** 23

2.2 **Data Processing** 26

2.2.1 **Time Domain Analysis** 27

2.2.2 **Frequency Domain Analysis** 36

Chapter 3 **Experimental Tests** 39

3.1 **Acquisitions after Physical Stimulation** 39

3.2 **Acquisitions during Acoustic Stimulation** 41

Chapter 4 **Physical Stimuli Test Results** 45

4.1 **Results of the Time Domain Analysis** 51

4.1.1 **Comparison among Subjects** 51

4.1.2 **Comparison among Different Intensities of Physical Efforts** 56

4.2 **Results of the Frequency Domain Analysis** 58

4.2.1 **Comparison among Subjects** 59

4.2.2 **Comparison among Different Intensities of Physical Efforts** 64

4.2.3 **Comparison among Different Frequency Bands** 66

Chapter 5 **Auditory Stimuli Test Results** 70

5.1 **Results of the Time Domain Analysis** 72

5.1.1 **Comparison among Subjects** 73

5.1.2 **Comparison among Pleasant, Neutral and Unpleasant Sounds** 81

5.2 **Analysis of the SAM Scores Given by Enrolled Subjects** 84

Chapter 6 **Conclusion** 86

Chapter 7 **Limitations and Future Developments** 88

References 89

Introduction

Emotions play a key role in human life. Their recognition is a powerful tool for a wide range of applications, among which industrial and medical ones [1]. Initially, human emotions were evaluated by using self-reports, facial expression and speech analytics, however these are not completely reliable tools to detect emotional changes of users [2]. For this reason, in the last decades researchers have tried to develop methods to automatically recognize the emotional arousal of individuals starting from physiological changes [3]. Indeed, since emotions regulate the Autonomic Nervous System (ANS) producing variations in heart rate, respiration rate and sweat secretion, the physiological changes are considered reliable to examine the psychological and emotional states of subjects [2].

Among physiological signals, the Galvanic Skin Response (GSR) is one of the most interesting in emotion research. GSR is a biometric index reflecting changes in the electrical properties of the skin [4]. When humans are exposed to stimuli such as images, sounds and physical efforts, the sympathetic division of ANS induces a sweat reaction. Sweat glands become more active and sweat is secreted on the skin surface. Consequently, Na^+ and Cl^- ions concentration on the skin rises causing an increase of the electrical conductance of the skin. Fluctuations of the skin's electrical properties can be measured using two electrodes positioned on specific regions of the skin surface [5]. The recent development of wearable devices has made possible the acquisition of GSR signals even outside the laboratory settings. The information content and the easiness of acquisition of the GSR signal have elevated it to a role of strong interest among the biomedical signals analyzed for the purpose of emotion recognition [6].

The aim of this thesis is to go through the whole process of acquisition, elaboration and analysis of the GSR signal. In particular, GSR signals were recorded on male and female individuals of different ages, when they were submitted to physical and auditory stimuli. A Matlab program developed on purpose was used to implement algorithms to analyze the collected measurement data in both time and frequency domains. Results were examined in

order to understand the effects that different kinds and levels of stimuli have on the electrical properties of the skin.

The thesis is organized into seven main Chapters. In the first Chapter, the GSR signal characteristics and the state of art analysis are presented. In the second Chapter, the device used to measure the GSR signal, called Empatica E4 wristband, and the Matlab toolbox used for the signal's analysis, named Ledalab [7], are described. Additionally, in this Chapter the code implemented in Matlab to process the GSR signal in the time and frequency domain is explained. The third Chapter, titled "Experimental Tests", provides detailed information about the characteristics of the population of subjects involved in the experiments and about their execution. The fourth and the fifth Chapters show the results obtained from the analysis of the GSR signals acquired after physical activity and during auditory stimulation, respectively. Conclusions drawn from the results are presented in the sixth Chapter, while the last Chapter discusses the limitations of this work and presents some ideas about how to proceed in the future to further develop the study of the GSR signal in response to arousal stimuli.

Chapter 1

Galvanic Skin Response Signal

Galvanic Skin Response (GSR), also known as Electrodermal Activity (EDA) and Skin Conductance (SC), is a biometric signal that reflects the variations in the electrical properties of the skin, resulting from Autonomic Nervous System (ANS) activity. These fluctuations are caused by the triggering of sweat glands that cannot be controlled consciously [4]. When such glands become more active, moisture and sweat are secreted through pores on the skin surface [6]. This secretion produces a variation of the charge carriers' concentration (ions Na^+ and Cl^-) on the skin surface that can be recorded with an appropriate equipment. These concentration changes are reflected in a variation SC that can be measured applying two electrodes on the skin surface.

The skin electrical properties, influenced by the Sympathetic Nervous System (SNS) only, are biomarkers of physiological and psychological arousal. Therefore, the time changes analysis of GSR gives direct information on the activity of the SNS and, by extension, on the emotional and cognitive activity [4].

Thanks to the measure simplicity and the richness of the extractable information, this signal has been widely used in the last years [6].

1.1 Skin and Sweat Glands Anatomy and Physiology

The skin is the outer covering of the body that consists of a complex set of organs. It is composed of three different layers: *epidermis*, *dermis* and *hypodermis (Figure 1)*. The dermis and epidermis compose the cutis, while the subcutis is made up of hypodermis [8].

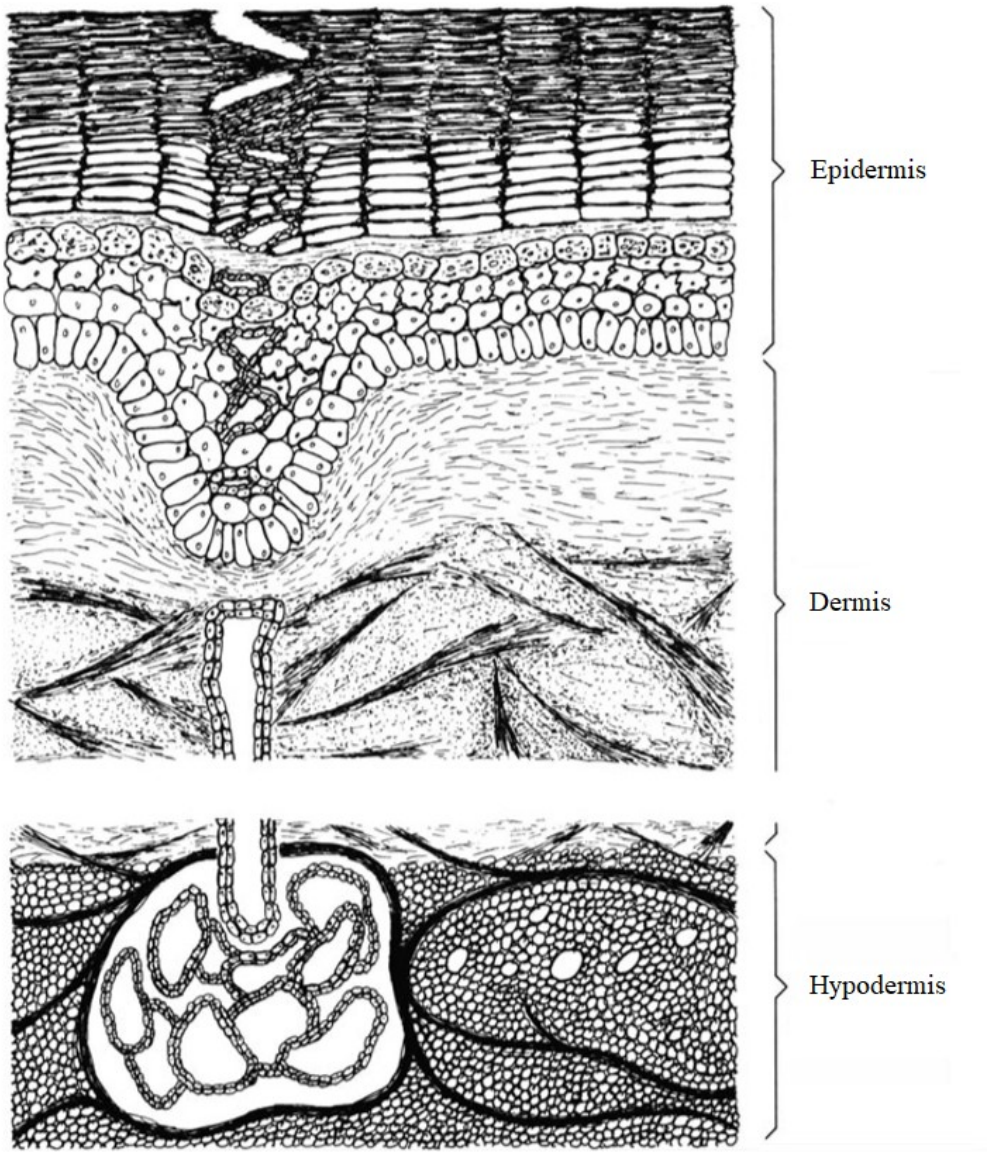

Figure 1 - Layered composition of the human skin [8].

Epidermis. It is the upper layer of the cutis and is located on the skin surface. It consists of epithelial tissue, which becomes progressively hornier closer to the surface [8]. This region of the skin plays a key role in the electrodermal phenomenon, because it is a dry layer that becomes wet during the sweat secretion.

Dermis. The dermis is the thicker region of the cutis and consists of two dermal layers. The layer closest to the epidermis is known as *papillary dermis*. Here, blood vessels end in a capillary net, and receptor organs, melanocytes, as well as free collagen are included in this

layer. The inner dermal layer is called the *reticular dermis*, made by strong collagenous fibers, giving the skin a high resistance against rupture [8].

Hypodermis. It is composed of loose connective tissue which forms the transitional layer between the skin and the connective tissue covering the muscles. It contains the secretory part of the sweat glands, the hair follicles, the nerves and vessels which supply the skin [8].

The main functions of the skin are protection, sensation and regulation. Skin acts as a selective barrier providing protection to the body from environmental threats such as temperature, chemical, mechanical and infectious agents. Skin contains an extensive network of nerve cells and houses various receptors to provide afferent information related to touch, pain, and temperature. And, finally, it regulates body temperature and skin moisture through the production of sweat and by controlling vascular tone.

The sweat is secreted directly onto the skin's surface by the sweat glands. The human body has about three million sweat glands distributed in the body with different density. The greatest amount being found on the palms, soles, and forehead, and the lower density on the arms, legs, and trunk. The sweat glands can be divided into *eccrine* and *apocrine* [8]. Eccrine sweat glands are present in a larger quantity than apocrine ones and they are involved in the variations of the electrical properties of the skin. This kind of glands is composed of secretory segment and duct *(Figure 2)*. The secretory segment is located in the hypodermis or in the dermis. It consists of a tube which is irregularly coiled into a rounded mass of a diameter approximately 0.4 mm long. From it originates the duct, characterized by a straight course through the dermis and then a spiral course through the epidermis. The duct opens onto the skin surface through a little pore [8].

The secretory part of the sweat glands is innervated by many different sympathetic fibers, called postganglionic sudomotor neurons. Central control of their activity is attributed to the hypothalamic area, especially the paraventricular and posterior nuclei and to many other cortical and subcortical regions. Sudomotor fibers descend via hypothalamic-reticular-spinal sympathetic pathways in close proximity to other sympathetic fibers ending at the preganglionic sudomotor neurons. The preganglionic neurons leave the spinal cord ipsilaterally via the lateral horn leading to the sympathetic trunk, where they are switched to postganglionic sudomotor unmyelinated fibers [8].

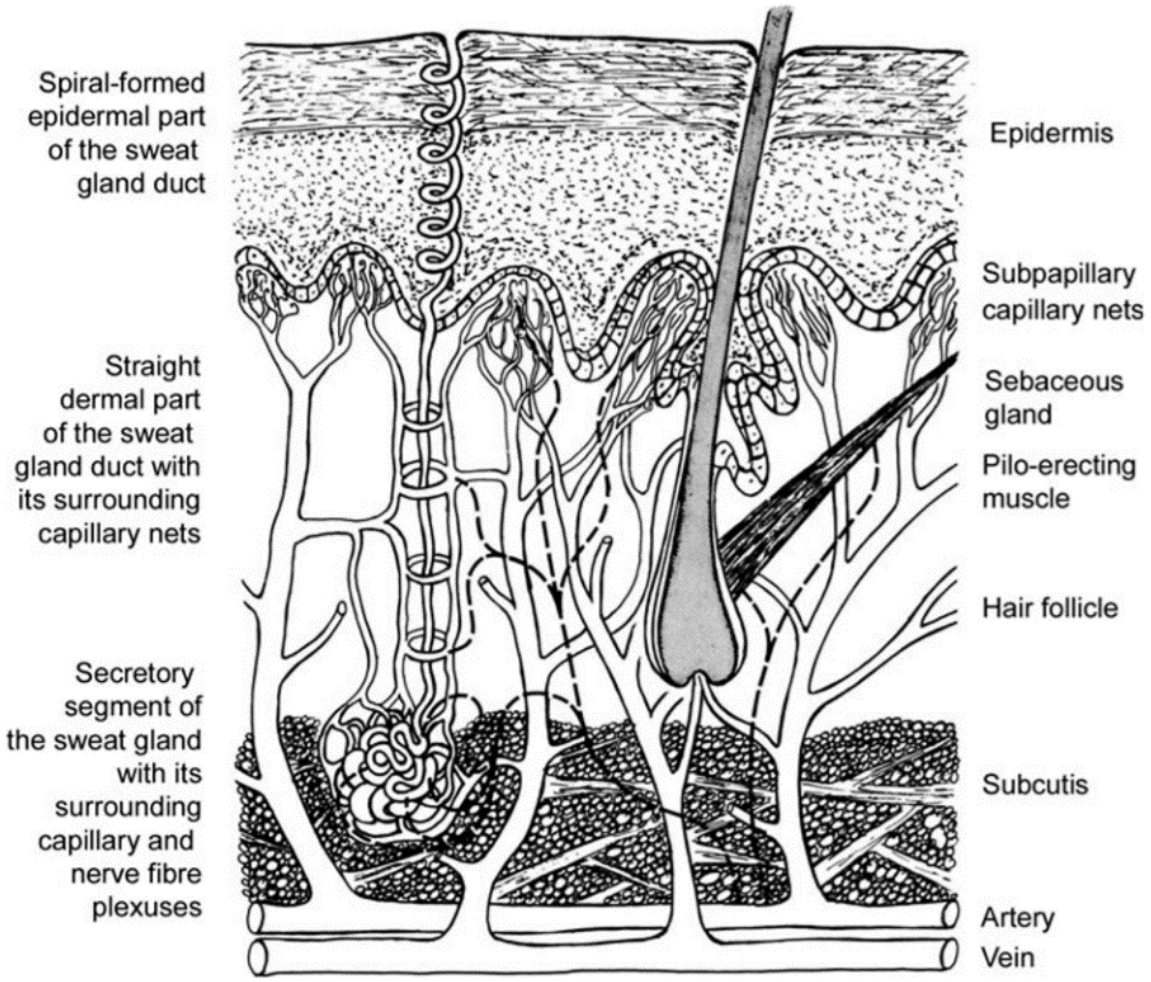

Figure 2 - Vertical section of the skin with the schematic representation of an eccrine sweat gland (left) and a hair (right) [8].

Although the sweat glands are principally involved in thermoregulation, besides the thermal sweating other five kinds of sweating exist, and they are classified according to the stimuli eliciting them [8]. All of these types use the same postganglionic sympathetic neuron, but their mechanisms of Central Nervous System (CNS) elicitation are partially different. Among these types, the emotional sweating is the most interesting in the context of the GSR. Indeed, in this kind of sweating, the increased sweat gland activity is related to a concomitance of psychological and emotional states, connected with either external or internal stimuli generating arousal or stress. As a result, the emotional sweating is observed mainly where the sweat glands' density is higher, namely on palmar and plantar sites [8][9].

1.2 **Emotion Recognition using GSR Analysis**

Emotions play a key role in everyday life of human beings. Their detection can improve several applications, like human communication with a computer, they can be used in psychology and medicine for diagnosis of a user's mental state and also in evaluating neuromarketing strategies [1].

The importance of emotions motivated the researchers to develop automatic methods to recognize the emotional state of individuals. Initially, facial expression and speech analytics have been used for emotion recognition [2]. However, using this couple of information is not reliable to detect emotion, especially when people want to conceal their feelings. Compared with facial expression, physiological signals represent a more reliable approach to probe the internal cognitive and emotional changes of users. Emotions regulate the ANS producing variations in sweat secretion on the skin's surface, as well as changes in the respiration rate and heart rate [2].

Skin reacts when it is exposed to emotionally loaded images, videos, events, or other kinds of stimuli. In particular, emotional changes induce a sweat reaction. As a result, the amount of Na^+ and Cl^- ions on the skin surface rises causing an increase of the skin's electrical conductance. The resulting changes in the electrical properties of the skin are measurable and can be processed to extract information about the emotional involvement of a subject [2].

There are several ways to identify emotions, however the best-known models for emotion recognition are the Discrete Emotion Model and the Emotion Dimensional Model [10]. The first one categorizes the emotions into six basic emotion states: happiness, anger, sadness, surprise, disgust, and fear. In contrast to this categorical model, the Emotion Dimensional Model describes the emotions as a combination of several psychological dimensions. The most well-known dimensional model is the Valence-Arousal Dimensional Model *(Figure 3)* [10]. In particular, the valence represents a form of pleasure level and it ranges from negative to positive. While, the arousal ranges from low to high and it indicates the psychological and physiological level of being awake [10].

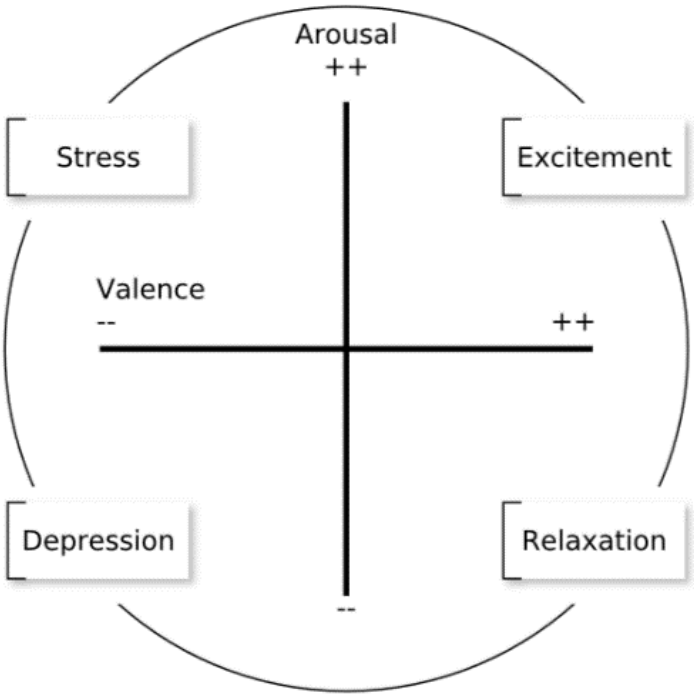

Figure 3 - Valence-Arousal Dimensional Model of emotions. The intersection between the valence and arousal axes splits the space into four regions. Each region is correlated with a particular emotional state [4].

Most of the studies demonstrate that GSR signal is sensitive only to the arousal dimension, not to the valence of the emotion involved [2]. Involving additional physiological signals as skin temperature, heart rate and electromyography, some information related to the valence of the emotion is added to the data obtained from the GSR signal, in order to obtain a more accurate recognition of the emotions.

However, physiological signals can be affected by artefacts and can present limitations. For this reason, such measures are usually coupled to questionnaires or self-assessment scales. In 1994, Bradley and Lang proposed the Self-Assessment Manikin (SAM) scale, that is one of the most famous among the existing self-reporting tools *(Figure 4)*. This scale measures the dimensions of valence (first row), arousal (second row) and dominance (third row) using a series of manikins horizontally organized according to a 9-points scale. Valence varies from a frowning figure to a smiling one and arousal ranges from a sleepy to a widely awake character showing an incremental explosion at the center. The dominance dimension

represents changes in control with changes in manikin's size. It spans form a very small to a very large figure, where the largest figure describes maximum control in situation [11].

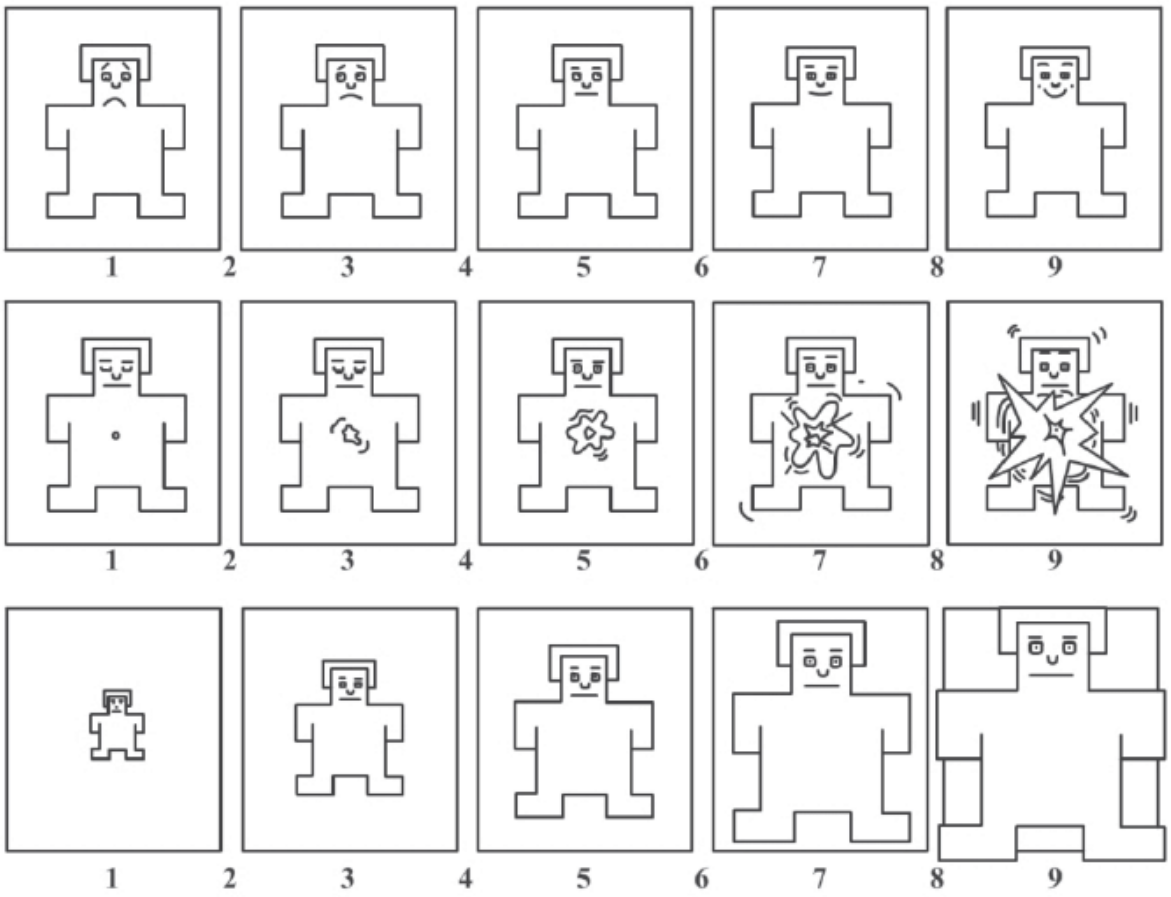

Figure 4 - Self-Assessment Manikins (SAM) scales for valence (top), arousal (middle) and dominance (bottom) [12].

1.3 **GSR Signal Analysis**

In this section, the characteristics of the GSR signal and the materials and procedures for the data acquisition are explained in detail. Finally, a brief outline of the processing techniques of the GSR signal is presented.

1.3.1 **GSR Signal**

GSR is a time variable biometric signal that may be analyzed in the time domain or in the frequency one [13].

In the time domain, the GSR consists of two components, namely *tonic* and *phasic* levels *(Figure 5)*.

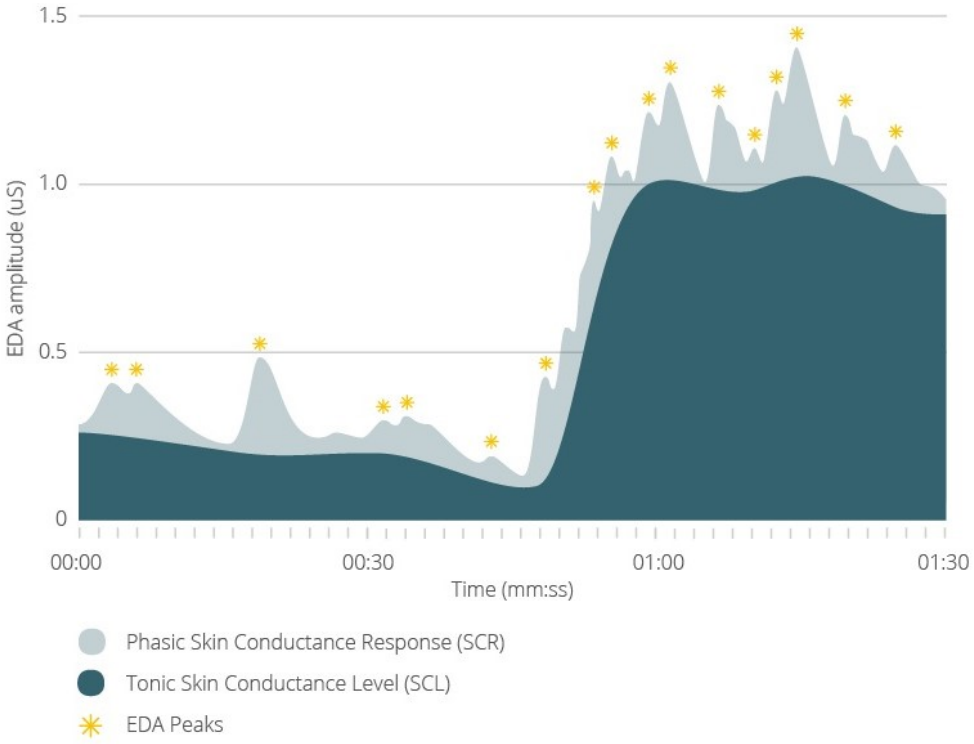

Figure 5 - Example of Galvanic Skin Response signal time representation [6].

Tonic component, also known as Skin Conductance Level (SCL), is the low-frequency component of GSR. The SCL is a slowly changing component that can be affected by external and internal factors such as psychological state or skin properties. It can be recorder in the absence of any environmental event or external stimuli and represents the activation level of the individual's nervous system. Such component can vary substantially between

subjects depending on their hydration, skin dryness and autonomic regulation. Due to interpersonal differences, the SCL-only analysis is not commonly used [5][14].

Phasic component is the high-frequency component representing the fast fluctuations caused by the sympathetic arousal response to a stimulus. Those variations are generally called Skin Conductance Responses (SCR) and are identifiable as "GRS peaks". SCR may be event related SCR (ER-SCR) or non-specific SCR (NS-SCR). ER-SCR is the response with respect to some events or external stimuli (images, sounds, and smells), while NS-SCR represents the phasic changes related to internal stimuli (thoughts, memories and emotions). The number of peaks varies subject by subject depending on their level of reactivity [5].

According to their definition and meaning, such components are characterized by different information content and distinct frequency bands. Therefore, generally after applying a subtraction algorithm in the time domain to isolate the SCR from the SCL, each component is analyzed separately.

The GSR signal should be recorded during a period in which the subject is not stimulated (baseline) in order to evaluate the characteristics of that signal [6]. In this circumstance, the activity recorded represents the spontaneous variability of the signal that is composed only by the tonic component and the NS-SCR. The baseline acquisition is a fundamental step for a later accurate extraction of the phasic component from the GSR curve. Since the analysis of ER-SCR gives a direct measure of the arousal level and emotional involvement of the subject, four significant parameters are extracted from each SCR *(Figure 6)*.

These parameters are:

- *Latency:* defined as the time distance between the stimulus and the onset of the peak. Typically, the ER-SCRs arise 1-5 seconds after the stimulus. The peak onset is generally set to the time point where the GSR curve exceeds a minimum amplitude criterion (0.01μS).
- *Peak amplitude:* that is the amplitude difference between the onset and the maximum of the peak.
- *Rise time:* defined as the time difference between the onset and the maximum of the peak.
- *Recovery time:* that is the duration from peak to total recovery.

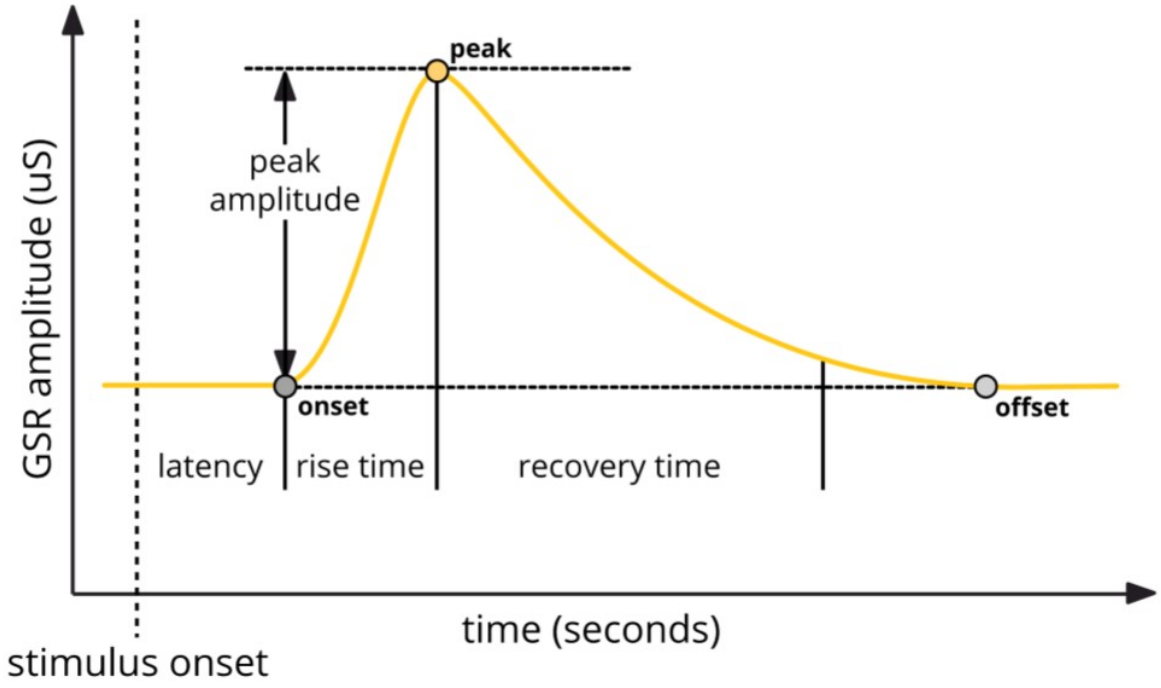

Figure 6 - Time representation of a Galvanic Skin Response peak and the related four most significant parameters [6].

The time domain analysis of the GSR signal provides a lot of information. However, the GSR analysis is quite difficulty, especially because the signal's components have high inter-subject variability, and the high occurrence of confounding factors (e.g. motion artefacts) may affect the four parameters defined above [13].

In order to overcome that kind of limitations, in the last years, researchers have developed methods to analyze the GSR in the frequency domain by computing the signal's Power Spectral Density (PSD) [15]. The spectral analysis of the GSR is easier to implement, and it provides less but more consistent details, particularly when the subject undergoes specific types of stimuli [13]. Finally, comparing the time domain with the frequency domain measures, the latter exhibit a lower variability. Indeed, the most of the GSR's spectral power (about the 95%) is usually concentrated in the range 0 to 0.25 Hz and, in particular, it is confined in the frequency band 0.045-0.25 Hz for all subjects [13][15]. Similar results were obtained by Posada-Quintero H. F. et al. that have performed the time-frequency analysis of the GSR signal applying the signal's spectrogram [16].

1.3.2 **GSR Signal Acquisition**

The sweat glands are present on almost all parts of the body, however certain areas respond more strongly to emotional stimuli. Those regions are the fingers, the palmar sites, the foot and the wrist. In these sites the eccrine sweat glands' density is higher compared to other body areas *(Figure 7)*.

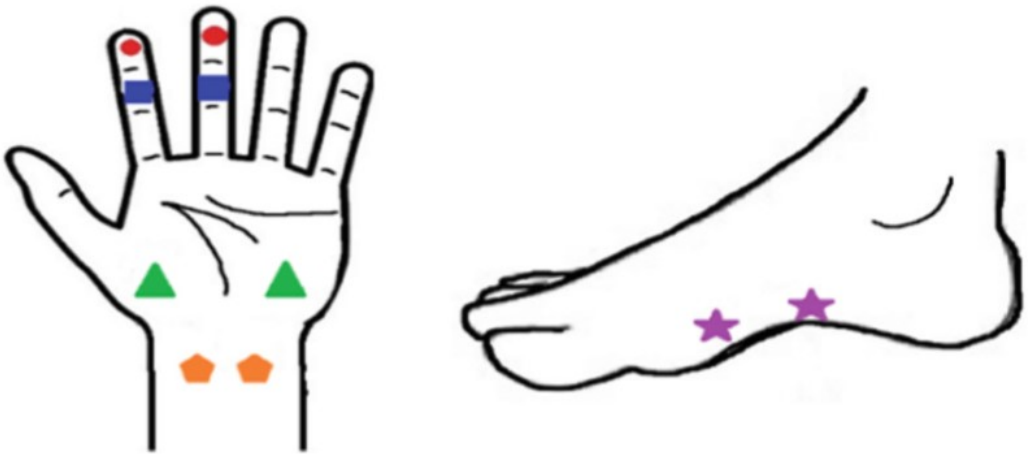

Figure 7 - Measurement sites for Galvanic Skin Response signal. These regions are: medial (blue) and distal (red) phalanges of middle and index finger, thenar and hypothenar eminence areas (green), feet (purple) and wrist (orange) [5].

GSR is typically measured non-invasively by attaching two electrodes to the skin. In this way, the electrical properties of the skin in between are passively recorded. GSR sensors generally have a measurement surface of Ag/AgCl (silver/silver-chloride) electrodes in order to minimize the polarization and bias potentials. Other types of electrodes, such as dry carbon/salt adhesive electrodes or textile Ag/AgCl type electrodes, also have been proposed. A gel with a specific chloride salt (NaCl or KCl) concentration is sometimes applied between the skin and the electrodes in order to reduce the impedance between them [5].

There are three different methods for the measurement of the GSR: (1) without the application of an external current, that is called *endosomatic* method, and two *exosomatic*

techniques, which either (2) apply Direct Current (DC) on the skin or (3) Alternating Current (AC) instead [17].

(1) *Endosomatic measurement.* An electrical potential difference can be measured across the palmar and plantar skin in the absence of any applied voltage or current. A single electrode is placed on the active site with a reference electrode at a relatively inactive site such as the forearm [17].
(2) *Exosomatic measurement with direct current.* Applying a constant small voltage (e.g. 0.5 V) between the two electrodes placed in close proximity on the skin surface, a weak current flowing into the skin can be measured. As result, using the principles of the Ohm's law (R=V/I where R is the skin resistance, V the voltage applied and I the current measured) the Skin Resistance (SR) or its reciprocal, the Skin Conductance (SC), can be estimated [17].
(3) *Exosomatic measurement with alternating current.* This technique is less commonly used and allows the measurement of the Skin Impedance (SZ) or of its reciprocal, defined as the Skin Admittance (SY) [17].

During the years, several applications and devices have been developed to measure the GSR signal and consequently the emotion arousals of the individuals. Most of the time, these are also able to measure some other physiological parameters as heart rate, body temperature and blood volume pressure that combined with the GSR signal give more precise information on the emotional involvement of a subject.

1.3.3 **GSR Signal Processing**

The raw GSR signal has to be processed in order to analyze the data correctly. At first, data has to be filtered and the motion artefacts removed; once the implementation of these steps is completed, the GSR signal can be decomposed in SCL and SCR. A low-pass filter with a very small cut-off frequency (e.g. less than 1 Hz) is implemented in order to remove the electrical noise from the signal [5]. The motion artefacts are removed adding to the low pass filtering a manual inspection of the signal. Once the signal is cleaned, the GSR curve is

decomposed because the individual analysis of the two overmentioned components (in particular of SCR) provides richer information on the arousal level of the person. Over the years, several methods have been developed to separate the phasic component from the tonic one [5].

One of the earlier methods is the traditional analysis, where the significance of SCR is determined by the amplitude of SCR peaks. This technique, known as standard peak detection or Trough-To-Peak (TTP) detection method, relies on the detection of peaks and troughs in the signal time-series [18]. The presence of a peak or a trough is established by finding the points where the signal derivative is zero. Once the onset and the maximum of the peak are found, all the features of interest can be extracted for each peak. Despite its simplicity, this analysis has some disadvantages. When SCRs overlap, the tail of the preceding SCR creates a higher baseline for the following SCR. For this reason, the measured SCR amplitude will be smaller than the true amplitude, because it is calculated relative to a higher baseline [18]. Moreover, the tail of the preceding SCR will also cover the initial effects of the next SCR, producing an erroneous assessment of the onset time that will be delayed respect to the true one. As a consequence, the measured rise time will also be less than true rise time. More generally, the problem of overlapping SCRs introduces distortions into all SCR measures [18].

To overcome these problems, different mathematical models have been developed for analyzing GSR more accurately using more features.

Alexander et al. introduced a method based on the deconvolution of the GSR signal. They suppose that GSR data originates from a convolution process between the sudomotor nerves activity (corresponding to a driver function) and an impulse response function (IRF). The IRF is modelled with a biexponential function and represents the basic SCR shape that would result from a unit impulse. The driver function is obtained deconvolving the SC data by the IRF. It is characterized by a sequence of discrete bursts having a shorter time constant than the SCRs. Peak detection is performed on the driver function and the individual SCRs are reconstructed performing a convolution between the identified peaks and the biexponential function. Finally, for each single non-overlapped SCR, the phasic parameter can be computed. This method has an advantage of separating overlapping SCR peaks, but it

assumes a perfect IRF for GSR, which causes the ignorance of tonic activity reflection on the phasic one [18].

In order to address this problem, Benedek and Kaernbach developed a model based on a nonnegative deconvolution to decompose GSR, named discrete decomposition analysis (DDA). This method claims non-negativity of the driver and maximal compactness of the impulses. Initially, a standard deconvolution is performed to obtain the driver function and the tonic activity is estimated fitting the inter-impulse intervals of the driver. Then, subtracting the SCL from the SC data, phasic activity can be extracted. On the phasic SC data, the non-negative deconvolution is applied that results in two phasic signals, a non-negative phasic driver and a remainder. The first exhibits distinct peaks on a zero baseline, while the reminder signal captures all deviations from the standard SCR shape. Performing a convolution between the extracted driver function and an IRF, a valid reconstruction of the original SC data can be accomplished through this method [19].

Later, Benedek and Kaernabach proposed an improved model called Continuous Decomposition Analysis (CDA). The aim of this approach is to establish a continuous measure that reflects more closely the original properties of the sudomotor nerve activity. This procedure involves three steps where the SC data are deconvolved applying a standard deconvolution into driver function and IRF and, then, the tonic and phasic activities are estimated [20].

Furthermore, Benedek and Kaernabach developed a useful Matlab toolbox, known as Ledalab toolbox, where the SC data can be analyzed performing the DDA or CDA.

Chapter 2
Materials and Methods

This chapter is divided into two main sections. In the first one, the functioning of tools used to acquire and analyze GSR signal are explained in detail, while in the second section algorithms, implemented in Matlab, for the analysis of the GSR data are described step by step.

2.1 **Tools**

Data was acquired using a single wearable wireless device, called *Empatica E4* wristband. During each measurement, subjects wore the Empatica E4 wristband on the dominant wrist. Once recorded, data can be downloaded and analyzed using specific software as Ledalab or algorithms implemented using programming software as Matlab.

2.1.1 **Empatica E4 Wristband**

Empatica E4 wristband is a multi-sensor device designed for real-time, continuous and comfortable data acquisition in everyday life *(Figure 8)*.

According to the datasheet provided by the manufacturer, four sensors are embedded in such device, specifically [21]:

- *Photoplethysmography (PPG) sensor*. It measures Blood Volume Pulse (BVP). From it, some cardiovascular parameters as heart rate and heart rate variability can be derived.
- *3-axis Accelerometer*. It records motion along the X, Y and Z axis.
- *EDA sensor*. It measures SNS arousal and, by extension, provides information about involvement, excitement and stress of a subject.
- *Infrared Thermopile*. It records skin temperature.

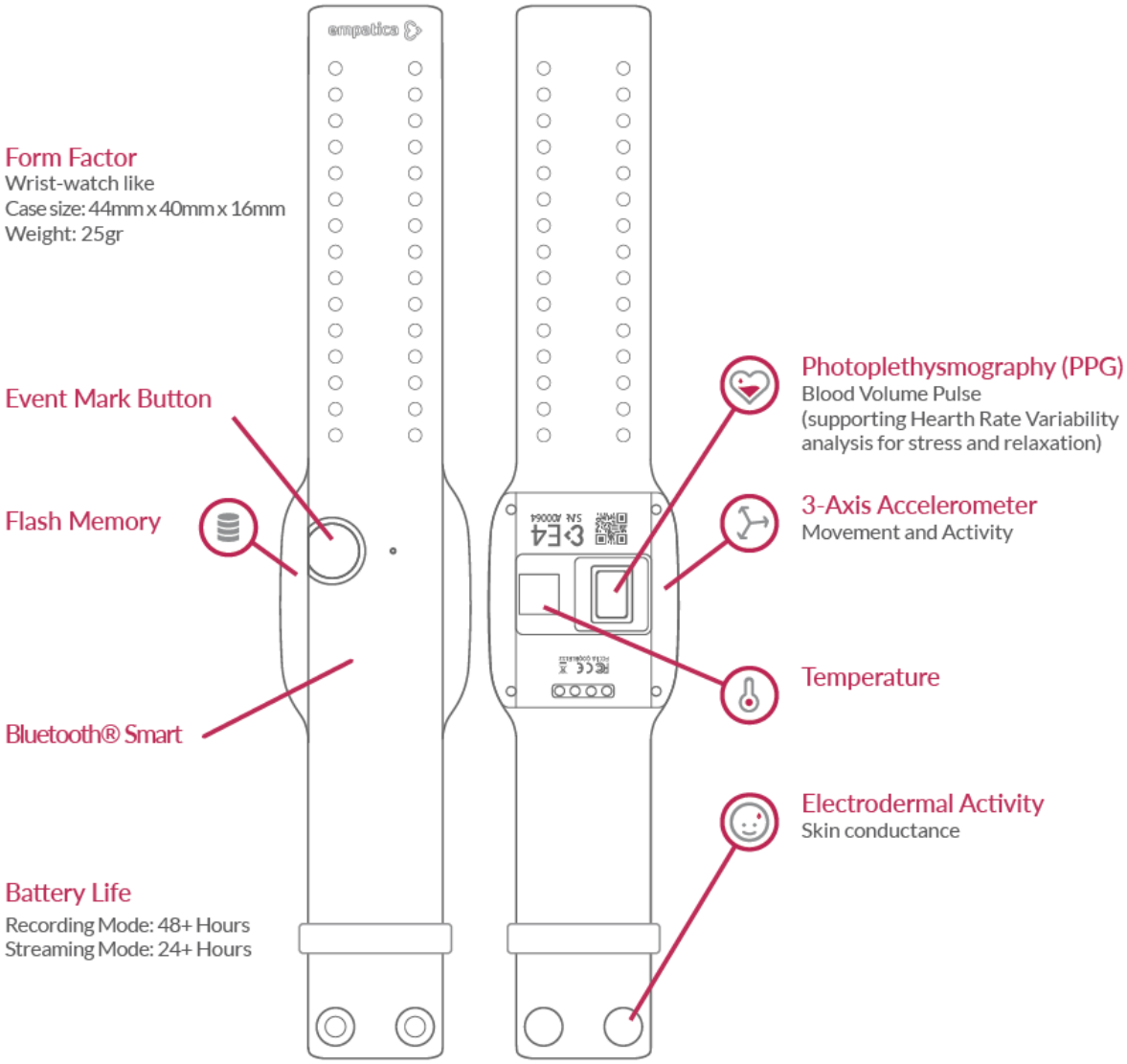

Figure 8 - Empatica E4 wristband [21].

Moreover, the E4 wristband is provided with an event mark button that allows subjects to tag the start of external stimulations.

At the beginning of each recording, the device automatically performs calibration procedure lasting 15 seconds [21]. For this reason, during the processing stage, the 60 samples corresponding to the calibration period were removed.

In order to reach the aim of this work, data used were only data recorded by the event mark button and EDA sensor. This latter uses two silver-coated electrodes that have to be positioned in the ventral region of the wrist to measure the electrical conductance of the skin. In particular, the EDA sensor records SC in the range of [0.01, 100] μSiemens with a resolution of 900 picoSiemens and a sampling rate of 4 Hz [21].

E4 wristband may work in two distinct modalities: memory mode and recording mode *(Figure 9)*.

The recording modality allows capturing and storing data in an internal flash memory for up to 60 hours. Once the data are acquired, the device has to be connected via USB to a computer in order to import information to a secure cloud platform, named *E4 Connect*. This operation is performed automatically by a desktop application, the *E4 Manager*. As soon as the user has logged in and the wristband is connected, the app transfers all data acquired to the Empatica cloud server [22][23]. Differently, operating in streaming mode, the E4 wristband connects to smartphones or tablets via Bluetooth. A mobile application, *E4 Realtime*, allows the real-time visualization of data being acquired on the smartphone. In particular, E4 Realtime provides the real-time curves of the BVP and EDA and displays heart rate and skin temperature values. When the acquisition ends, raw data is automatically uploaded to E4 Connect [22][23].

Data, securely saved on E4 Connect, may be online analyzed and managed by researchers. Otherwise, acquired measurement samples can be downloaded in CSV format and easily processed using third-party applications [21]. Among all the files downloaded only the “EDA.csv” and “tags.csv” files were used in this study. In particular, the EDA file contains in the first row the start time of acquisition, and in the second row the sampling frequency. While the tags file contains the moments of time value when the event mark button of the wristband was pushed.

Figure 9 - Working modalities of E4 wristband. The recording mode is depicted in the left chain (1) while the streaming mode in the right one (2) [23].

2.1.2 **Ledalab Toolbox**

In order to provide robust and sensitive estimates of sympathetic arousal, many software packages are available for use.

In this study, the so-called Ledalab tool version 3.4.9 was used to decompose the GSR signal and identify GSR peaks. Ledalab is a Matlab toolbox for the analysis of GSR data, available for free from http://www.ledalab.de/ website. The Ledalab.m file, contained in the downloaded zip folder, has to be run on Matlab to start the Graphical User Interface (GUI) of Ledalab software for the first time. Then, it can be lunched by just typing “Ledalab” in the Command Window of Matlab. In addition to the GUI, Ledalab can be used via batch-mode, by entering commands directly in the Matlab Command Window [7].

Ledalab is the tool recommended by Empatica E4 wristband manufacturers to decompose GSR signals into their tonic and phasic components and analyze their features [21]. The Ledalab software supports the import of various data formats such as Matlab and text data

files [7]. GSR data, acquired using the E4 wristband, can be loaded on Ledalab following the steps shown in the block diagram below (*Figure 10*).

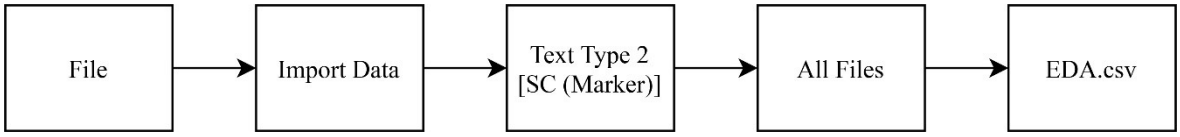

Figure 10 - Block diagram representing the procedure executed to import EDA files acquired using E4.

Once the signal is imported, the GUI of Ledalab appears as in *Figure 11*.

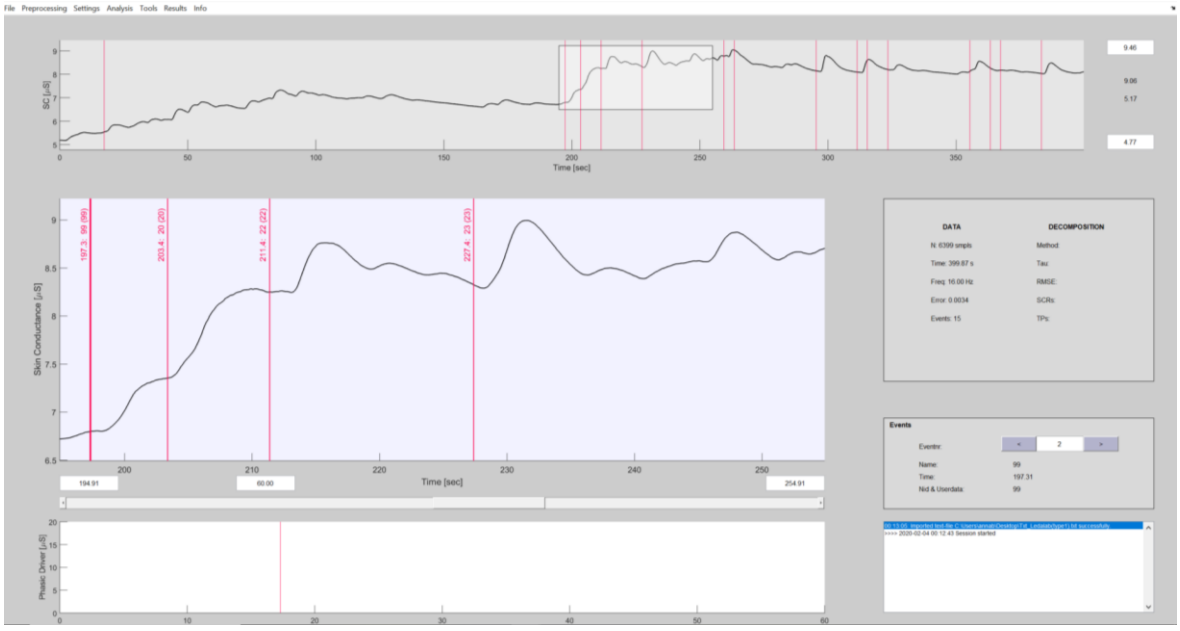

Figure 11 - Graphical User Interface of Ledalab toolbox where an imported GSR signal is represented.

The window on the top shows the GSR amplitude in µS over time given in s, in the middle window a GSR segment view is reported, while the last window shows the phasic driver view. The lateral panels contain information about data, events and operations carried out.

Moreover, the events related to external stimuli are depicted on the first and second windows as red vertical lines.

As soon as the GSR signal is loaded, it may be elaborated by performing the data preprocessing. For this purpose, Ledalab is provided of preprocessing functions like cutting, down-sampling, smoothing and artifacts correction [7]. Then, the GSR signal can be analyzed to extract and separate the tonic and phasic activity, with related parameters. Ledalab executes automatically the TTP analysis of the signal [7]. Additionally, Ledalab software provides users with two more accurate GSR analysis methods, the CDA and DDA [7]. CDA is a fast and robust method to decompose a GSR signal into continuous tonic and phasic components using a Standard Deconvolution [20]. Conversely, applying a Nonnegative Deconvolution, DDA decomposes GSR signals into tonic and discrete phasic activity [19]. Once chosen the suitable analysis technique, it has to be optimized pushing the "Optimize" button and, then, applied to the GSR data [7]. The following block diagram (*Figure 12*) displays the set of commands used in this work to perform the GSR data decomposition and GSR peaks detection.

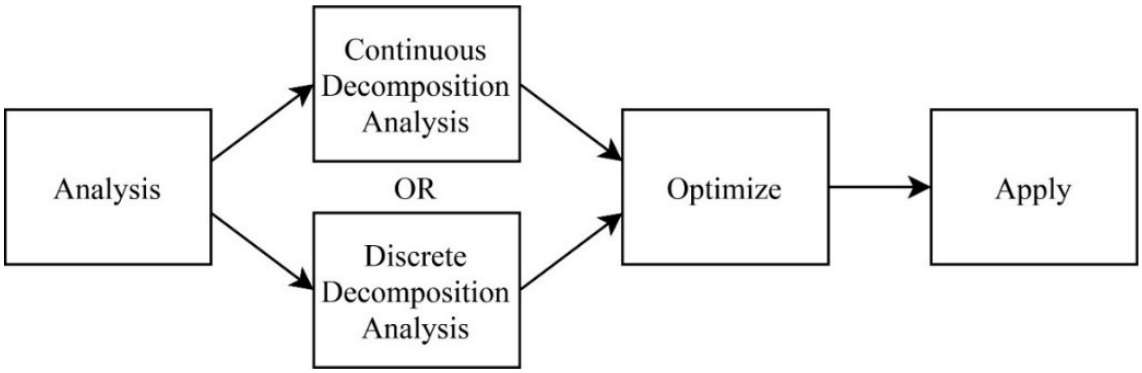

Figure 12 - Block diagram describing steps followed to perform the analysis of EDA signal.

Figure 13 represents an example of decomposition of the GSR signal performed by the software, using the CDA method.

Results obtained can be downloaded from the software and saved in an Excel file. An Excel sheet is created for each kind of analysis conducted. Here, the amplitude and the time location of each identified peak are collected.

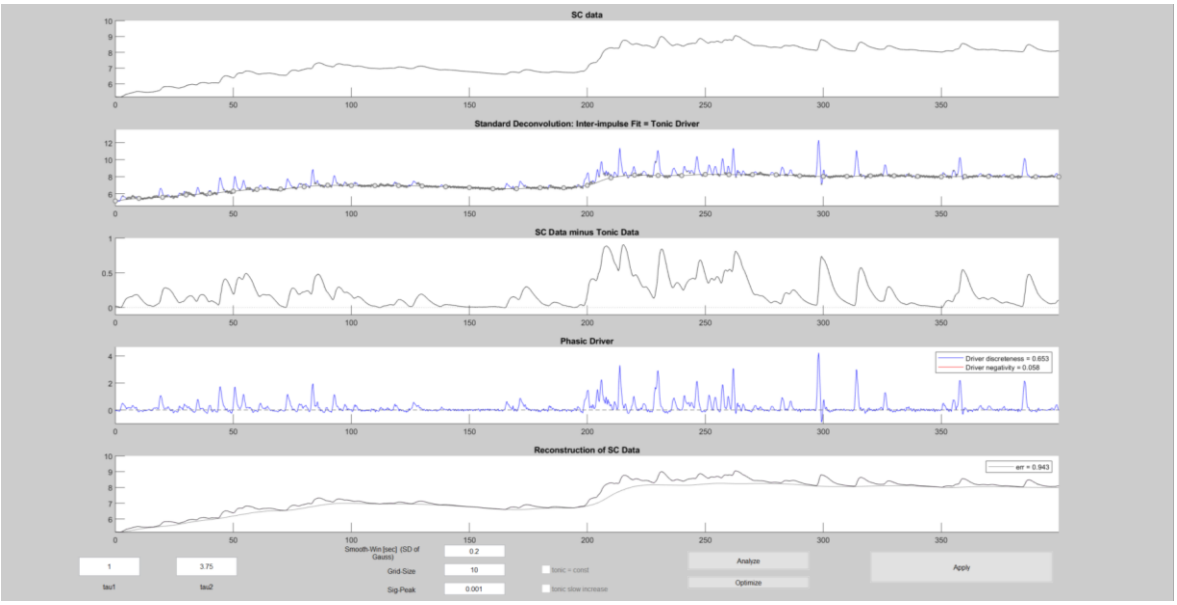

Figure 13 - Screen of the CDA steps performed by the Ledalab toolbox. From the top downwards, are shown: the SC data, the Standard Deconvolution (Tonic Driver), the SC Data minus Tonic Data, the Phasic Driver and, finally, the Reconstruction of SC Data.

2.2 **Data Processing**

Data has been processed using Matlab, approaching two different analyses. In the former, signals have been analyzed in the time domain following the procedure described in the GSR Pocket Guide [6], in order to identify and count the GSR peaks for each measured session. In the latter analysis, the raw data has been studied in the frequency domain computing the GSR signal Fast Fourier Transform (FFT) and the PSD of them.

Signals was acquired on voluntaries using the E4 wristband. GSR signal was measured on participants after they were subjected to physical stimulation and during auditory stimulation. The GSR signals resulting from the first test were analyzed in both the time and frequency domain, while on data acquired during the listening of acoustic stimuli only the analysis in the time domain was performed.

2.2.1 **Time Domain Analysis**

In order to accurately analyze the GSR signal, properly finding GSR peaks in time domain, it is necessary to remove the tonic component from the raw signal [6][19][20].

The algorithm described in the GSR Pocket Guide was implemented using Matlab. It is divided into three main steps: *down-sampling*, *filtering* and, *onset and peak detection*. Because the GSR signal is usually sampled at a higher sampling frequency than required, the first step allows reducing the number of samples per second without any risk of losing significant information [6]. The filtering step permits to remove the tonic component from the original GSR curve. Specifically, a median filter is applied in order to consider only the phasic component of the analyzed signal. In the last step, the phasic component is used to identify the onset and offset of each peak by setting two thresholds. A threshold th_{on} = 0.01 μS is used to detect the onsets, while the offsets are identified by setting a threshold th_{off} = 0 μS. Then, back to the original signal, for each onset-offset couple, the exact position of each peak is identified. Once peaks are detected, they can be counted. The peaks count is an interesting metric to examine in depth the emotional and psychological state of a person and to compare the collected data [6].

GSR data, downloaded from E4 Connect, was imported in Matlab and saved in an array data structure called `SC`.

Firstly, some samples at the beginning and at the end of the recorded signal were removed because they could be affected by motion artifacts. Moreover, this procedure allows obtaining signals of the same length (i.e. arrays containing the same amount of samples) thus allowing to compare the results obtained from different acquisitions. Because the duration of the acquisitions is different between the physical and auditory stimuli tests, the number of removed samples differs too. In particular, for the signals recorded after physical stimulation, 30 seconds at the beginning and 30 seconds at the end of the acquisition, amounting to a total of 240 samples, were removed. While, for the data acquired during auditory stimulation, only 16 samples were eliminated corresponding to the initial 2 seconds and the final 2 seconds.

Once the initial and last samples have been removed, the algorithm described above was applied to the resulting array.

Because the sampling rate of the E4 EDA sensor, equal to 4 Hz, is low enough [6], the first step of the Pocket Guide's algorithm was not applied. Therefore, the `SC` array was directly filtered applying a median filter as described below:

- For each sample of SC, the median GSR score of the surrounding 32 samples, corresponding to a time interval of 8 seconds centered on the current sample, was calculated.
- The outcomes, computed using the median function of Matlab, were saved in a new array called `SCL` corresponding to the tonic component of the GSR signal.
- Finally, the phasic component of the signal was obtained subtracting the `SCL` from `SC`. The array resulting from the subtraction was called `SCR`.

The Matlab code concerning this step of the algorithm is the following one:

```
% Median filter implementation
frequency = 4;
w = 4*frequency;
for i = w+1:length(SC)-w
     x = SC(i-w:i+w);
     SCL(i) = median(x);
     SCR(i) = SC(i)- SCL(i);
end
```

A `for` cycle was implemented to compute and subtract the median GSR value to the original collected signal. At first, the sampling rate of E4 wristband and the window length were defined in `frequency` and `w` variables, respectively. In the first row of the recursive cycle, the 32 samples surrounding the `i-th` sample were selected. In the second row, the median of the `x` interval, created in the previous row, was computed and saved in the `i-th` position of the `SCL` array. In the last raw, the phasic component (`SCR`) was computed subtracting sample by sample the tonic component (`SCL`) from the raw signal (`SC`).

The following flowchart details the procedure carried out for the definition of `SCL` array *(Figure 14)*.

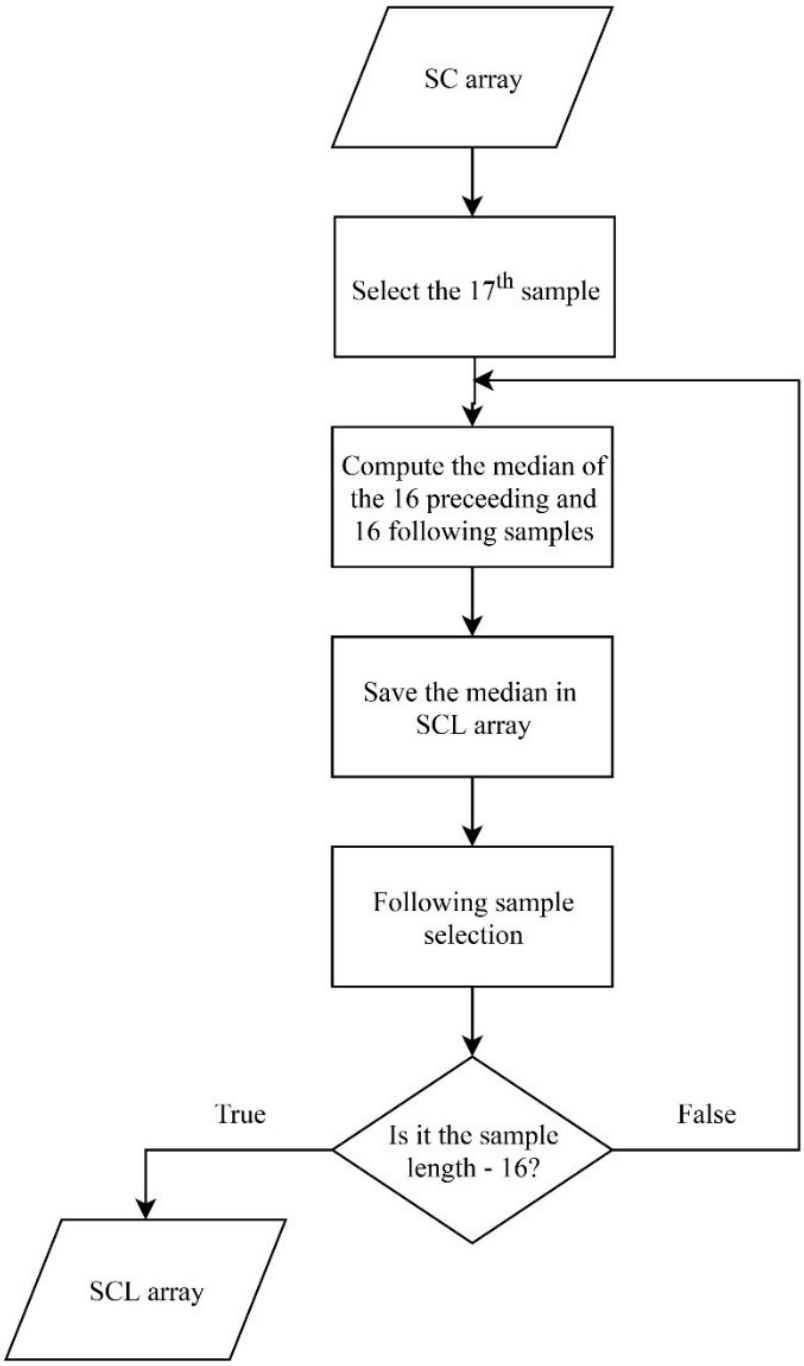

Figure 14 - Flowchart describing the SCL array building.

Once the phasic component of the GSR signal was computed, it was possible to automatize the peaks detection procedure. At first, peaks onset and offset were identified in the SCR signal, following the step described below:

- By setting an onset (> 0.01 μS) and an offset (< 0 μS) threshold, two arrays, called `onset` and `offset`, were defined.

The flowchart below presents the operations carried out to define the `onset` array (*Figure 15)*.

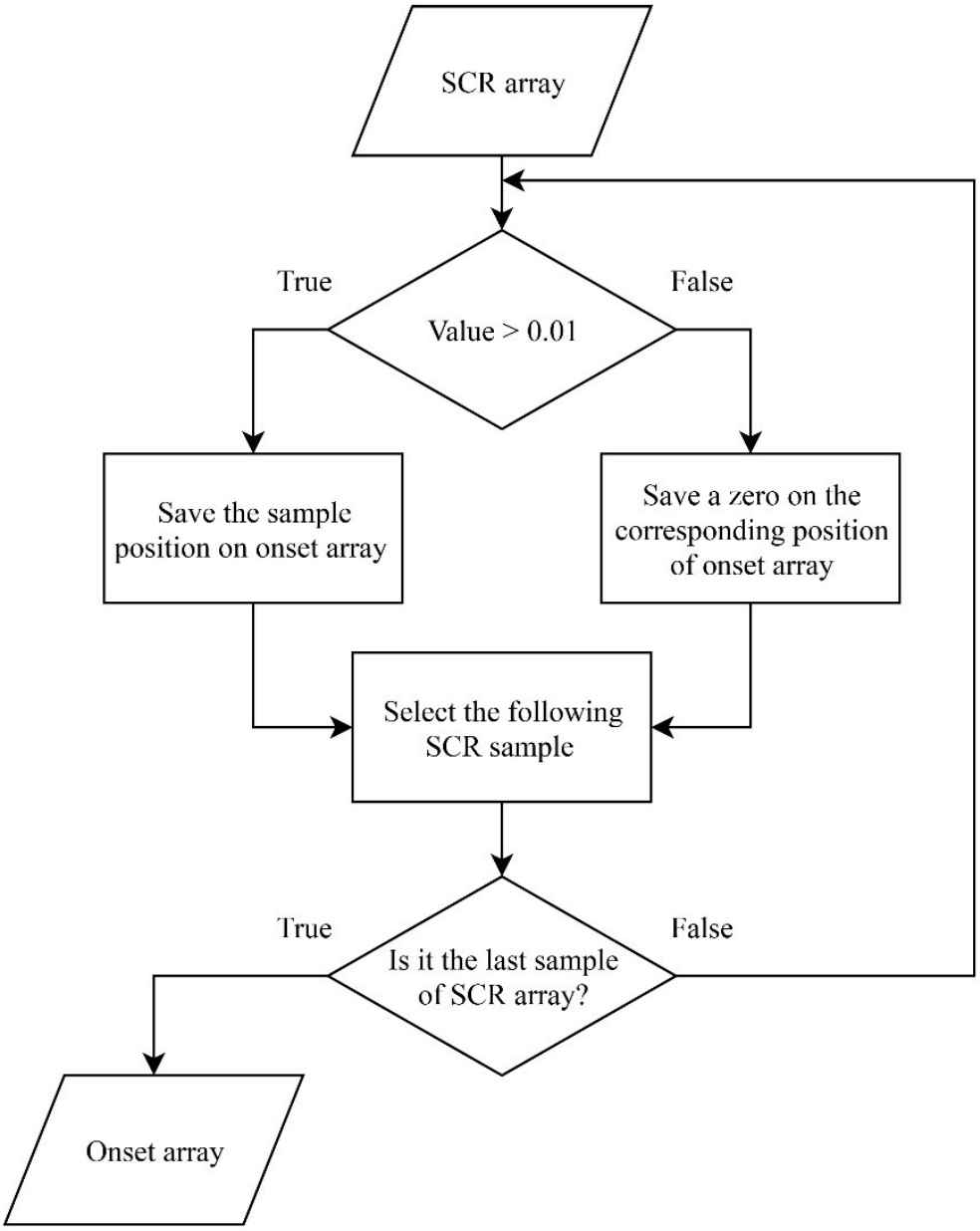

Figure 15 - Flowchart for the definition of the onset array. The construction process of the offset array may be described by an analogous flowchart.

The code related to the definition of `onset` array is displayed below:

```
% Onset array building
sup_threshold = 0.01;
for i = 1:length(SCR)
    if SCR(i) > sup_threshold
        onset(i) = i;
    else
        onset(i) = 0;
    end
end
```

The `onset` array was created implementing a `for` loop and imposing an `if-else` condition. In particular, the `SCR` array was scrolled sample by sample. The `i-th` position of the samples that satisfied the `if` condition was saved in the `i-th` position of the `onset` array, while the zeros were saved in all other positions. Similarly, a cycle was implemented to build the `offset` array, that differs from the one shown above just for the threshold value and the `if` condition.

All the samples satisfying the set thresholds were saved in the `onset` and `offset` arrays. However, the building of two different arrays did not allow the association of a specific `onset` to the corresponding `offset`. Therefore, in order to identify all the onset-offset pairs, the following step was implemented:

- A two-columns matrix called `on_off_couple` was created. The onset and the offset of each interval where a peak occurs were saved in this matrix. In particular, the first column contains the onsets, while the second one the offsets.

The Matlab code concerning the `on_off_couple` matrix creation is shown below:

```
% On_off_couple matrix creation
index = 1;
token = 1;
l = max(length(offset), length(onset));
on_off_couple = [];
for i = 1:l
```

```
        if token == 1
           while onset(index) == 0 && index < length(onset)
                 index = index+1;
           end
             on_off_couple(i,1) = index;
             token = 0;
        end
        if token == 0
           while offset(index) == 0 && index < length(offset)
                 index = index+1;
           end
             on_off_couple(i, 2) = index;
             token = (index <= length(onset));
        end
        if index == length(offset)
           break
        end
end
```

Using two auxiliary variables, the vectors containing the onset and offset positions were scrolled in order to build the matrix containing the onset-offset couple of each interval. In particular, the `index` variable was introduced to scroll both `onset` and `offset` arrays, while the boolean variable (i.e. `token`) was used to jump from the `onset` to the `offset` vector and conversely. A series of nested cycles was implemented to build the matrix. Depending on the current `token` value, only a portion of the `for` loop was run for each iteration. Specifically, when `token == 1`, the `onset` array was scrolled until it was equal to zero and lower than the total length of the array itself. When the `while` condition was not more satisfied, the `index` value was saved in the first column of the `on_off_couple` matrix and the `token` was set equal to 0. When `token == 0`, the operations described above were performed on the `offset` array.

The steps carried out to build the matrix containing the onset-offset pairs are specified in the following flowchart *(Figure 16)*.

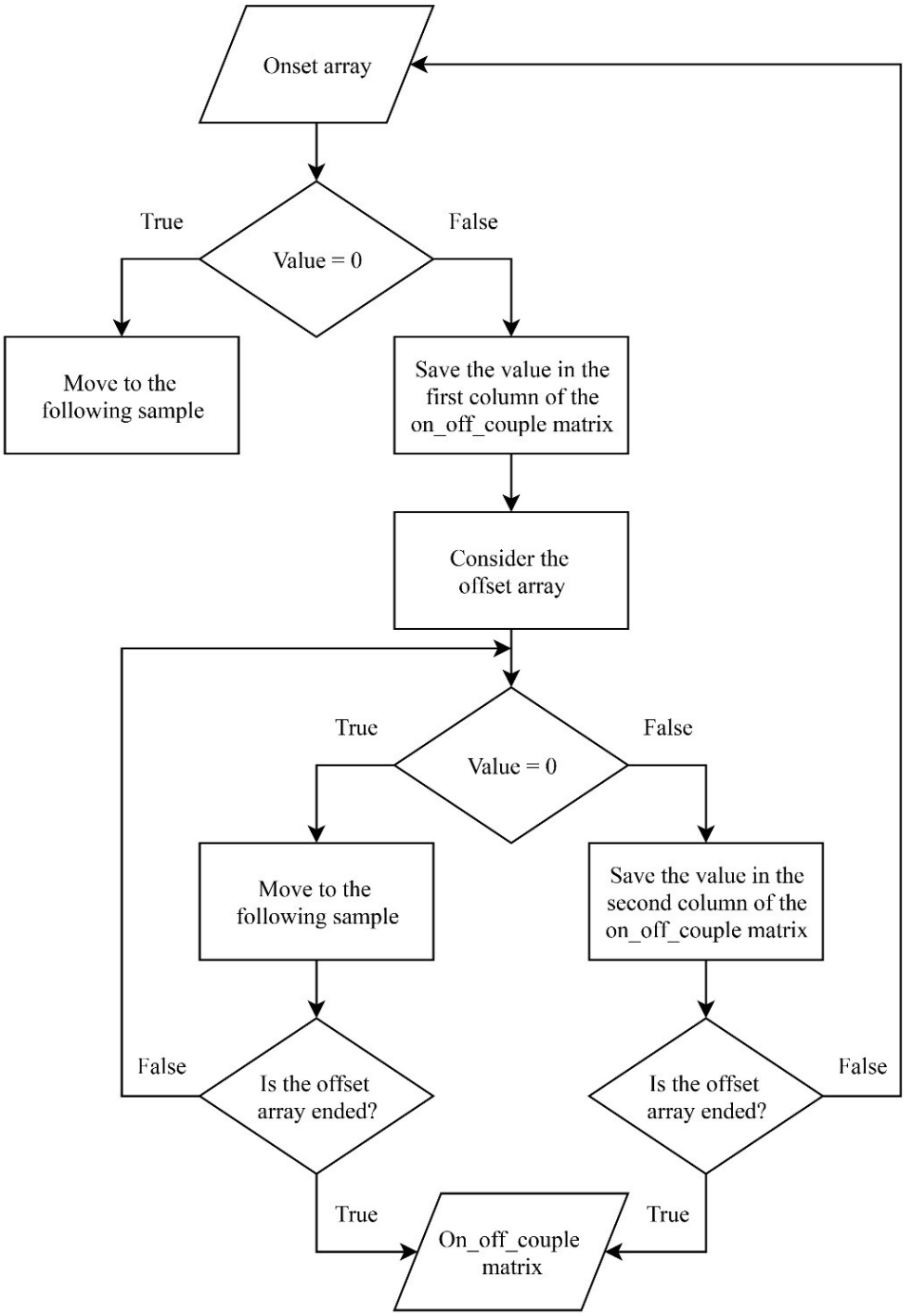

Figure 16 - Flowchart explaining the on_off_couple matrix building.

Once the onset and the offset of each interval were identified, the GSR peaks were detected in the original unfiltered signal as explained in the following steps:

- A new matrix called `interval` was defined. The `interval` matrix has a number of columns equal to the number of onset-offset couples identified in the previous step. In each column, the SC values between each pair of onset and offset were saved.
- For each column, the maximum value and its position were calculated using the `max` function of Matlab. Each maximum found corresponds to the GSR peak in that interval.

The for cycle developed to implement steps just described is displayed below:

```
% Interval matrix building and peaks identification
interval = [];
for i = 1:length(on_off_couple(:,1))
    j = 1;
    k = on_off_couple(i,1);
    while k <= on_off_couple(i,2)
        interval(j,i) = SC(k);
        j = j+1;
        k = k+1;
    end
    [max_vet(i), pos_max(i)] = max(interval(:,i));
    pos_max(i) = pos_max(i)+on_off_couple(i,1)-1;
end
```

The `while` loop, nested into a `for` cycle, was implemented to fill in the `interval` matrix. A `k` variable was introduced to carry out the matrix filling. Outside the `while` cycle, `k` was set equal to the `i-th` raw of the first `on_off_couple` column, corresponding to the sample at which the peak onset occurs. Then, the `k` value was increased until the `while` condition was satisfied. SC values corresponding to the `k-th` positions were saved in the `i-th` column of the `interval` matrix. This procedure was repeated for each pair of onset and offset. On each matrix column, the maximum value and its position were calculated and saved in the `max_vet` and `pos_max` vectors, respectively.

The flowchart below explains the steps followed to fill in the `interval` matrix *(Figure 17)*.

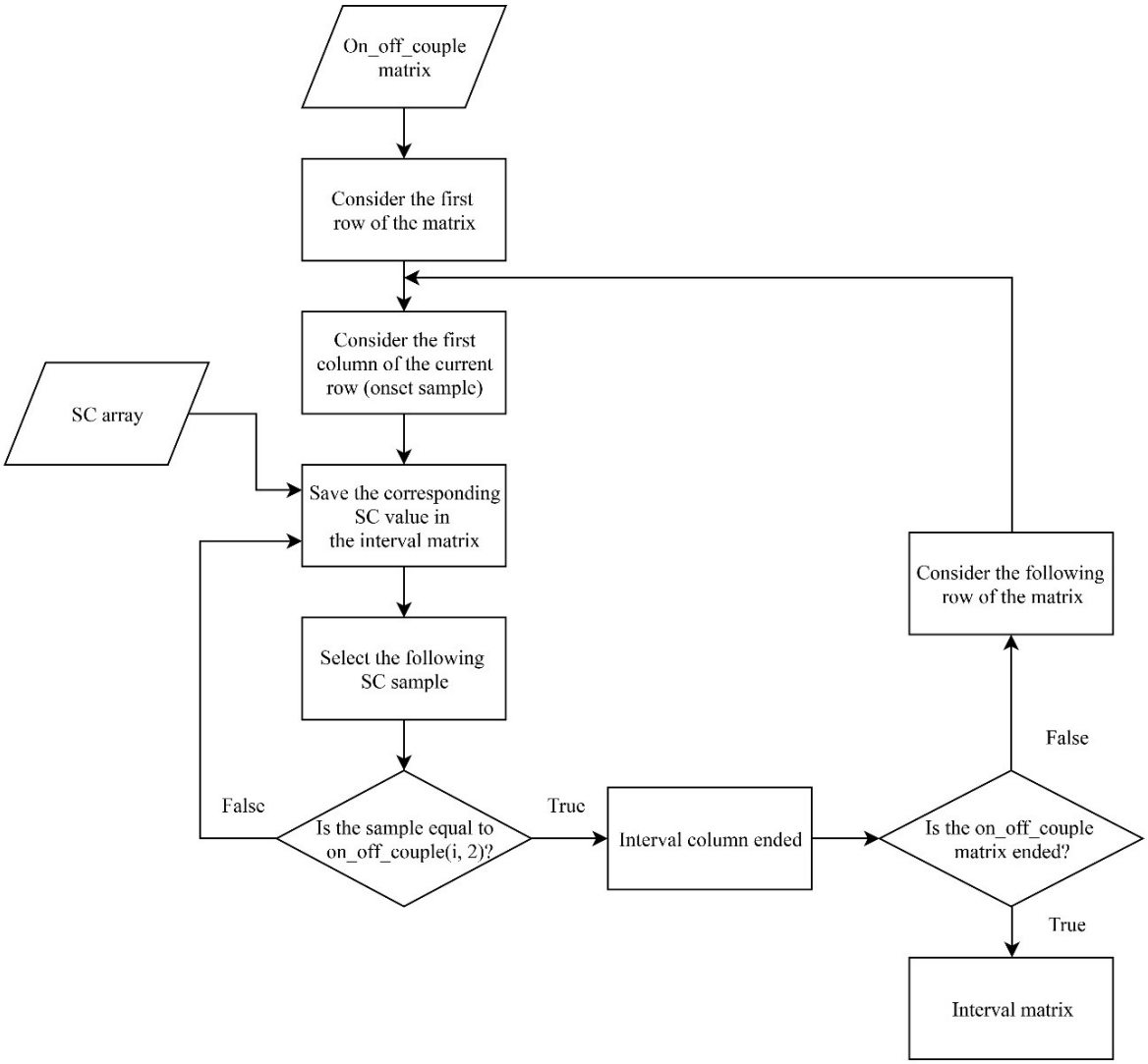

Figure 17 - Flowchart for the interval matrix construction.

Finally, because the maximum found for each interval corresponds to the GSR peak, the total amount of peaks was counted using the *length* function of Matlab, applied on the `max_vet` array.

The Matlab code relating to the peaks counting is shown below:

```
% Peaks number calculation
number_peak=length(max_vet);
```

Figure 18 contains an example of Matlab plot showing the results of the steps described above, computed on a signal acquired on Subject 1 after a session of high intensity exercise. Specifically, the blue curve represents the raw signal (i.e. SC array), while the red one is the phasic component of the original signal, computed applying the median filter. The green triangles represent the onsets, while the red ones the offsets. Finally, the peaks detected following the last steps are represented by yellow stars markers placed on the SC signal.

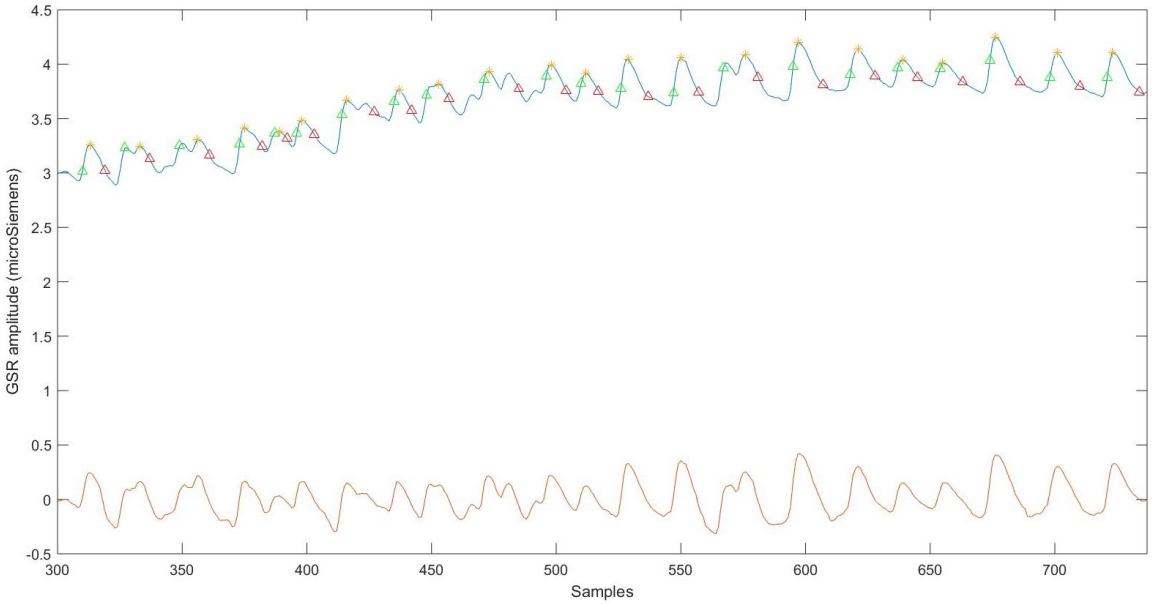

Figure 18 - Example of Matlab plot representing the original raw signal SC (blue), the filtered signal SCR (red) and the corresponding peaks detected (yellow stars).

2.2.2 **Frequency Domain Analysis**

Data, acquired using the E4 wristband after subjects performed physical efforts, was analyzed also in the frequency domain.

Raw signals were imported in Matlab and saved in the *sc* vector. Initial and final samples of the array were removed in order to avoid samples affected by motion artifacts and obtain

vectors of the same length for each acquisition. As in the time domain analysis, 240 samples were removed from signals acquired after physical stimulation.

No pre-processing was performed on the GSR signals, indeed the absolute value of the FFT was directly computed on the raw data. Moreover, the spectrogram and the PSD of the data were calculated to analyze GSR in both the time-frequency domain and time-invariant frequency domain, respectively. The computations of FFT and spectrogram were performed using the suitable and appropriate Matlab functions, while for the PSD, according to the definition, the following equation was implemented:

```
% Power Spectral Density calculation
PSD_SC = (1/(fs*l_freq)) * abs(sc).^2;
```

where `fs` is the sampling frequency of the signal corresponding to 4 Hz and `l_freq` is the length of the frequency vector.

Values obtained were saved in a vector called `PSD_SC`, while the ones achieved computing the absolute value (magnitude) of the FFT were saved in the `FFT_SC` array.

As explained in Chapter 1, several studies have shown that most of the total GSR's spectral power is usually in the range 0 to 0.25 Hz and, in particular, it is contained in the frequency band 0.045-0.25 Hz [13][15]. According to these studies, in this work, the Area Under the Curve (AUC) was computed for both the resulting FFT and PSD to assess the acquired GSR signals in the frequency domain.

Specifically, the AUCs of the `FFT_SC` and of the `PSD_SC` in the frequency ranges 0-0.25 Hz, 0.045-0.25 Hz and 0-0.4 Hz were calculated [13][15].

Finally, the area contained in the first and the second range was compared with the one of the last frequency band, thus computing the percentage ratio. The same steps were performed on the PSD of the GSR signal.

The following Matlab plot *(Figure 19)* shows an example of the absolute value of the PSD computed on the raw signal acquired on Subject 2 after a session of medium exercise. The three frequency bands of interest are represented by the vertical dashed lines. In particular, the first line is placed at 0.045 Hz, while the second one at 0.25 Hz.

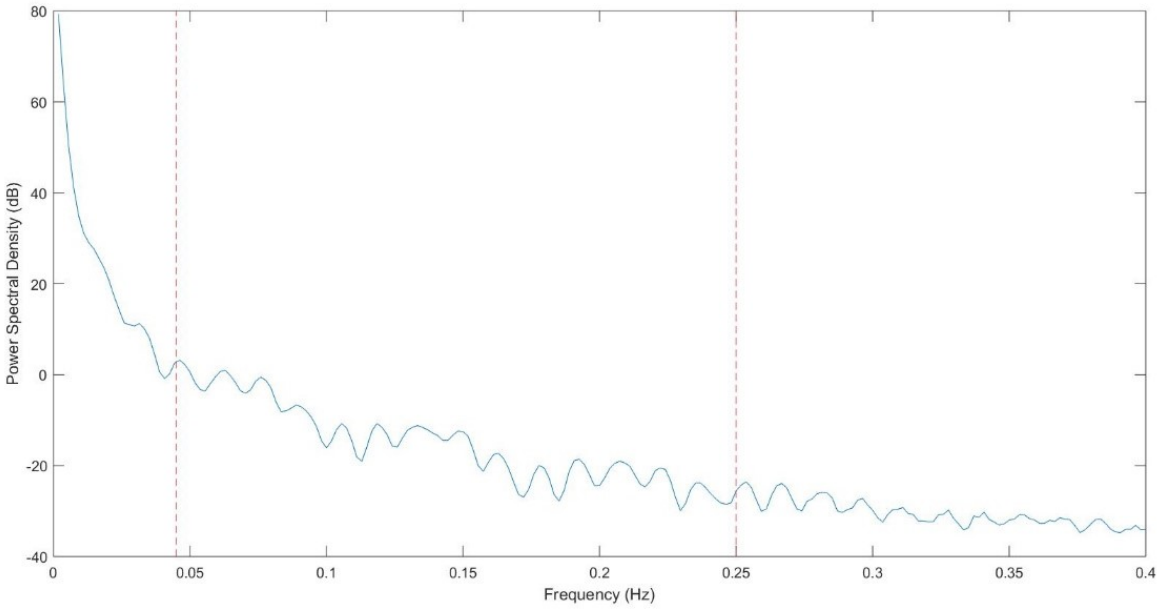

Figure 19 - Example of Matlab plot representing the PSD of the GSR signal. The red dashed lines represent the frequency thresholds defined above.

Chapter 3
Experimental Tests

The experimental tests conducted during this thesis work are described in detail in this chapter. Before the beginning of the acquisitions, subjects were informed on the experiment functioning and a written consent was obtained from each of them. Participants were contributed to two different tests in order to evaluate GSR's changes in response to physical and auditory stimuli. During each measurement, subjects wore the Empatica E4 wristband on the dominant wrist, lying on the bed in a comfortable position. Moreover, in order to the minimize artifacts, prior to collect data it was asked to the subjects to maintain regular breathing and avoid moving and talking.

3.1 Acquisitions after Physical Stimulation

Data were acquired on eight subjects, three males and five females *(Figure 20)*, with a mean age of 35.4 ± 16.4 years *(Figure 21)*.

Each subject performed different sessions of physical activities. Data were recorded for a period of 15 minutes in resting condition, for a duration of 10 minutes after a session of medium exercise and after one of hard exercise. Some examples of medium exercise are 10 minutes of brisk walking or climbing stairs, while during the hard exercise session participants were subjected to physical efforts like 10 minutes of quick run. Data acquired in resting condition was used as baseline signal. Acquisitions were carried out during different times of the day: in the morning until 1:00 pm, during the afternoon, and in the evening after 8:00 pm.

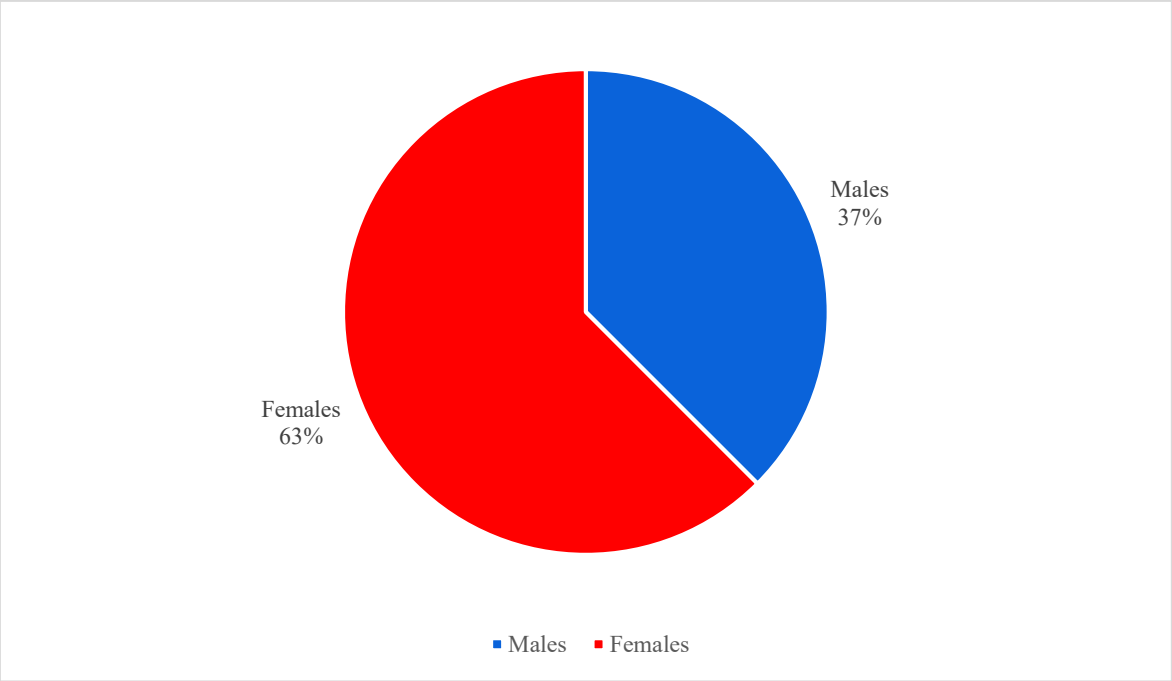

Figure 20 - Percentage of males and females in test population.

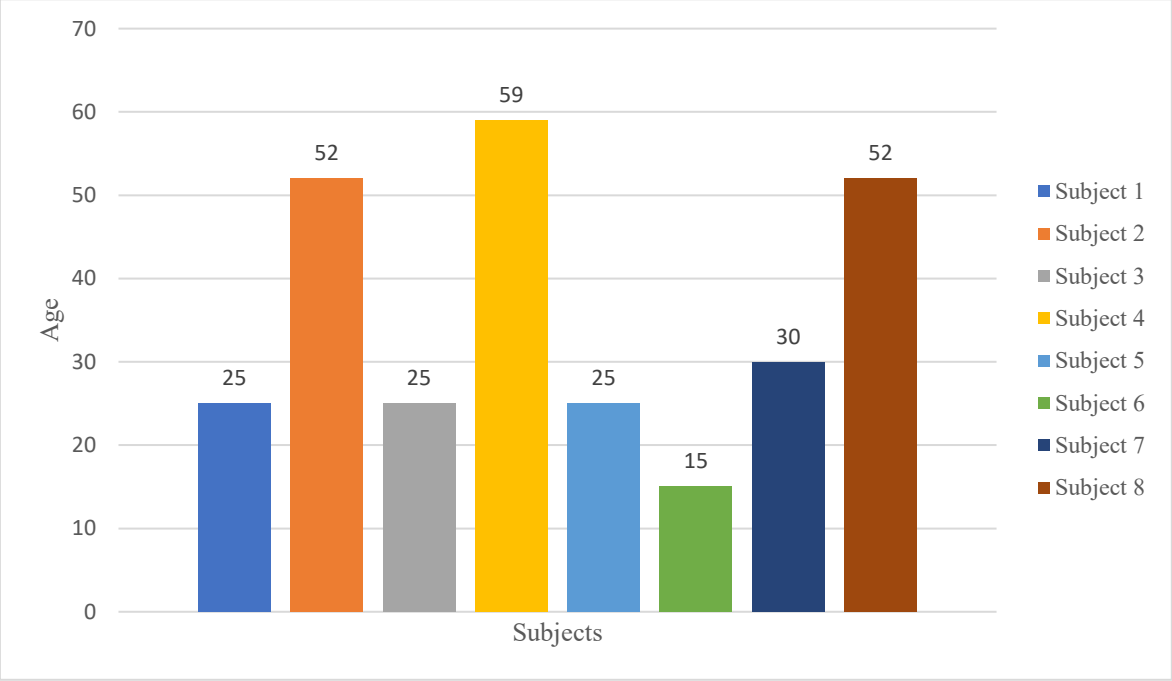

Figure 21 - Age distribution of the selected subjects.

After of each trial session, it was asked to participants to rate their emotional state using the SAM scale described in Chapter 1. This scale measures the valence, arousal and dominance dimensions. However, only the valence and arousal dimensions are used in this experimental test because they are the most used in literature and the ones most clearly perceived by the users [11]. The valence and arousal score were chosen by subjects involved in the experiment selecting the manikin describing more faithfully their current condition.

3.2 **Acquisitions during Acoustic Stimulation**

Seven subjects, two males and five females (*Figure 22*) with an age (mean ± standard deviation) of 35.7 ± 17.9 years, were enrolled (*Figure 23*).

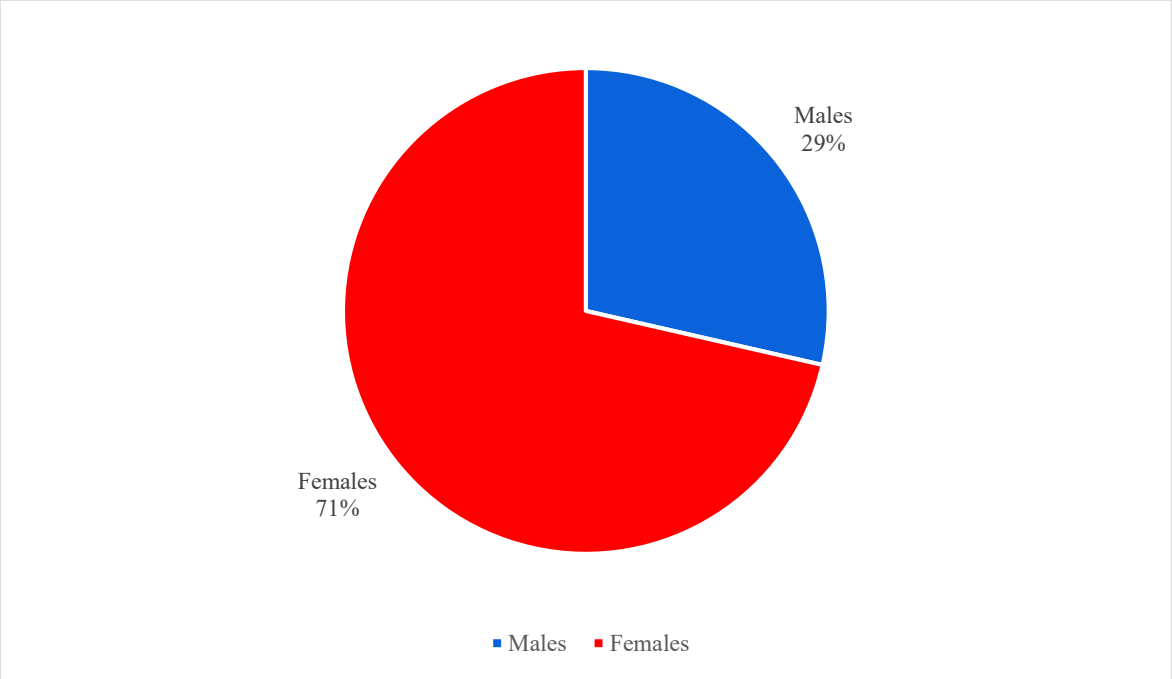

Figure 22 - Percentage of males and females in test population.

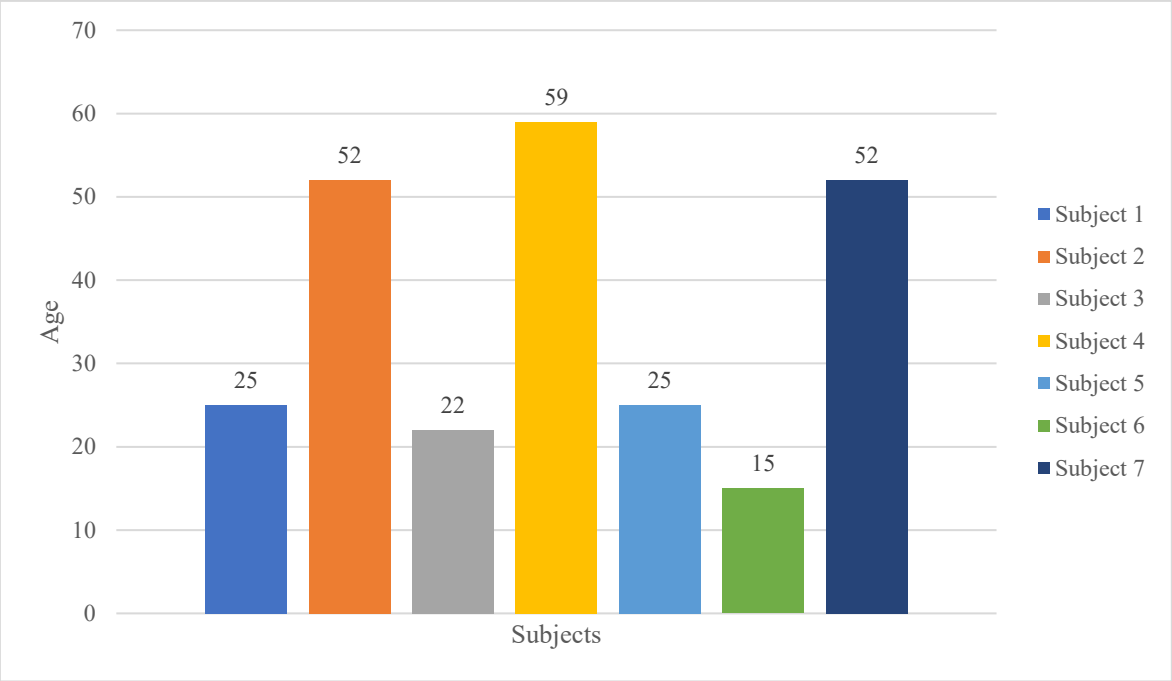

Figure 23 - Age distribution of the selected subjects.

Each subject was submitted to six sessions of acquisition during which an acoustic stimulus was played. Three sessions last about eleven minutes and are divided into three phases. For the first and last five minutes within each session, the GSR signals were recorded at resting condition, while in the central minute participants were listened to a sound. The remaining sessions have a duration of twelve minutes and are composed by five minutes of acquisition at resting condition, followed by 2 minutes of GSR signal recording during sound reproduction, and five minutes of acquisition without stimulation. Acoustic stimuli were played by a Bluetooth speaker inside a bedroom where the participants lied in a comfortable position, keeping their eyes closed. The examiner was placed outside the room in order to avoid interferences with the experiment. Finally, subjects were asked to push the event marker button of the wristband at the beginning and at the end of the acoustic stimulus.

Sounds were selected from the International Affective Digitized Sounds (IADS-2) database. This database contains a collection of sounds rated in terms of valence, arousal and dominance using the SAM scale [24][25]. Considering the valence score, a pleasant, a neutral and an unpleasant sound were chosen for the tests performed in this work. The scores of sounds selected are presented in *Table 1*, *Table 2* and *Table 3*. The first Table shows the

overall scores, while the second and the third ones contain scores considering only a female population or a male population, respectively.

Table 1 - Valence, arousal and dominance scores (dimensionless values) of the selected sounds in a mixed population.

Sound Description	Valence	Arousal	Dominance
RockNRoll	7.90 ± 1.53	6.58 ± 2.16	6.86 ± 1.99
Walking	4.83 ± 1.22	4.97 ± 1.82	4.66 ± 1.49
Scream	2.05 ± 1.62	8.16 ± 2.15	2.55 ± 2.01

Table 2 - Valence, arousal and dominance scores (dimensionless values) of the selected sounds in a female population.

Sound Description	Valence	Arousal	Dominance
RockNRoll	8.13 ± 1.41	6.75 ± 2.28	6.99 ± 1.99
Walking	5.02 ± 1.19	4.87 ± 1.86	4.85 ± 1.41
Scream	1.65 ± 1.16	8.35 ± 1.32	2.11 ± 1.74

Table 3 - Valence, arousal and dominance scores (dimensionless values) of the selected sounds in a male population.

Sound Description	Valence	Arousal	Dominance
RockNRoll	7.56 ± 1.65	7.00 ± 1.77	6.67 ± 2.00
Walking	4.61 ± 1.22	5.08 ± 2.00	4.45 ± 1.56
Scream	2.49 ± 1.94	7.96 ± 1.67	3.04 ± 2.19

The sounds of the IADS-2 database have a duration of 6 seconds. Since some studies have found that stimuli lasting from 2 to 4 minutes are enough to produce variations of some physiological parameters as GSR [26], it was thought to reproduce the same sound more

times. Specifically, for each sound two playlists were created using Windows Media Player. In the first playlist the auditory stimulus was reproduced ten times obtaining a one-minute-long sound, while in the second playlist the acoustic file was repeated twenty times in order to reach a total duration of two minutes. The use of the same audio track for different time lengths allows comparing the resulting GSR signals in order to understand the effect of the stimuli length on the physiological signals. Sounds were randomly reproduced and, between one recording and the next, the E4 was removed from the wrist of the subject in order to restore the resting condition. At the end of each acquisition, participants rate the listened sound using the valence, arousal and dominance dimensions of the SAM scale. These scores will then be compared with the ones presented in the Tables shown above.

Chapter 4
Physical Stimuli Test Results

This chapter presents the results obtained from the analysis of GSR signals acquired after participants have performed physical efforts of different intensities.

Signals were recorded on 8 individuals (3 males and 5 females) with an age ranging from 15 to 59 years. The E4 wristband was used to acquire GSR data that was recorded on subjects at resting condition and, following medium and high-intensity physical efforts. Later, data was processed in Matlab following the algorithms described in Chapter 2. Specifically, they were analyzed in time and frequency domain in order to identify common features in the GSR pattern of different subjects, when they perform physical exercises of different intensities.

By making just a visual inspection of raw GSR signals, it is possible to easily identify some differences between signals acquired at resting condition and the ones recorded after physical stimulation. Conversely, finding clear differences between raw signals arising from different levels of physical activity is much harder, by just inspecting the plot of the GSR data.

Figures 24, 25 and *26* show the raw GSR signals at resting condition, after medium physical exercise and after strong physical efforts, respectively. All the Matlab plots have the sample number in the abscissa axis and the amplitude of the GSR signal expressed in μS along the vertical one.

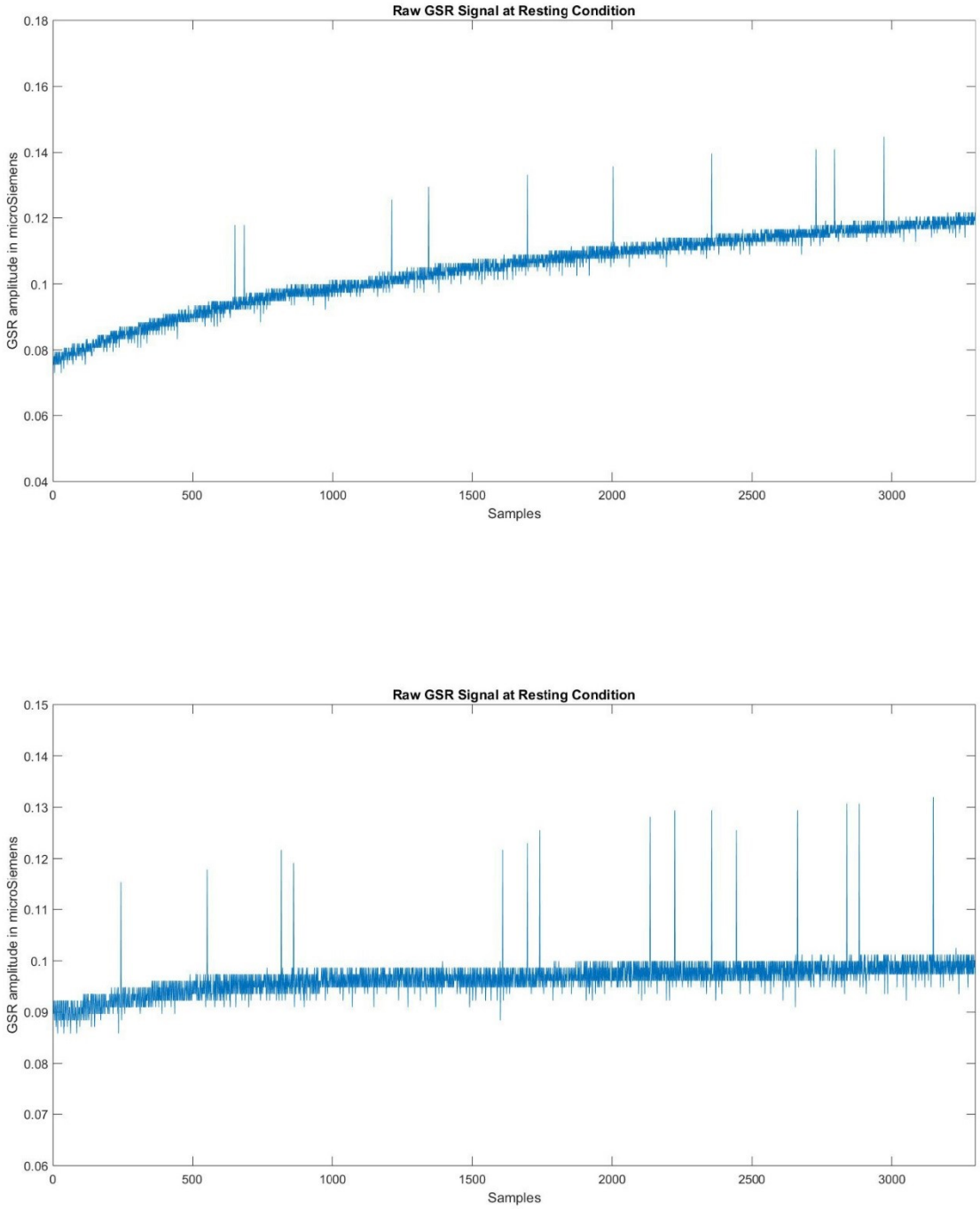

Figure 24 - Two examples of Matlab plots of raw GSR signals recorded during on subject 1 at resting condition.

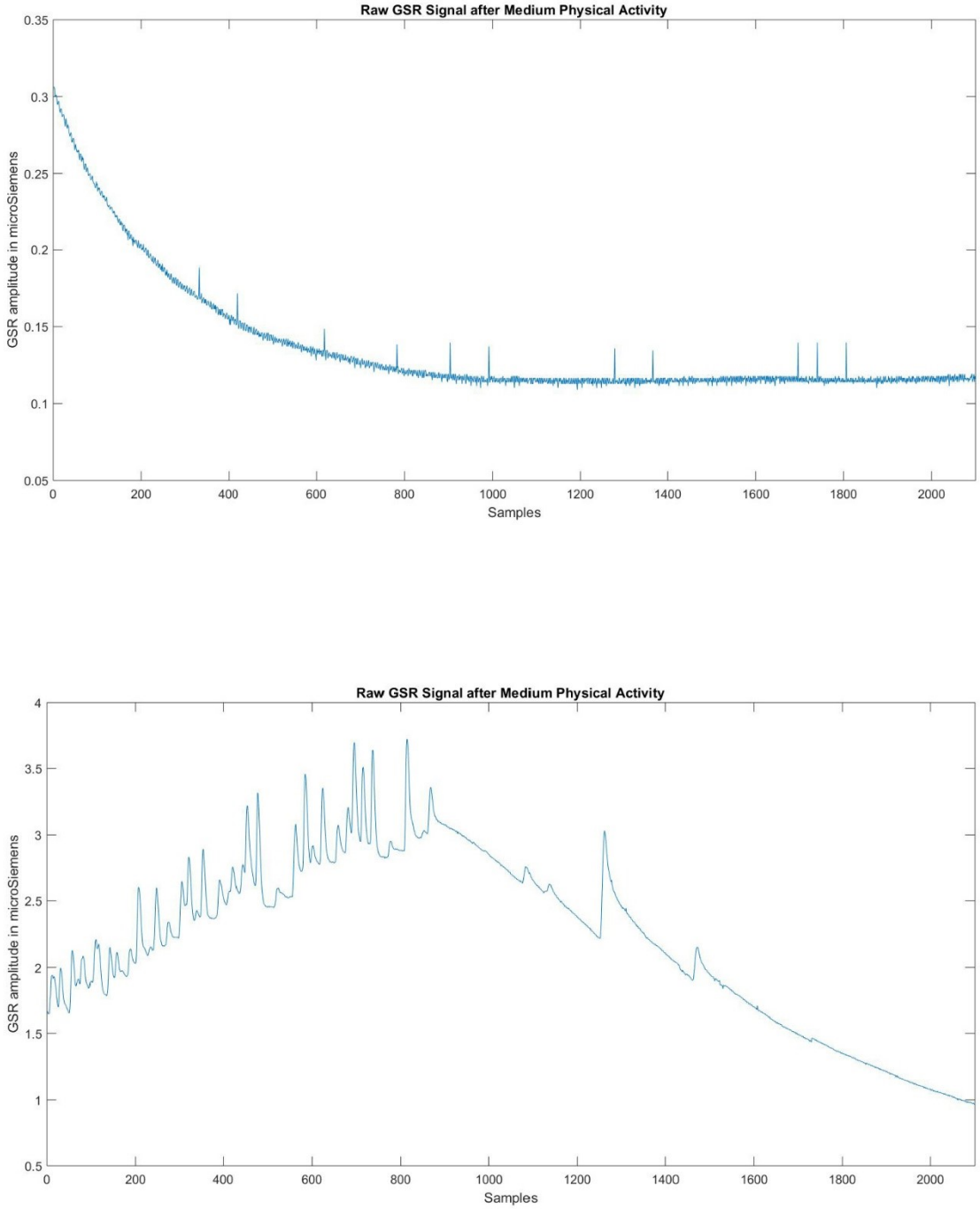

Figure 25 - Two examples of Matlab plots of raw GSR signals recorded after subject 1 has performed physical exercise of medium intensity.

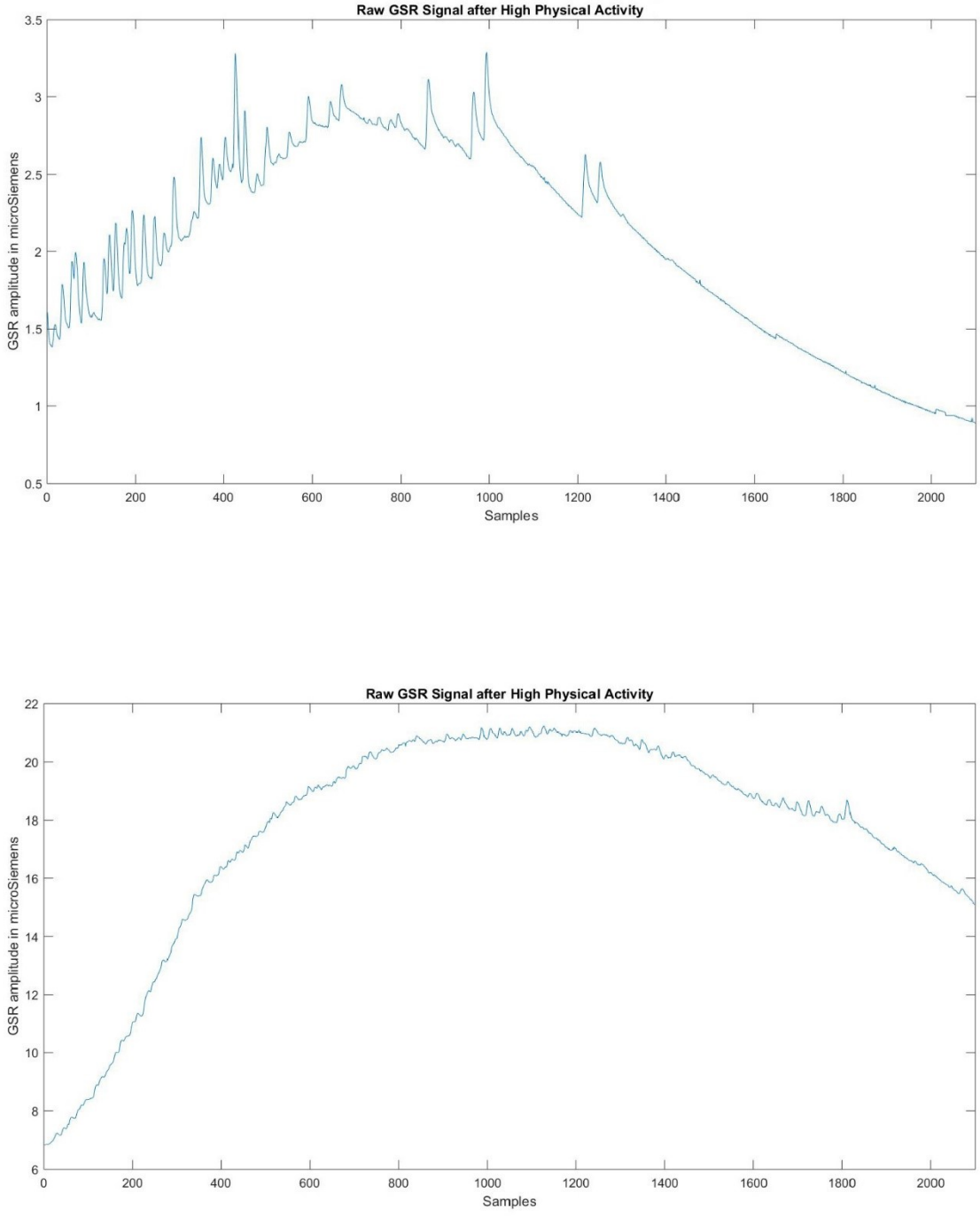

Figure 26 - Two examples of Matlab plots of raw GSR signals recorded after subject 1 has performed physical exercise of high intensity.

By analyzing the images shown above, it is possible to notice that the pattern of the raw GSR signal acquired at resting condition is similar in both the plots (*Figure 24*). The amplitude of the signal is very low and rather constant. Conversely, GSR signals recorded after medium and high intensity physical activity are strongly variable in different sessions. Specifically, GSR signals resulting from physical activity of medium intensity appear usually as in *Figure 25*. Often, the signal trend is similar to the first plot: it has high magnitude at the beginning of the acquisition and gradually decreases as time passes, reaching after some minutes of recording a shape similar to the one of the GSR signal acquired at resting condition. Instead, in other cases, the GSR pattern is similar to the one shown in the second plot. In this case, the GSR signal increases, and then decreases its amplitude, showing very evident peaks. As it is possible to notice from the first plot of *Figure 26*, frequently the pattern of GSR data acquired after physical exercise of high intensity is very similar to the one resulting from the medium physical exercise. However, sometimes the raw GSR signal appears as in the second plot of *Figure 26.* Here the GSR amplitude variation is much greater and GSR peaks are much more frequent, but with smaller amplitude.

Table 4 shows the mean GSR amplitude and the standard deviation for each subject, at different levels of physical exercise.

Table 4 - Mean amplitude and standard deviation of the raw GSR signal at rest condition and after physical activity of medium and high intensity, for each subject.

	Rest (µS)	**Medium (µS)**	**High (µS)**
Subject 1	0.11 ± 0.02	1.00 ± 1.31	5.30 ± 6.45
Subject 2	1.31 ± 0.91	3.37 ± 1.08	26.90 ± 13.10
Subject 3	0.24 ± 0.07	0.49 ± 0.73	3.05 ± 3.56
Subject 4	0.16 ± 0.01	0.17 ± 0.01	0.15 ± 0.02
Subject 5	0.55 ± 0.14	4.48 ± 5.99	6.47 ± 4.98
Subject 6	0.14 ± 0.03	0.96 ± 1.14	18.19 ± 8.96
Subject 7	0.17 ± 0.01	2.39 ± 0.64	14.16 ± 9.41
Subject 8	0.15 ± 0.06	0.15 ± 0.02	14.75 ± 15.69

Although the raw GSR pattern is quite variable from one acquisition to the other, especially comparing the medium and high intensity physical exercises, *Table 4* shows that, in seven of the eight subjects, the mean amplitude of raw GSR data increases when the intensity of physical exercise increases. Indeed, excluding the subject 4 and, partially, the subject 8, all the other individuals present values that grow with the increasing of the physical exercise intensity. This evidence can be noticed also by inspecting *Figure 27* shown below. The graph has along the abscissa axis the subjects, while along the vertical axis the mean amplitude of the raw GSR is reported.

The different colors of the bars represent different intensities of physical effort. The blue color indicates the mean GSR amplitude at resting condition, the orange bar shows the mean amplitude of raw GSR obtained after physical efforts of medium intensity, while the gray color states the mean GSR amplitude resulting from high levels of physical exercise.

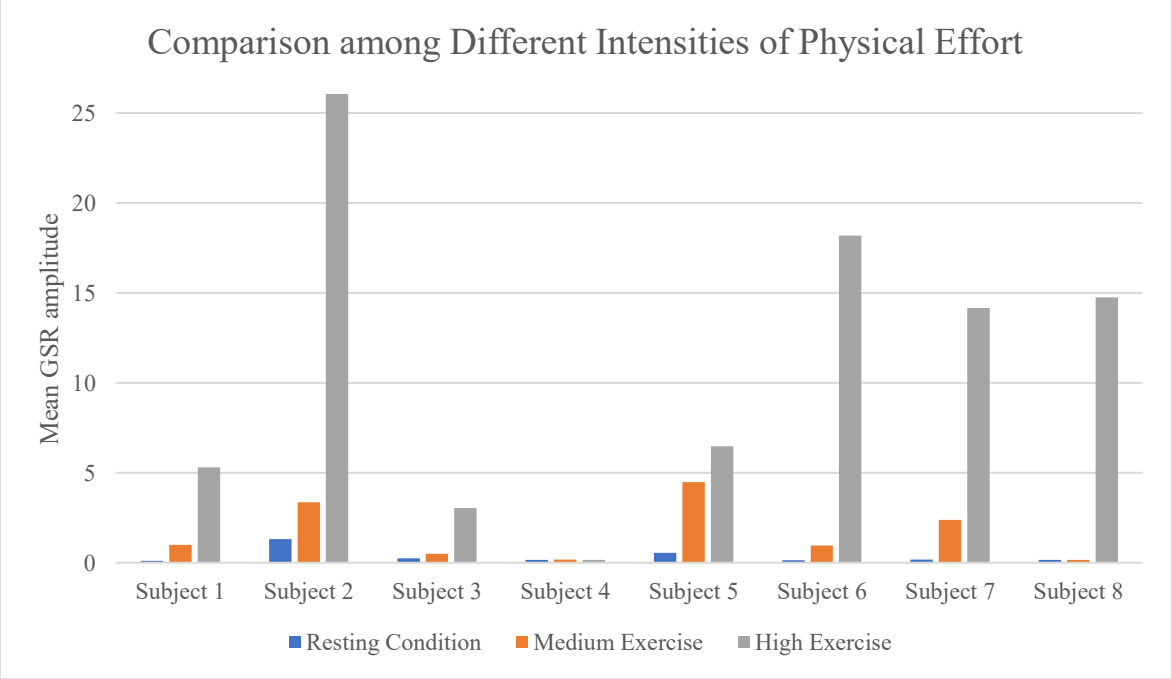

Figure 27 - Comparison of mean GSR amplitude among different levels of physical effort.

Analyzing *Figure 27*, the high variability of GSR signal acquired after physical exercises of medium and high intensity is confirmed.

4.1 **Results of the Time Domain Analysis**

GSR data was analyzed in the time domain using the algorithm proposed by the Pocket Guide [6]. It was implemented in Matlab following the sequence of steps presented in Chapter 2. In particular, such algorithm allows the identification of GSR peaks and the computation of some other parameters as the GSR peaks number, the mean of GSR raw signal and of its tonic component. Initially, the raw signal was decomposed in tonic and phasic components by using a median filter. The intervals containing peaks were identified on the phasic component by setting two thresholds. Finally, the GSR peaks were identified back to the original raw data.

The results obtained are presented below. Specifically, in the 4.1.1 sub-chapter, the number of peaks in GSR signals is compared among subjects, while in the following section GSR peaks numbers are compared among different levels of physical effort.

4.1.1 **Comparison among Subjects**

In this section, the GSR peaks number is presented making a comparison among 8 subjects performing different levels of physical exercise. GSR peaks were computed by implementing the Pocket Guide's algorithm in Matlab. Mean and standard deviation of the outcomes were computed for each subject.

The results are shown in the Figures and Tables below. In particular, *Table 5* and *Figure 28* report the number of GSR peaks detected in GSR signals acquired on each subject at resting condition for a period of 14 minutes. GSR peaks number counted in GSR data recorded on each subject after physical efforts of medium intensity is shown in *Table 7* and *Figure 29.* While *Table 9* and *Figure 30* show the number of GSR peaks identified in GSR signals resulting after subjects have performed physical exercises of high intensity. Both signals acquired after medium and high intensity physical exercise are recorded for a period of 9

minutes. Each graph has along the X-axis the subjects and along the Y-axis the number of GSR peaks computed for each signal.

Table 5 - Average and standard deviation of the number of GSR peaks computed on the GSR signal acquired at resting condition.

	Average Peaks Number	Standard Deviation
Subject 1	11.1	3.4
Subject 2	9.0	4.4
Subject 3	9.4	3.5
Subject 4	12.5	3.5
Subject 5	4.7	3.5
Subject 6	10.0	0.8
Subject 7	10.0	4.4
Subject 8	10.2	4.1

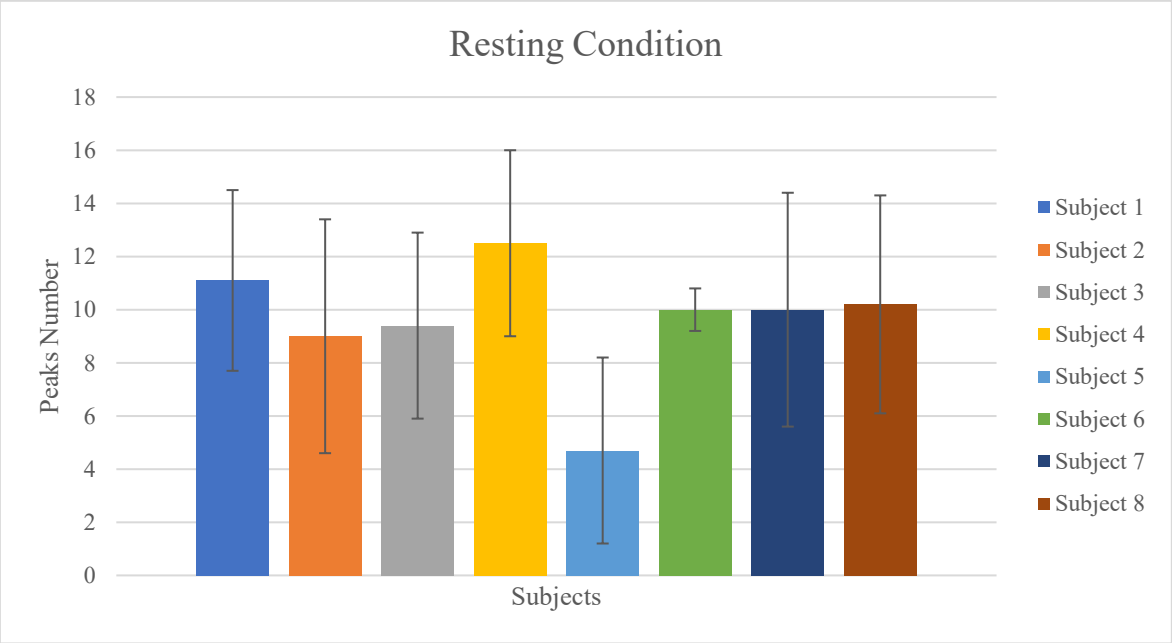

Figure 28 - Average and standard deviation of GSR peaks number computed for each subject, when they are not subjected to physical stimulation.

Looking at the results shown in *Table 5* and *Figure 28*, it is possible to notice that the lowest mean GSR peaks number is 4.7, related to the subject 5, while the highest one is obtained from subject 4, resulting in an average of number of peaks equal to 12.5. The highest standard deviation is equal to 4.4, corresponding to the subject 2 and subject 7, while the lowest is equal to 0.8, computed on the acquisitions performed on subject 6. However, except for the fifth subject, all the other subjects show a comparable number of GSR peaks. Indeed, computing the average peaks number among all the subjects and their standard deviation the values obtained are the ones presented in *Table 6*.

Table 6 - Average and standard deviation of the number of GSR peaks among all subjects, at resting condition.

	Average Peaks Number	**Standard Deviation**
All Subjects	9.6	2.2

Table 7 - Average and standard deviation of the number of GSR peaks computed on the GSR signal acquired after physical exercise of medium intensity.

	Average Peaks Number	**Standard Deviation**
Subject 1	18.6	16.4
Subject 2	16.5	6.4
Subject 3	11.7	12.0
Subject 4	7.0	2.8
Subject 5	31.0	41.0
Subject 6	16.3	21.8
Subject 7	54.0	9.6
Subject 8	6.0	1.7

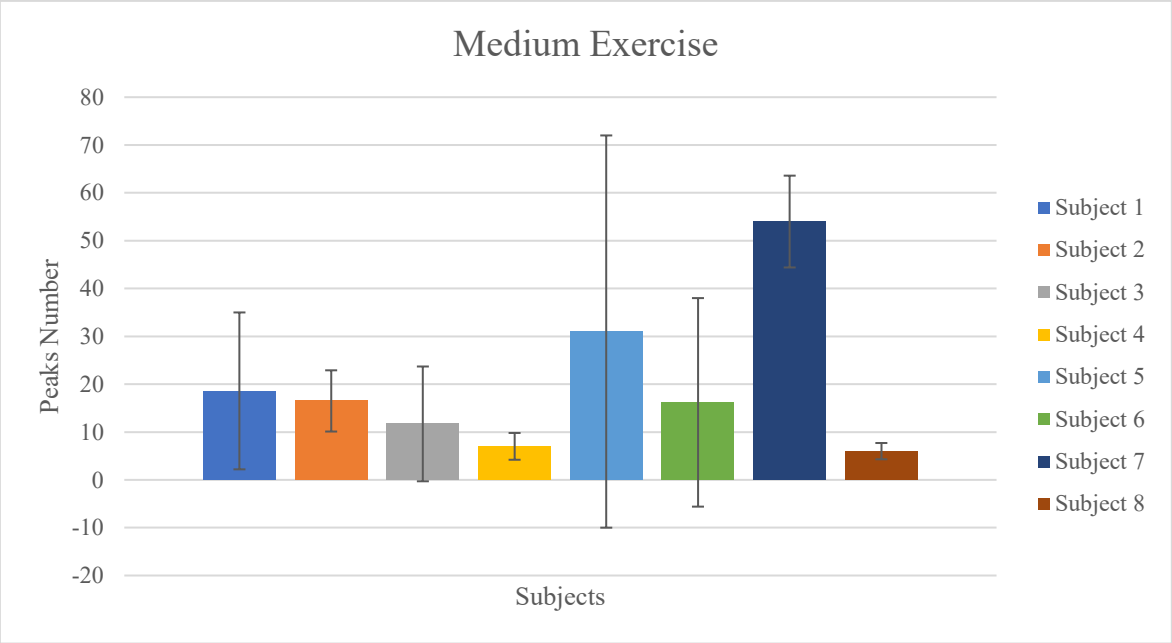

Figure 29 - Average and standard deviation of GSR peaks number computed for each subject, after they are subjected to physical exercises of medium intensity.

Table 7 and the corresponding *Figure 29* display the GSR peaks number calculated on each subject after they have performed physical activity of medium intensity. The obtained average peaks number and the related standard deviation show high variability as already mentioned in the introduction of the current chapter. Indeed, on the subject 7, a very high number of peaks (i.e. 54) is recorded while the lowest peaks number is recorded on the eighth subject, who presents just 6 peaks. The high variability is highlighted also by the high values of standard deviation obtained especially by the subjects 5 and 6. The considerations made are confirmed by *Table 5* that shows the average number of GSR peaks computed among all subjects after these have performed physical efforts of medium intensity.

Table 8 - Average and standard deviation of the number of GSR peaks among all subjects, acquired after physical activity of medium intensity.

	Average Peaks Number	**Standard Deviation**
All Subjects	20.1	15.8

Table 9 - Average and standard deviation of the number of GSR peaks computed on the GSR signal acquired after physical exercise of high intensity.

	Average Peaks Number	Standard Deviation
Subject 1	71.2	37.0
Subject 2	140.0	18.4
Subject 3	58.8	22.2
Subject 4	12.0	0
Subject 5	67.5	31.8
Subject 6	115.5	9.2
Subject 7	115.0	21.2
Subject 8	104.5	81.3

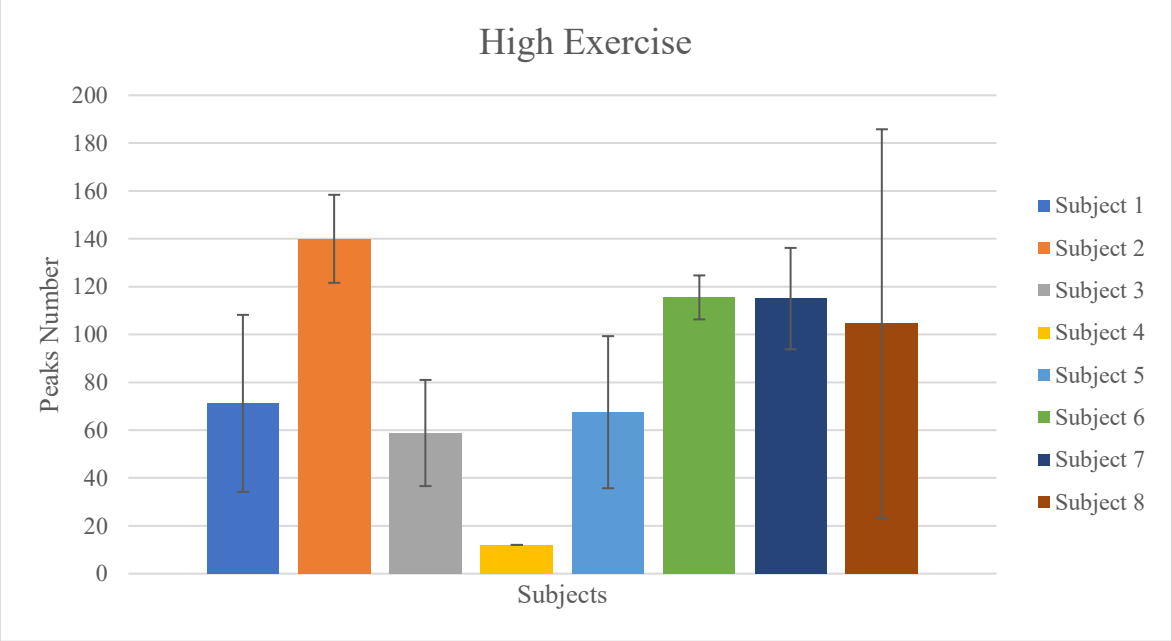

Figure 30 - Average and standard deviation of GSR peaks number computed for each subject, after they are subjected to physical exercises of high intensity.

Analyzing results presented in *Table 9* and *Figure 30*, similarly to the results obtained performing physical efforts of medium intensity and how highlighted in the introductive section of the current chapter, it is possible to notice that GSR peaks number average and standard deviation show very high inter-subject and intra-subject variability. Indeed, on the subject 4, just 12 peaks are recorded, while the highest number is obtained by the subject 2 who presents an average peaks number equal to 140. The high intra-subject variability is confirmed by the analysis of the standard deviation. The lowest standard deviation is equal to 0 while the highest is equivalent to 81.3. The high variability among subjects is confirmed, as in the other cases, calculating the average of GSR peaks number among subjects and computing the corresponding standard deviation. The values obtained are shown in *Table 10*.

Table 10 - Average and standard deviation of the number of GSR peaks among all subjects, acquired after physical activity of high intensity.

	Average Peaks Number	**Standard Deviation**
All Subjects	85.6	41.0

4.1.2 **Comparison among Different Intensities of Physical Efforts**

In this section, the number of GSR peaks resulting from different intensities of physical effort are compared. As detailed above, the acquisitions at resting condition have a duration of 14 minutes, while the ones recorded after medium and high physical stimulation last 9 minutes. Therefore, in order to rightly compare results obtained from different intensities of physical effort, the *GSR peaks number per minute* metric was computed. For each session of acquisition of each subject the number of GSR peaks per minute was computed, and the results obtained for each session were averaged in order to obtain a single value for each subject.

Table 11 and *Figure 31* show the number of GSR peaks per minute for each subject related to the kind of physical activity that he/she has performed. The graph has the subjects along the X-axis, while the Y-axis reports the GSR peaks number per minute values. The different bars colors represent the different levels of physical activity. The blue color indicates the resting condition, the orange bar shows the results for medium intensity physical effort, while the gray color corresponds to high levels of physical exercise.

Table 11 - Average number of GSR peaks per minute of each subject at resting condition and after medium and high intensity physical efforts.

	Resting Condition (peaks/minute)	**Medium Exercise (peaks/minute)**	**High Exercise (peaks/minute)**
Subject 1	0.8	2.1	7.9
Subject 2	0.7	1.8	15.5
Subject 3	0.6	1.3	6.5
Subject 4	0.9	0.7	1.3
Subject 5	0.4	3.4	7.5
Subject 6	0.7	1.8	12.8
Subject 7	0.7	6.0	12.7
Subject 8	0.7	0.7	11.6

Looking at the results shown in *Table 11* and in the following Figure (*Figure 31*), it is possible to notice that, generally, the number of GSR peaks per minute grows with the increase of the intensity of physical effort. In particular, with the exception of the fourth subject, all the individuals show at resting condition a much lower number of peaks per minute with respect to the one obtained from the analysis of the signals acquired after high level of physical exercise. The number of GSR peaks per minute computed on signals recorded after medium intensity exercise is more variable. Indeed, passing from GSR signals acquired at rest and GSR data recorded after medium exercise, in many subjects an evident increase of the peaks number per minute does not emerge.

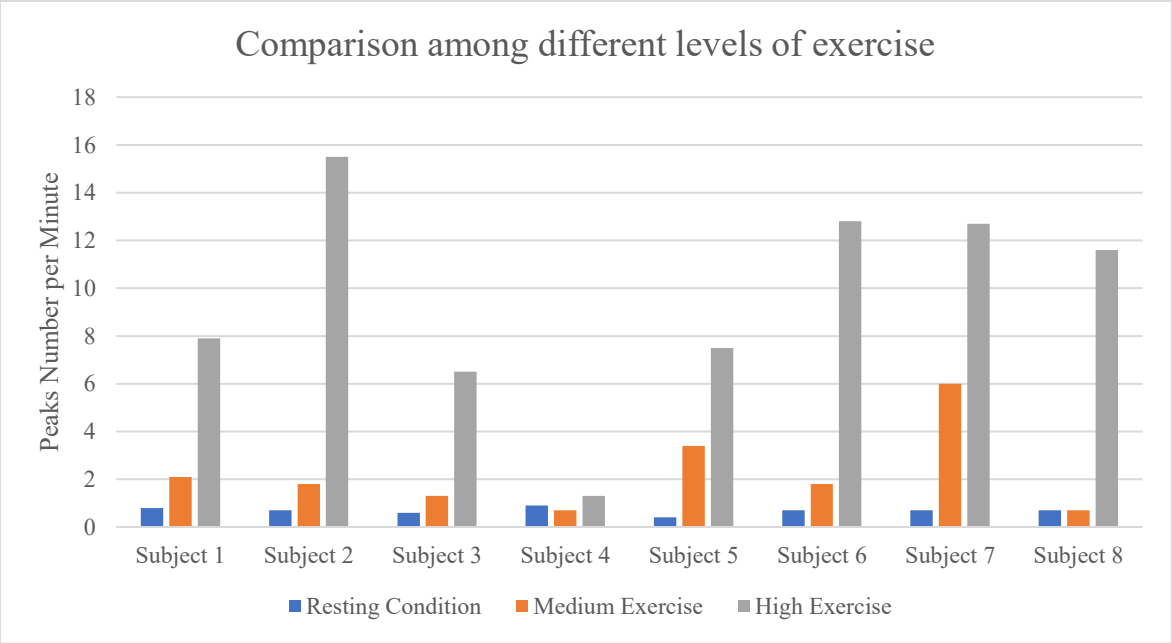

Figure 31 - Comparison among different intensities of physical efforts for each subject.

4.2 **Results of the Frequency Domain Analysis**

The analysis of GSR signals in the time domain provides a lot of physiological information. However, as shown in the previous section, GSR signals have high variability between subjects, especially when they are submitted to physical stimuli of medium and high intensity. For this reason, it was thought to analyze the GSR data in the frequency domain as already done by some researchers starting from 2016 [13][15][16]. To this end, the PSD of the raw GSR signals was computed. Specifically, the absolute value of the GSR signal FFT was calculated and then, by implementing the PSD definition on Matlab, also this parameter was computed. PSD was expressed in logarithmic scale. Then, in order to assess the spectral content of specific frequency bands of the GSR signal, the AUC of the PSD was computed. In particular, the spectral power contained in the frequency ranges 0-0.25 Hz and 0.045-0.25 Hz was computed and the results were compared with the spectral content of the entire frequency band, corresponding to 0-0.4 Hz.

The values resulting from this analysis are shown in the following sections. In particular, in the first sub-chapter, the AUCs computed for the PSD are compared among subjects for each level of physical activity, while in the sub-chapter 4.2.2 results are compared among different intensities of physical effort.

4.2.1 **Comparison among Subjects**

The results obtained from the analysis on the frequency domain are shown below making a comparison among 8 subjects performing physical efforts of different intensities. The percentages presented in this section were calculated comparing the AUC of PSD signal contained in the range 0-0.25 Hz with the AUC of PSD signal included in the entire frequency band (i.e. 0-0.4 Hz). Specifically, the PSD percentage values were calculated by dividing the PSD AUC in the range 0-0.25 Hz by the PSD AUC in the full range 0-0.4 Hz, the result was, then, expressed in percentage. Results were averaged for each subject and the standard deviation was computed in order to obtain a single value per subject.

In the following Figures and Tables, PSD percentages and standard deviations are presented. Specifically, *Table 12* and *Figure 32* show results obtained for each subject at resting condition. In *Table 14* and *Figure 33*, values resulting from the analysis of GSR data acquired after medium physical stimulation are presented. While *Table 16* and *Figure 34* contain results obtained from the frequency domain analysis of signals recorded after physical efforts of high intensity.

Graphs have the subjects along the abscissa, and along the vertical axis they show the PSD percentage values calculated as the ratio of the PSD AUC in the range 0-0.25 Hz over the PSD AUC in the full range 0-0.4 Hz.

Table 12 - Average and standard deviation of the percent GSR PSD AUC values for each subject at resting condition.

	Average Percentage	Standard Deviation
Subject 1	60.4 %	1.3
Subject 2	55.4 %	3.6
Subject 3	59.3 %	0.9
Subject 4	59.9 %	2.2
Subject 5	55.9 %	1.7
Subject 6	61.0 %	1.9
Subject 7	59.0 %	1.1
Subject 8	58.8 %	1.4

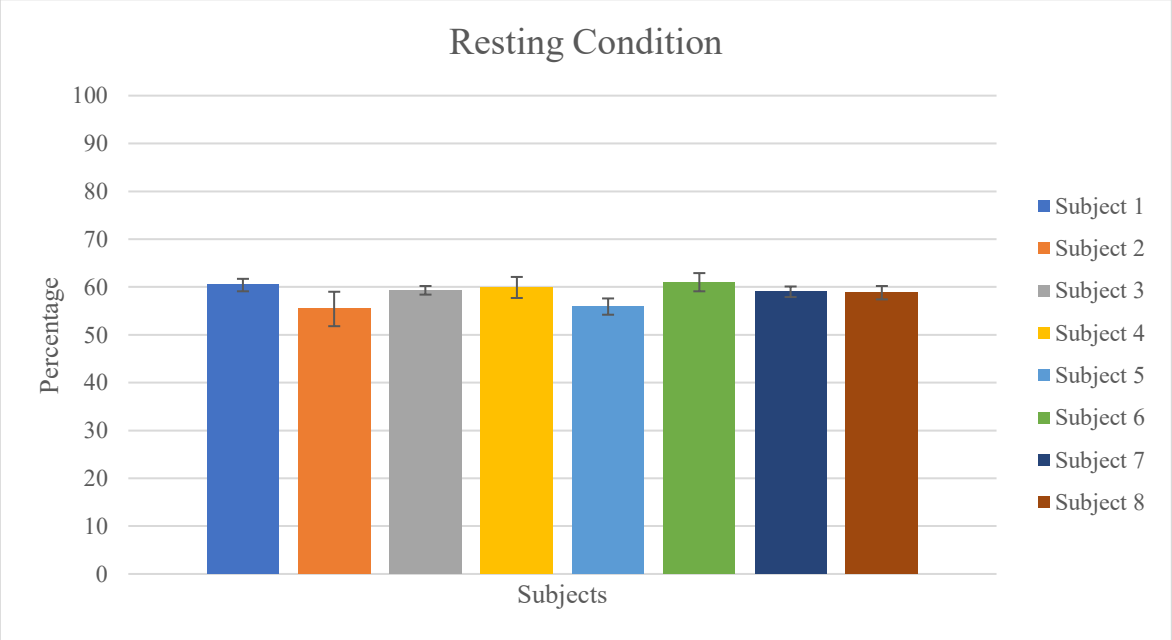

Figure 32 - Average and standard deviation of the percent GSR PSD AUC values for each subject at resting condition.

Looking at the results shown in *Table 12* and *Figure 32*, it possible to notice that about sixty percent of the spectral content is contained in the frequency range of interest (i.e. 0-0.25 Hz) for each subject. Results obtained for each subject present a very low variability. This is confirmed by the following Table (*Table 13*), which contains the average of the percentages over all the subjects and its standard deviation.

Table 13 - Average and standard deviation of the percent GSR PSD AUC values over all subjects acquired at resting condition.

	Average Percentage	**Standard Deviation**
All Subjects	58.7 %	2.0

Table 14 - Average and standard deviation of the percent GSR PSD AUC values for each subject after physical efforts of medium intensity.

	Average Percentage	**Standard Deviation**
Subject 1	54.5 %	3.3
Subject 2	50.2 %	1.3
Subject 3	58.1 %	2.6
Subject 4	57.7 %	0.8
Subject 5	53.2 %	8.3
Subject 6	52.9 %	3.4
Subject 7	52.9 %	0.7
Subject 8	58.6 %	2.9

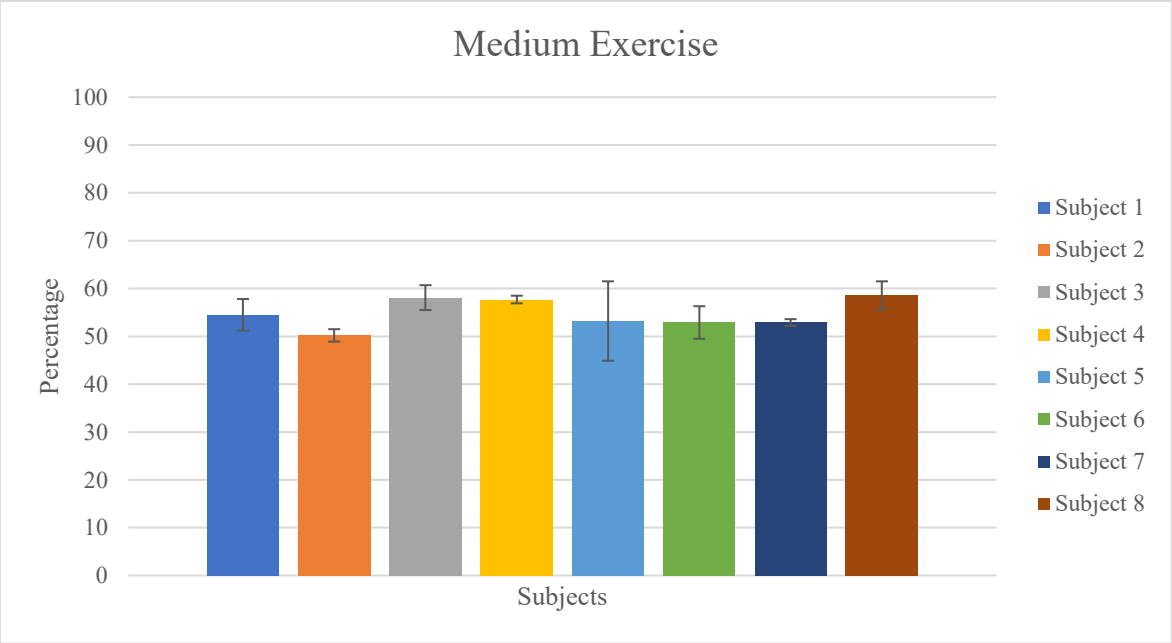

Figure 33 - Average and standard deviation of the percent GSR PSD AUC values for each subject after medium intensity exercise.

Percentages presented in *Table 14* and *Figure 33* show lower values than the results obtained analyzing signals acquired at resting condition, however, these values are even higher than fifty percent. Percentage values range from 50.2 for the 2nd subject to 58.6 for the subject no. 8; the maximum standard deviation was found on subject 5 and it is equal to 8.3. Evaluating these results, it possible to notice that they are not highly variable, as confirmed by the following Table (*Table 15*). *Table 15* presents the mean percentage GSR PSD AUC over all subjects and its standard deviation, after they perform physical activity of medium intensity.

Table 15 - Average and standard deviation of the percent GSR PSD AUC values over all subjects acquired after physical efforts of medium intensity.

	Average Percentage	**Standard Deviation**
All Subjects	54.8 %	3.0

Table 16 - Average and standard deviation of the percent GSR PSD AUC values for each subject after physical efforts of high intensity.

	Average Percentage	Standard Deviation
Subject 1	48.8 %	1.9
Subject 2	48.6 %	0.1
Subject 3	49.6 %	3.0
Subject 4	58.0 %	3.9
Subject 5	49.6 %	0.5
Subject 6	50.6 %	4.1
Subject 7	49.0 %	0.9
Subject 8	50.7 %	2.8

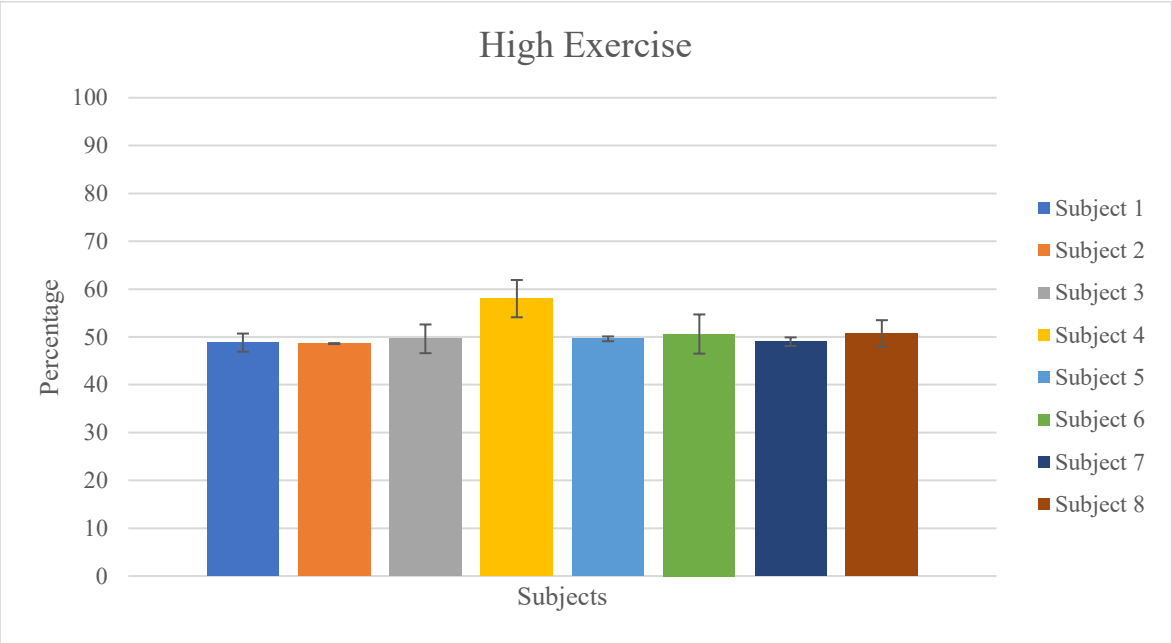

Figure 34 - Average and standard deviation of the percent GSR PSD AUC values for each subject after high intensity exercise.

By evaluating the results presented in *Table 16* and *Figure 34*, it is evident that all the subjects show a comparable behavior. Whit the exception of subject 4, presenting a

percentage value of about ten percentage points above the others, the percentage of any other individual is included between 48.8 and 50.7. These values are about ten percent lower than the ones obtained analyzing signal acquired at resting condition and about four percent lower than percentages computed on data recorded after medium level exercise. These considerations are confirmed by *Table 17* that shows the percentage mean value and relating standard deviation of all the subjects submitted to physical efforts of high intensity.

Table 17 - Average and standard deviation of the percent GSR PSD AUC values over all subjects acquired after physical efforts of high intensity.

	Average Percentage	**Standard Deviation**
All Subjects	50.6 %	3.1

4.2.2 **Comparison among Different Intensities of Physical Efforts**

In this section, the percentages obtained considering the AUC of GSR PSD in the range 0-0.25 Hz and the AUC of GSR PSD in the range 0-0.4 Hz are compared in relation to different intensity of physical activity. For each session of acquisition of each subject, the percentage was computed, the result obtained from each session were averaged in order to obtain a single value for each subject.

Table 18 and *Figure 35* show the percentage AUC of GSR PSD for each subject, related to the kind of physical activity that participants have performed. The graph has in the X-axis the subjects, while in the Y-axis the percentage values.

Bars of various colors represent different levels of physical activity. The blue color indicates signals acquired at resting condition, the orange bar shows results obtained on GSR data acquired after physical efforts of medium intensity, while the gray color states the percentages resulting from high level physical exercises.

Table 18 - Average percent AUC of GSR PSD for each subject at resting condition and after medium and high intensity physical effort.

	Resting Condition	Medium Exercise	High Exercise
Subject 1	60.4 %	54.5 %	48.8 %
Subject 2	55.4 %	50.2 %	48.6 %
Subject 3	59.3 %	58.1 %	49.6 %
Subject 4	59.9 %	57.7 %	58.0 %
Subject 5	55.9 %	53.2 %	49.6 %
Subject 6	61.0 %	52.9 %	50.6 %
Subject 7	59.0 %	52.9 %	49.0 %
Subject 8	58.8 %	58.6 %	50.7 %

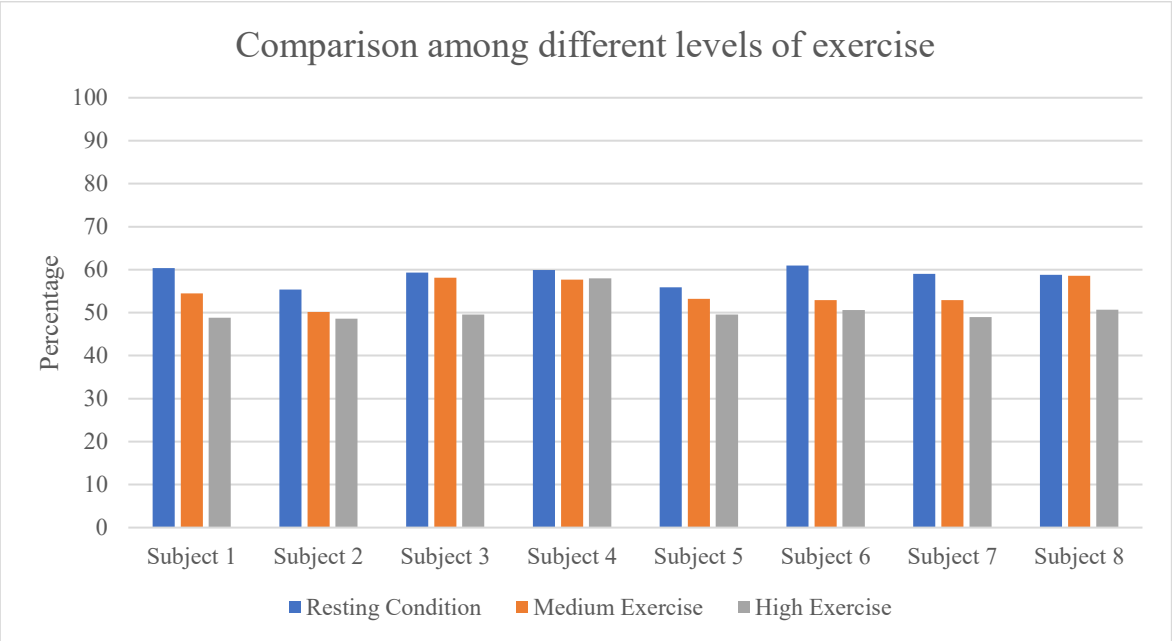

Figure 35 - Comparison among different intensities of physical efforts for each subject.

Examining the results presented in *Table 18* and *Figure 35*, it is evident that, generally, the amount of spectral power contained in the rage 0-0.25 Hz decreases with the increase of the

intensity of physical activity. Specifically, except the fourth and eighth subjects, all the participants present a higher percentage of the power spectrum in the considered range at resting condition, while this percentage is lower analyzing data acquired after physical exercise of medium intensity, and even lower examining results obtained from signals recorded after high level of physical effort.

4.2.3 **Comparison among Different Frequency Bands**

Recently, several researchers have analyzed GSR signals in the frequency domain. These studies have shown that the bulk of GSR's spectral power is usually contained in the range 0 to 0.25 Hz and, in particular, most of it is confined in the frequency band 0.045-0.25 Hz for all subjects [13][15][16]. In order to verify whether our findings are similar to the ones exposed in the previous researches, the percentage of PSD contained in the range of frequencies 0.045-0.25 Hz was compared to the one present in the frequency band 0-0.25 Hz.

The results are presented in this section and, in particular, *Table 19*, *Figure 36*, *Figure 37* and *Figure 38* show the percentages for each range computed by analyzing GSR signals acquired at resting condition and after medium and high level of physical exercise. The values found for each subject were averaged in order to get a percentage for each level of physical activity and for each range.

Figures present three colored circles, the yellow one represents the percentage of power spectral contained in the range 0-0.4 Hz, PSD percentage included in the frequency band 0-0.25 Hz is represented by the blue color, the orange states the spectral content in percentage contained in the range of frequencies 0.045 to 0.25 Hz.

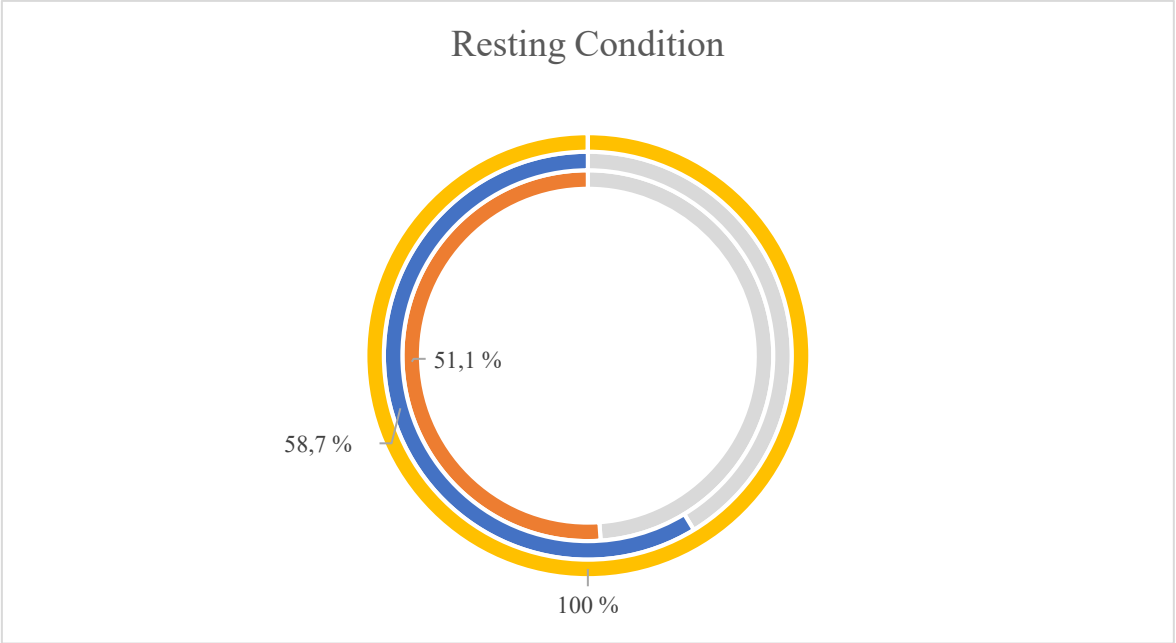

Figure 36 - PSD percentage contained in different frequency ranges at resting condition.

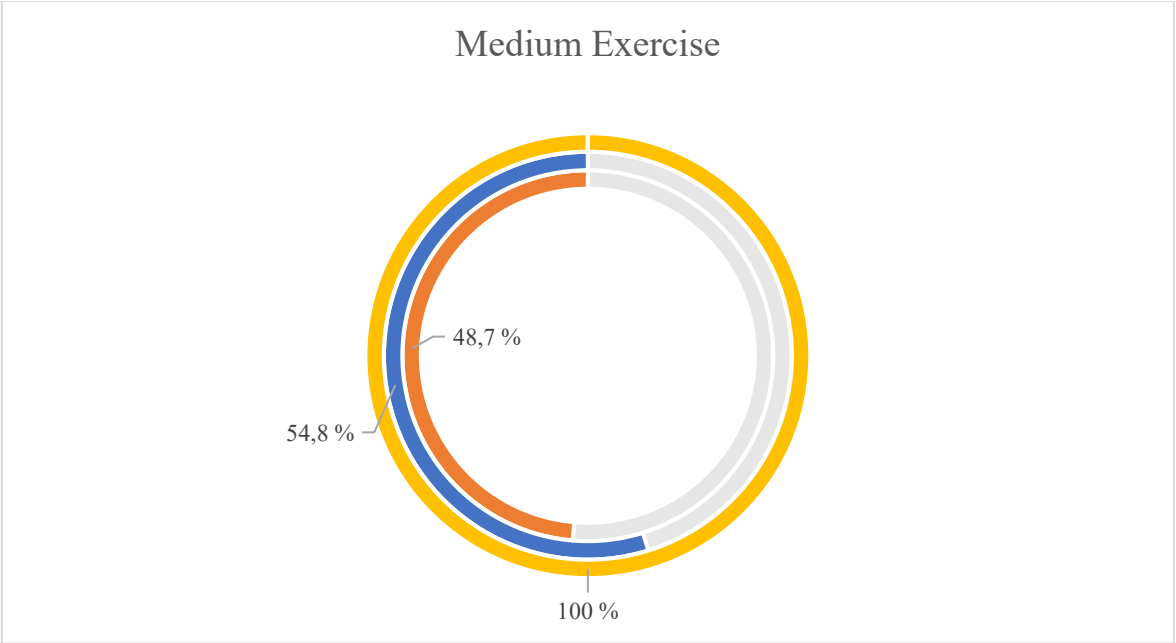

Figure 37 - PSD percentage contained in different frequency ranges of signals acquired after exercise of medium intensity.

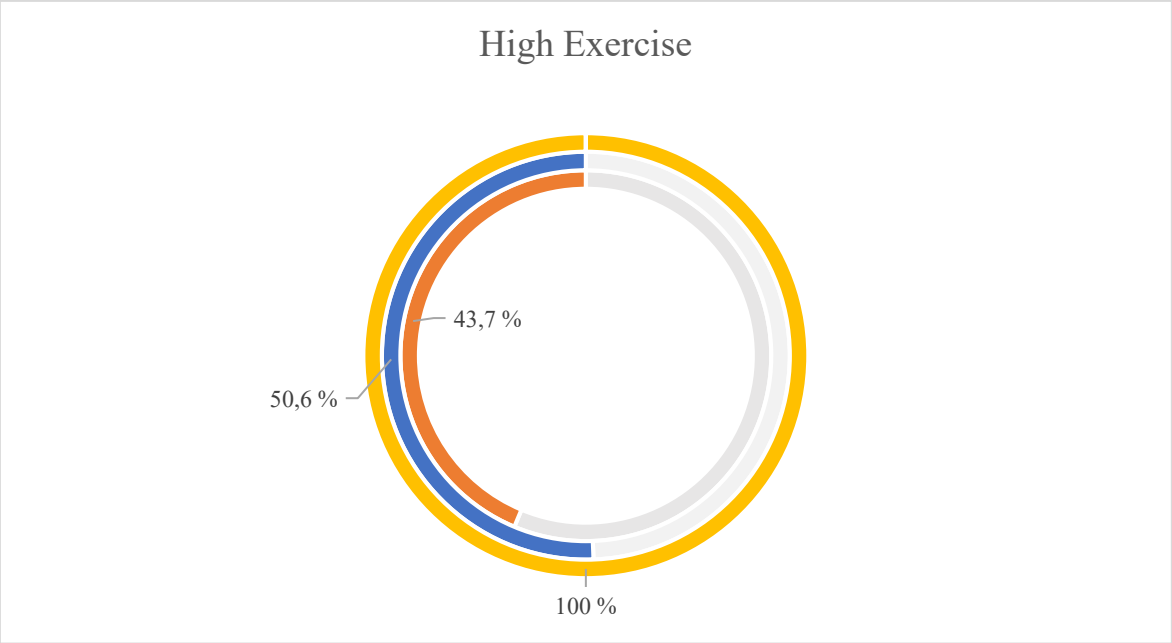

Figure 38 - PSD percentage contained in different frequency ranges of signals acquired after exercise of high intensity.

Table 19 - Average percent PSD contained in different frequency ranges computed on signals acquired at resting condition and after physical exercise of various intensities.

	Resting Condition	**Medium Exercise**	**High Exercise**
Range 0.045-0.25 Hz	51.1 %	48.7 %	43.7 %
Range 0-0.25 Hz	58.7 %	54.8 %	50.6 %

Looking at the results presented on the Figures and Table above, it is possible to notice that more than fifty percent of PSD is contained in the frequency band 0-0.25 Hz for each level of physical stimulation. In addition, more than forty percent of the total PSD is between the frequencies 0.045-0.25 Hz, for all kinds of physical activity.

As shown in *Table 20*, almost ninety percent of the PSD included in the range of frequencies 0 to 0.25 Hz is contained in the range 0.045-0.25 Hz.

Table 20 - Percentage of PSD contained in the range 0.045-0.25 Hz with respect to the one included in the range 0-0.25 Hz.

	Resting Condition	**Medium Exercise**	**High Exercise**
Range 0.045-0.25 Hz over Range 0-0.25 Hz	87.0 %	88.9 %	86.4 %

Chapter 5
Auditory Stimuli Test Results

Results obtained from the analysis of GSR signals acquired while listening to acoustic sounds are presented in this section. Data were recorded on two males and five females aged from 15 to 59 years by using the E4 wristband. Each participant was subjected to six sessions of acquisition during which a pleasant, neutral or unpleasant sound was played through the use of a Bluetooth speaker. Then, collected GSR signals were processed in the time domain using an algorithm implemented in Matlab, described in Chapter 2. For each acquired signal some GSR parameters such as the number of peaks were calculated, in order to understand if acoustic sounds of different duration and valence scores produce different changes of the GSR data. Finally, at the end of each session of acquisition, subjects were asked to rate the emotions evoked by the listened stimuli by using the valence, arousal and dominance dimensions of the SAM scale.

By analyzing the raw GSR data just visually, it is not possible to identify evident differences among signals acquired while listening to pleasant sounds, neutral sounds, and unpleasant sounds, as shown in the following Figures. Specifically, the first Figure (*Figure 39*) shows the raw GSR signal acquired during the listening of a pleasant sound, GSR data recorded while listening a neutral sound are represented in the *Figure 40*, while the last Figure (*Figure 41*) presents the raw signals resulting from the listening of an unpleasant sound.

All the Matlab plots have samples along the X-axis and GSR amplitude expressed in μS along the Y-axis. Moreover, in each plot, two vertical lines may be identified. They indicate the sound's instant of beginning and end. Indeed, during this experimental test, the acquisition's period was divided into three main phases. GSR data was acquired for the first five minutes in the absence of any stimuli, while listening to acoustic stimuli for the following one or two minutes, and, finally, for a duration of other five minutes, at resting condition and no stimulation.

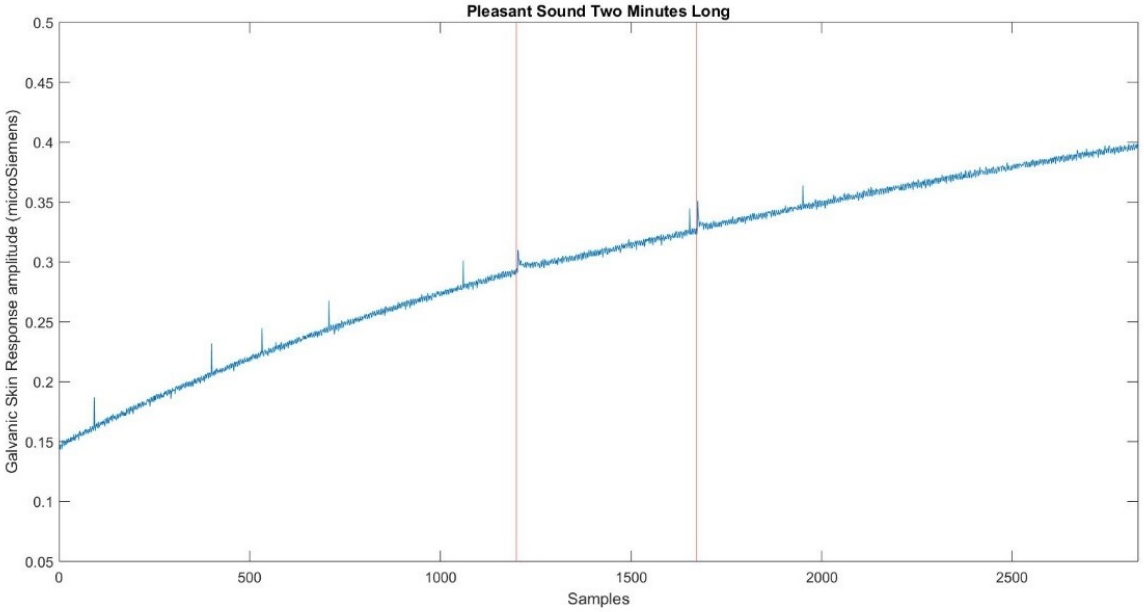

Figure 39 - An example of GSR signal acquired before, during and after the acquisition of a pleasant sound two minutes long.

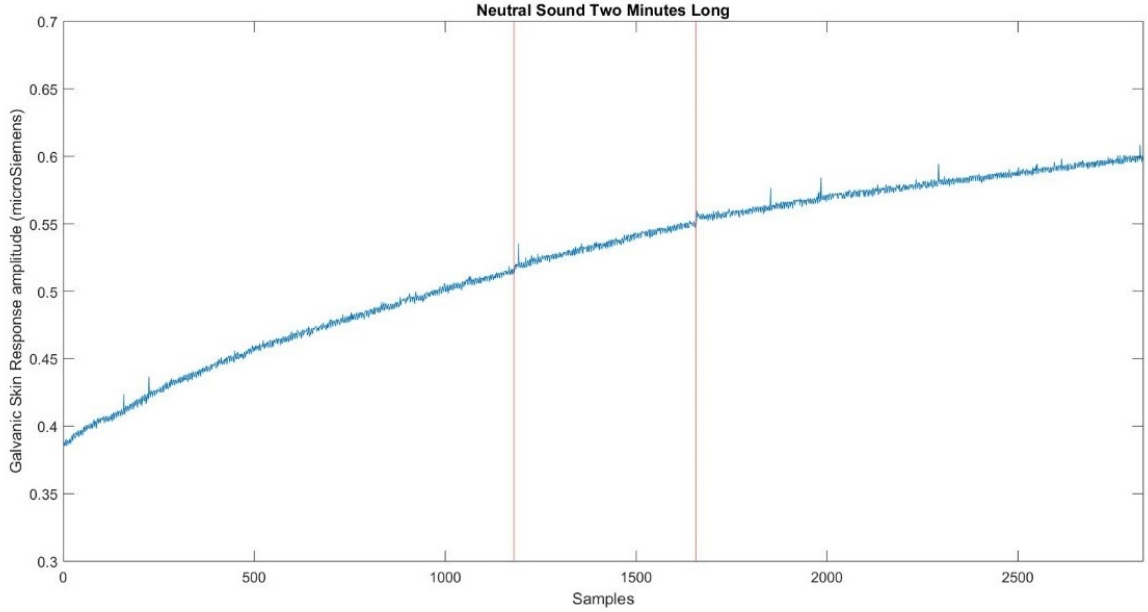

Figure 40 - An example of GSR signal acquired before, during and after the acquisition of a neutral sound two minutes long.

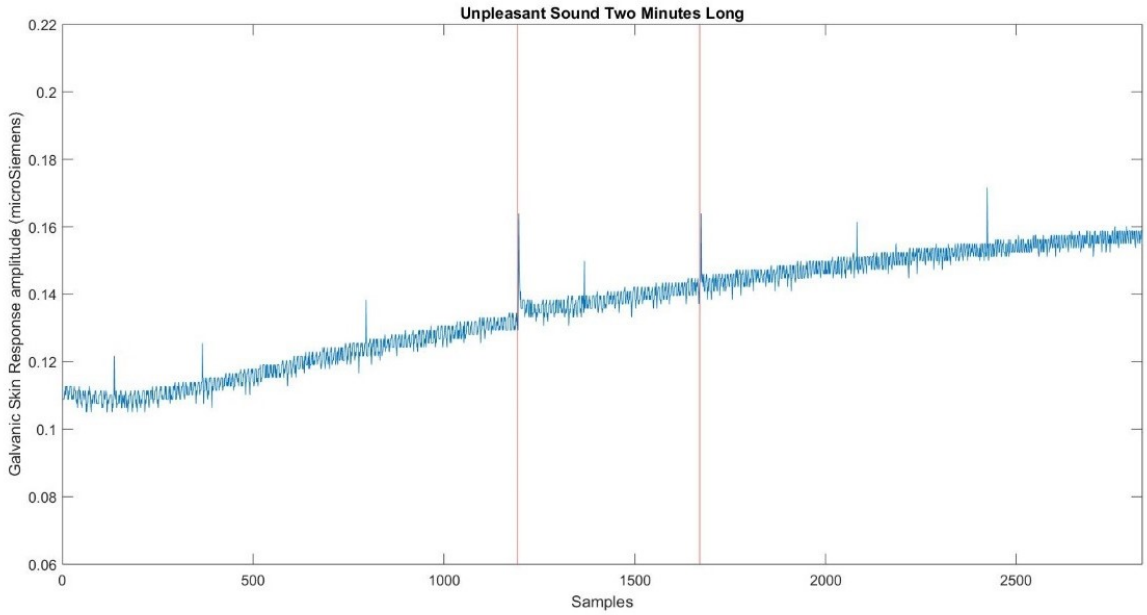

Figure 41 - An example of GSR signal acquired before, during and after the acquisition of an unpleasant sound two minutes long.

By examining the Figures above, these appear very similar. Indeed, the trend of the GSR signal recorded during the listening of pleasant, neutral and unpleasant sounds does not seem to suffer deviations from the baseline. The amplitude of the GSR signal is very low and quite constant during the whole length of the signal. However, some GSR curves show a slight deflection in close proximity to the beginning and end of the acoustic stimulation as in *Figure 41*.

5.1 **Results of the Time Domain Analysis**

GSR signals acquired during the listening of acoustic stimuli were analyzed in the time domain applying the algorithm proposed by the Pocket Guide [6]. The algorithm was implemented in Matlab in order to detect and count the GSR peaks, as explained in Chapter 2. Specifically, the original GSR signal was decomposed in tonic and phasic components by

using a median filter. On the phasic component, the intervals containing GSR peaks were identified by using two thresholds. Then, back to the original signal, the GSR peaks were detected and counted. In the following sections, the number of GSR peaks resulting from this analysis are described in detail.

5.1.1 **Comparison among Subjects**

In this section, the results obtained are presented by making a comparison among 7 subjects. Pocket Guide's algorithm was implemented in Matlab in order to compute the peaks number for each GSR signal. Each session of acquisition is composed by three phases of different duration as explained in Chapter 3. For this reason, the peaks number per minute was computed for each phase in order to understand if the peaks frequency during the time of listening is higher, lower or the same than the rate of GSR peaks calculated in the absence of acoustic stimuli. Each subject has listened to the same audio track two times. The first time, the sound was reproduced for one minute, while the second one, it lasted two minutes. In this section, results obtained from both the acquisitions are presented. In the specific, the results obtained from the shortest acquisition are shown before. Then, the GSR peaks rate computed during the longest session of recording is presented. The Figures below show the GSR peaks rate for each acquisition phase. For each subject, the orange bar represents the peaks frequency in the first five minutes of acquisition (i.e. in the absence of sound stimuli), the yellow bar in the middle indicates the rate of GSR peaks in the period of auditory stimulation, while the green bar states the number of peaks per minute computed on the five minutes of acquisition following the end of the sound. *Table 21* and *Figure 42* show the frequency of GSR peaks on the signal acquired before, during and after the listening of a one-minute-long pleasant sound. The rate of peaks of the signal recorded while listening to a one-minute-long neutral sound and during the five minutes before and after is reported in *Table 22* and *Figure 43*. Finally, *Table 23* and *Figure 44* show the results obtained from the analysis of a GSR signal acquired before, during and after the listening of an unpleasant sound lasting one minute. Each graph has along the X-axis the subjects and along the Y-axis the number of GSR peaks per minute.

Table 21 - Number of peaks per minute recorded on a signal acquired during the listening of a one-minute-long pleasant sound for each subject.

	Peaks per Minute (0-5 minutes)	Peaks per Minute (5-6 minutes)	Peaks per Minute (7-11 minutes)
Subject 1	0.6	0	0.4
Subject 2	1.0	0	0.8
Subject 3	0.4	2.0	0.8
Subject 4	0	1.0	0.8
Subject 5	0.2	2.0	0.6
Subject 6	1.0	1.0	0.8
Subject 7	0.8	0	0.6

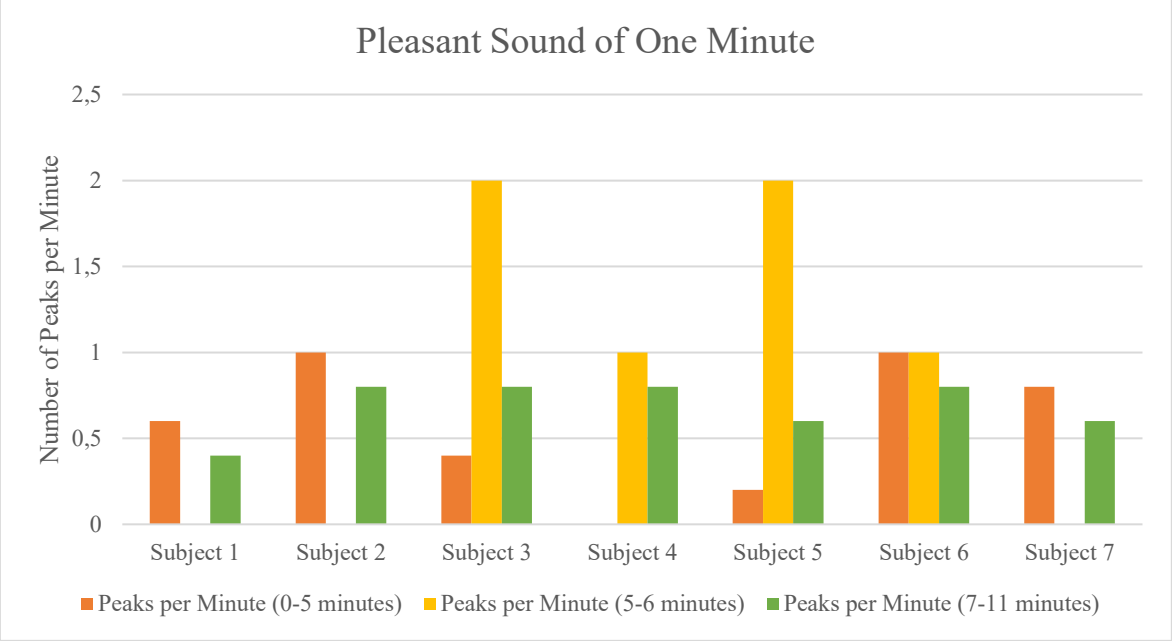

Figure 42 - Number of peaks per minute recorded on a signal acquired during the listening of a one-minute-long pleasant sound for each subject.

The listening of a pleasant sound one-minute-long does not produce the same effect on all subjects as shown in *Table 21* and *Figure 42*. Indeed, by analyzing the results obtained from the subjects 3, 4 and 5, it possible to notice that these subjects present an increase of the number of GSR peaks per minute when they are subjected to neutral acoustic stimuli, while the remaining subjects show a decrease or constant rate of GSR peaks.

Table 22 - Number of peaks per minute recorded on a signal acquired during the listening of a one-minute-long neutral sound.

	Peaks per Minute (0-5 minutes)	Peaks per Minute (5-6 minutes)	Peaks per Minute (7-11 minutes)
Subject 1	0.2	2.0	0.6
Subject 2	1.2	0	0.6
Subject 3	0.6	1.0	0.6
Subject 4	1.2	0	0.8
Subject 5	0.2	0	0.8
Subject 6	0.4	1.0	1.2
Subject 7	0.6	0	1.2

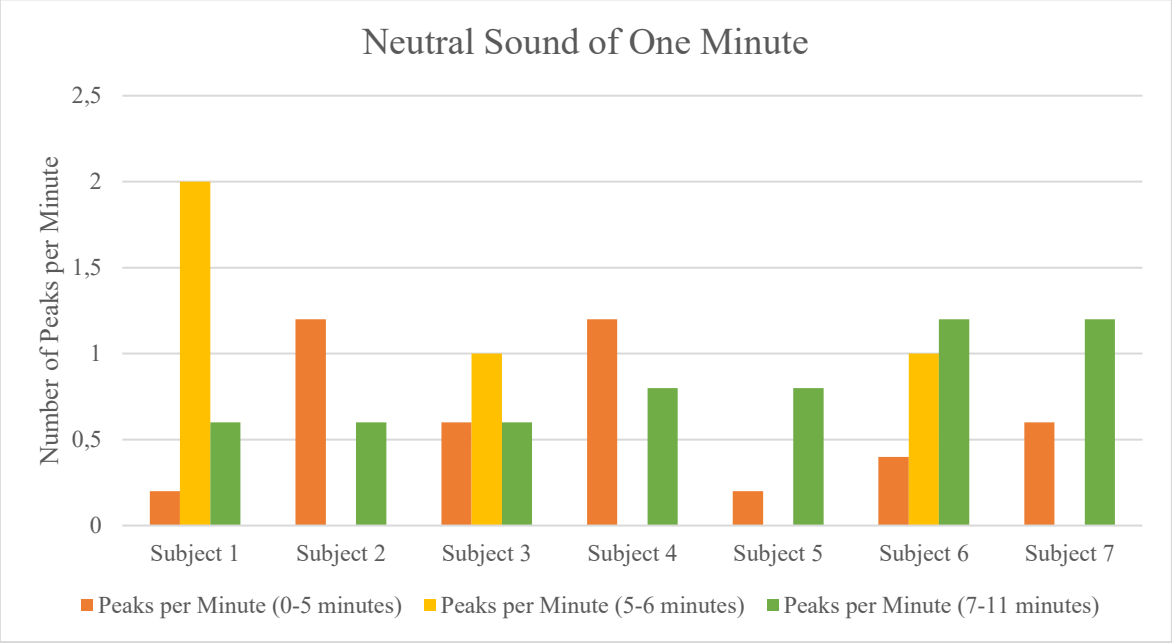

Figure 43 - Number of peaks per minute recorded on a signal acquired during the listening of a one-minute-long neutral sound for each subject.

By analyzing the results shown in *Table 22* and *Figure 43*, it possible to notice that there is not a precise correlation between one-minute-long neutral acoustic stimuli and the rate of GSR peaks. Indeed, some subjects such as the first, the third and the sixth present an increase of the GSR peaks frequency during the listening of the neutral sound with respect to the

peaks rate of the first five minutes of acquisition, while other subjects show no peak at all during the period of listening.

Table 23 - Number of peaks per minute recorded on a signal acquired during the listening of a one-minute-long unpleasant sound.

	Peaks per Minute (0-5 minutes)	Peaks per Minute (5-6 minutes)	Peaks per Minute (7-11 minutes)
Subject 1	0.4	1.0	1.0
Subject 2	0.6	2.0	0.6
Subject 3	0.8	0	0.4
Subject 4	1.0	1.0	0.8
Subject 5	0.4	2.0	0.8
Subject 6	1.2	3.0	0.8
Subject 7	0.8	4.0	0.6

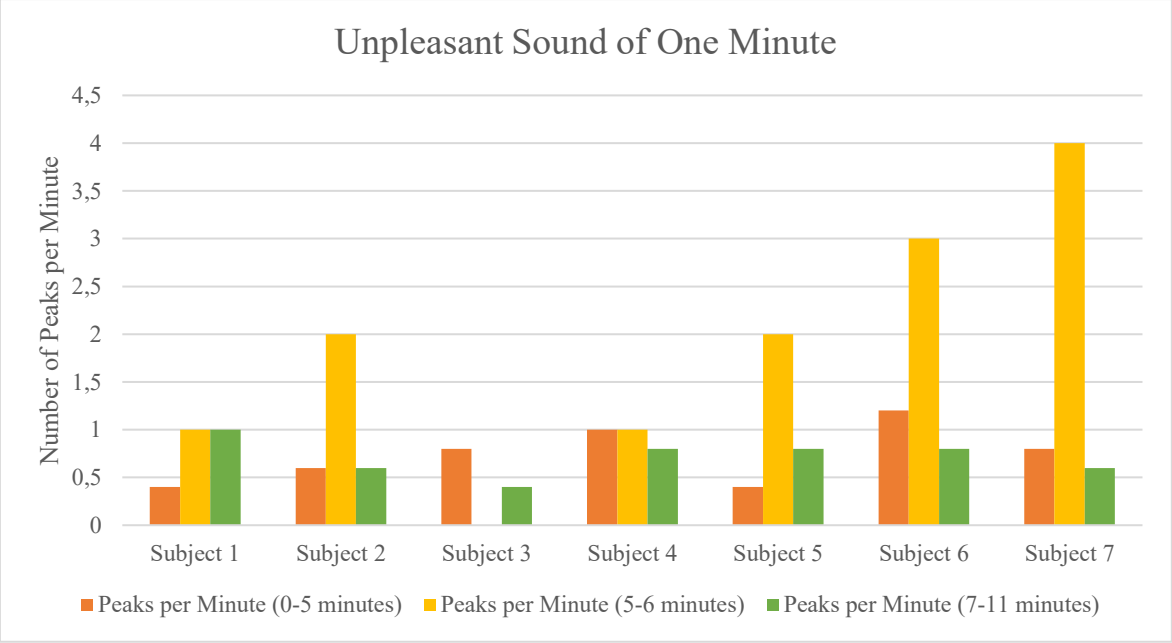

Figure 44 - Number of peaks per minute recorded on a signal acquired during the listening of a one-minute-long unpleasant sound for each subject.

Table 23 and Figure 44 show an evident increase of GSR peaks frequency during the listening of a one-minute-long unpleasant sound for the subjects 2, 5, 6 and 7. Subject 1 presents an increase in the peaks number per minute during the listening and, the increase remains constant after the end of the sound. The subject 3 and 4 seem to not suffer the effect of the listened sound.

The results obtained from the analysis of signal recorded before, during and after the listening of sounds lasting two minutes are shown below. Specifically, the rate of peaks of the signal recorded while listening to a pleasant sound two minutes long and during the five minutes before and after is reported in *Table 24* and *Figure 45. Table 25* and *Figure 46* show the frequency of GSR peaks on the signal acquired before, during and after the listening of a neutral sound lasting two minutes. Finally, *Table 26* and *Figure 47* show the results obtained from the analysis of a GSR signal acquired while listening to an unpleasant sound two minutes long.

Table 24 - Number of peaks per minute recorded on a signal acquired during the listening of a two minutes long pleasant sound.

	Peaks per Minute (0-5 minutes)	**Peaks per Minute (5-7 minutes)**	**Peaks per Minute (7-12 minutes)**
Subject 1	0.6	1.0	1.0
Subject 2	0.6	0.5	0.2
Subject 3	0.6	0	0.4
Subject 4	1.0	0.5	0.6
Subject 5	0	0	0.2
Subject 6	0.8	1.0	0.2
Subject 7	1.0	1.5	0.2

Looking at *Table 24* and the following Figure (*Figure 45)*, the pleasant sound of two minutes does not seem to produce the same effect on all subjects. Indeed, in the first, the sixth and the seventh subject, the GSR peaks rate increases with respect to the frequency recorded in the initial five minutes of acquisition in the absence of acoustic stimuli. The remaining

subjects, instead, show a number of peaks per minute lower than the one recorded before and after the listening of the pleasant sound.

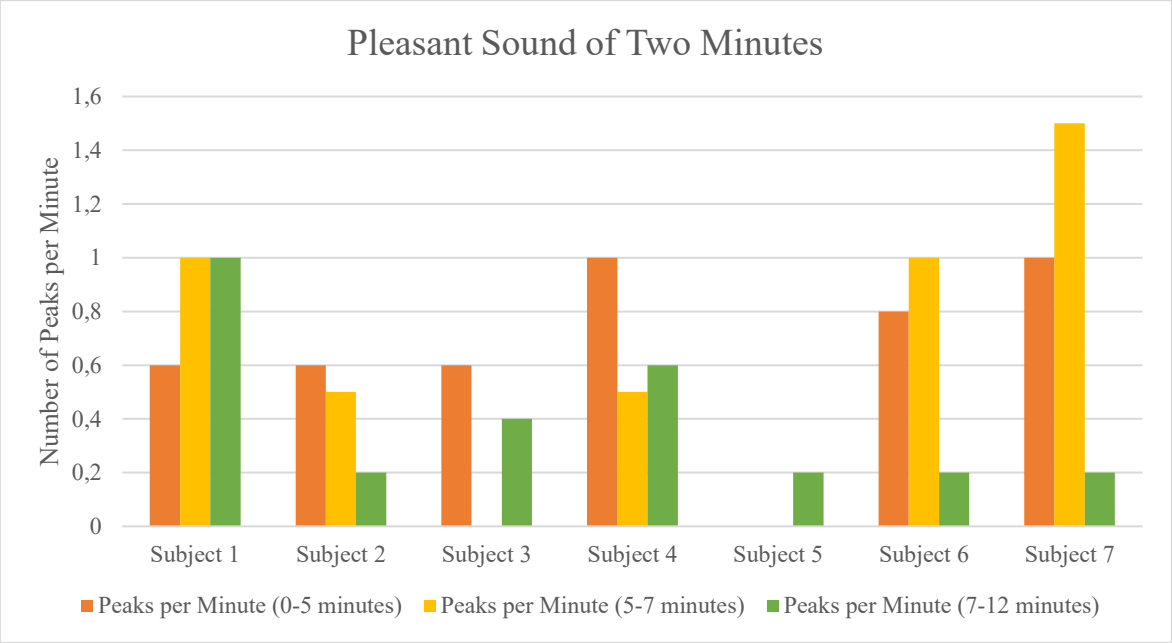

Figure 45 - Number of peaks per minute recorded on a signal acquired during the listening of a two minutes long pleasant sound for each subject.

Table 25 - Number of peaks per minute recorded on a signal acquired during the listening of a two minutes long neutral sound.

	Peaks per Minute (0-5 minutes)	**Peaks per Minute (5-7 minutes)**	**Peaks per Minute (7-12 minutes)**
Subject 1	0.8	2.0	0.6
Subject 2	1.0	0.5	0.8
Subject 3	1.0	0.5	1.4
Subject 4	0.4	1.0	0.8
Subject 5	0.4	0.5	0.6
Subject 6	1.2	0	0.6
Subject 7	1.2	1.5	0.8

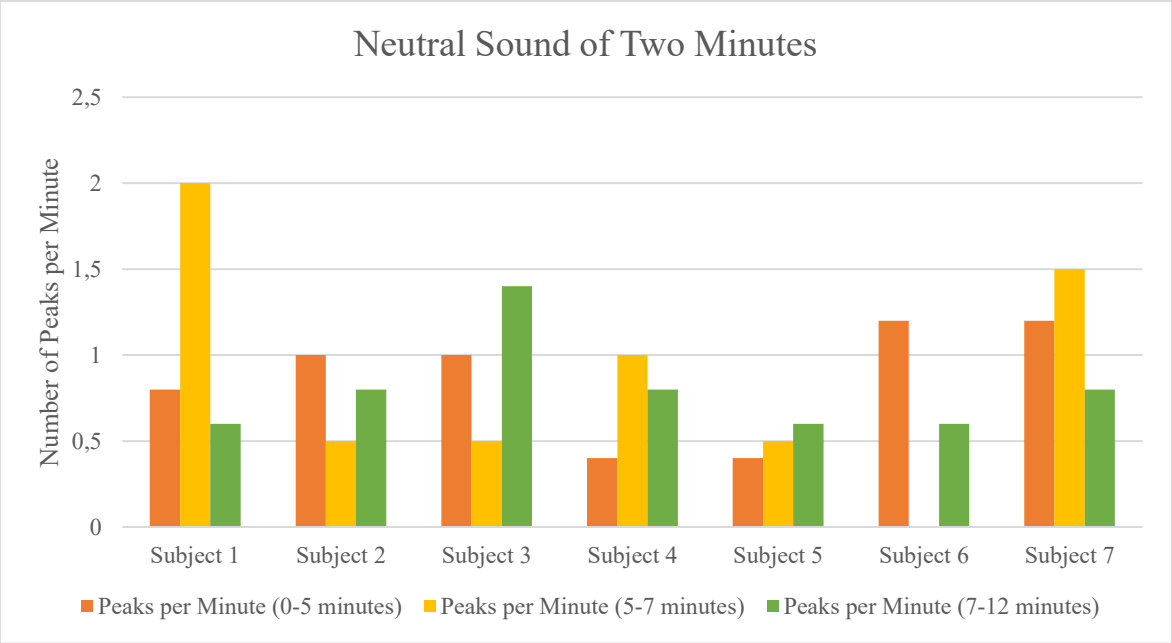

Figure 46 - Number of peaks per minute recorded on a signal acquired during the listening of a two minutes long neutral sound for each subject.

Similar to the case of pleasant sound, the listening of two minutes long neutral sound does not produce the same effect on all subjects, as shown in *Table 25* and *Figure 46*. Indeed, an increase in the number of GSR peaks per minute is recorded in subjects 1, 4 and 7, while the rate decreases in subjects 2, 3 and 6, listening to neutral sounds. Finally, subject 5 shows a slight and constant growth of the peaks rate during the three phases of the acquisition.

Table 26 - Number of peaks per minute recorded on a signal acquired during the listening of a two minutes long unpleasant sound.

	Peaks per Minute (0-5 minutes)	**Peaks per Minute (5-7 minutes)**	**Peaks per Minute (7-12 minutes)**
Subject 1	1.0	1.5	0.6
Subject 2	0.8	0.5	0.4
Subject 3	0.6	1.5	0.4
Subject 4	1.0	0	0.4
Subject 5	0.6	0.5	0.6
Subject 6	0.8	0.5	1.0
Subject 7	0	1.0	1.4

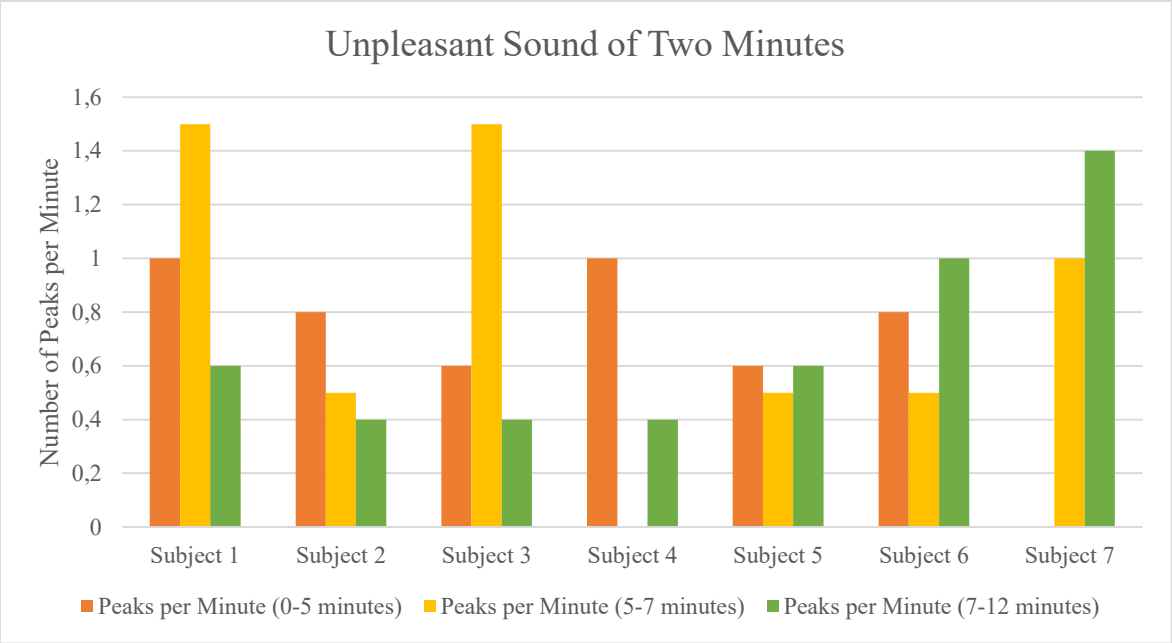

Figure 47 - Number of peaks per minute recorded on a signal acquired during the listening of a two minutes long unpleasant sound for each subject.

By analyzing the *Table 26* and *Figure 47*, it possible to notice that the listening of an unpleasant sound two minutes long has not the same effect on all individuals involved in the experimental test. Specifically, the first and third subjects show a peaks rate higher during the listening of the sound than in the signal acquired before and after the listening of the sound. All the other subjects present a rate of peaks lower during the listening of the sound than in the absence of any stimulation.

By making a comparison between results obtained from the analysis of signals acquired during the listening of sounds one minute and two minutes long, there is no way to understand if hearing longer-lasting acoustic stimuli produces greater changes of the GSR signal. On the contrary, by analyzing the effect of the unpleasant sound on the GSR signals, generally, the one-minute-long sound produces an increase of the peaks' frequency with respect to the number of peaks per minute computed in the absence of stimuli. However, subjects 1 and 3 appear to be more sensitive to unpleasant sounds of longer duration. By examining, instead, the pleasant sound, it possible to notice that while the fourth, fifth and sixth subjects appear to be more sensitive to sound lasting one minute, the subjects one, six and seven are more sensitive to pleasant sound two minutes long. Finally, considering the

values resulting from the analysis of GSR signals recorded during the listening of neutral sound, no considerations can be done.

5.1.2 **Comparison among Pleasant, Neutral and Unpleasant Sounds**

In this section, the results obtained from the analysis of signals acquired during the listening of pleasant, neutral and unpleasant sounds are compared. In particular, the peaks rate computed for each subject was averaged in order to obtain a value for each sound listened to. The frequency of GSR peaks calculated for the first, the second and the third period of acquisition are represented graphically and linked by a broken line.

Since the same audio track was listened from individuals two times, the first time for one minute while the second for two minutes, the results of both analyses are shown below. Specifically, the results obtained from the shortest acquisitions are shown before. Then, the GSR peaks rate computed in the longest sessions of recording is presented.

Table 27 and *Figure 48* present the frequency of GSR peaks during each acquisition phase for each kind of sound listened for one minute.

Table 27 - Average GSR peaks rate computed over all subjects on the GSR signals acquired before, during and after the listening of pleasant, neutral and unpleasant sounds lasting one minute.

	Average Peaks per Minute (0-5 minutes)	**Average Peaks per Minute (5-6 minutes)**	**Average Peaks per Minute (7-11 minutes)**
Pleasant Sound	0.57	0.86	0.68
Neutral Sound	0.63	0.57	0.83
Unpleasant Sound	0.74	1.86	0.71

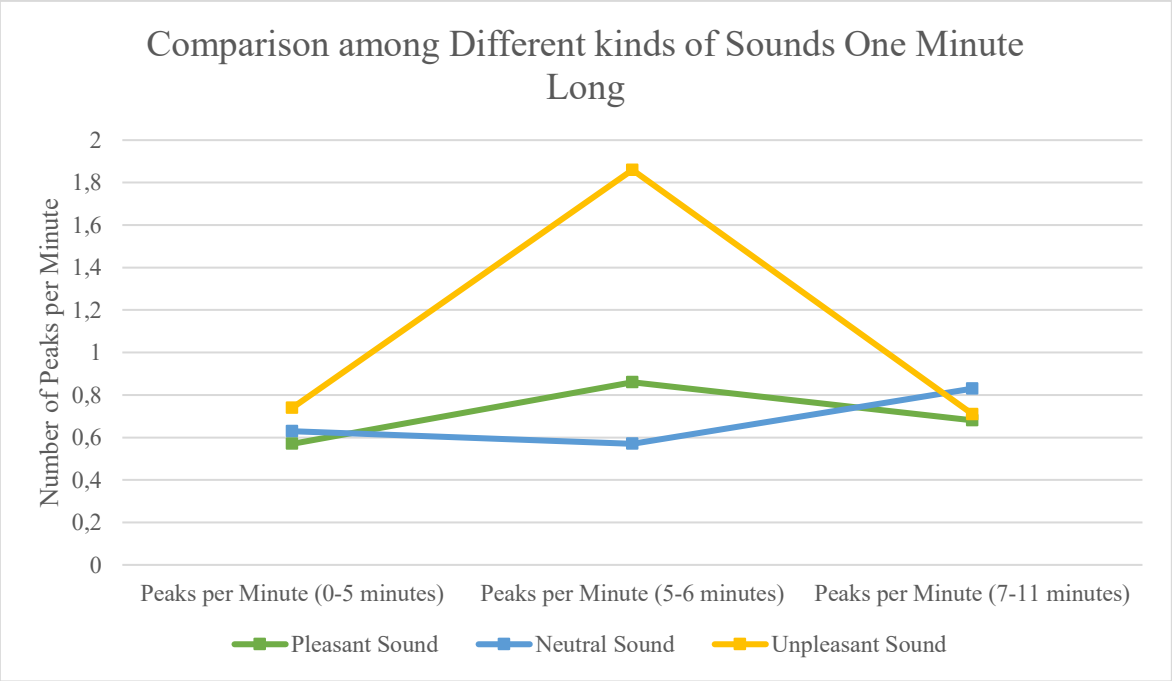

Figure 48 - Average GSR peaks rate before, during and after the listening of pleasant, neutral and unpleasant sounds lasting one minute, over all subjects.

Table 28 and *Figure 49* show the GSR peaks rate of each phase of recording for each sound listened for two minutes.

Table 28 - Average GSR peaks rate computed over all subjects on the GSR signals acquired before, during and after the listening of pleasant, neutral and unpleasant sounds lasting two minutes.

	Average Peaks per Minute (0-5 minutes)	**Average Peaks per Minute (5-7 minutes)**	**Average Peaks per Minute (7-12 minutes)**
Pleasant Sound	0.66	0.64	0.40
Neutral Sound	0.86	0.86	0.80
Unpleasant Sound	0.68	0.78	0.68

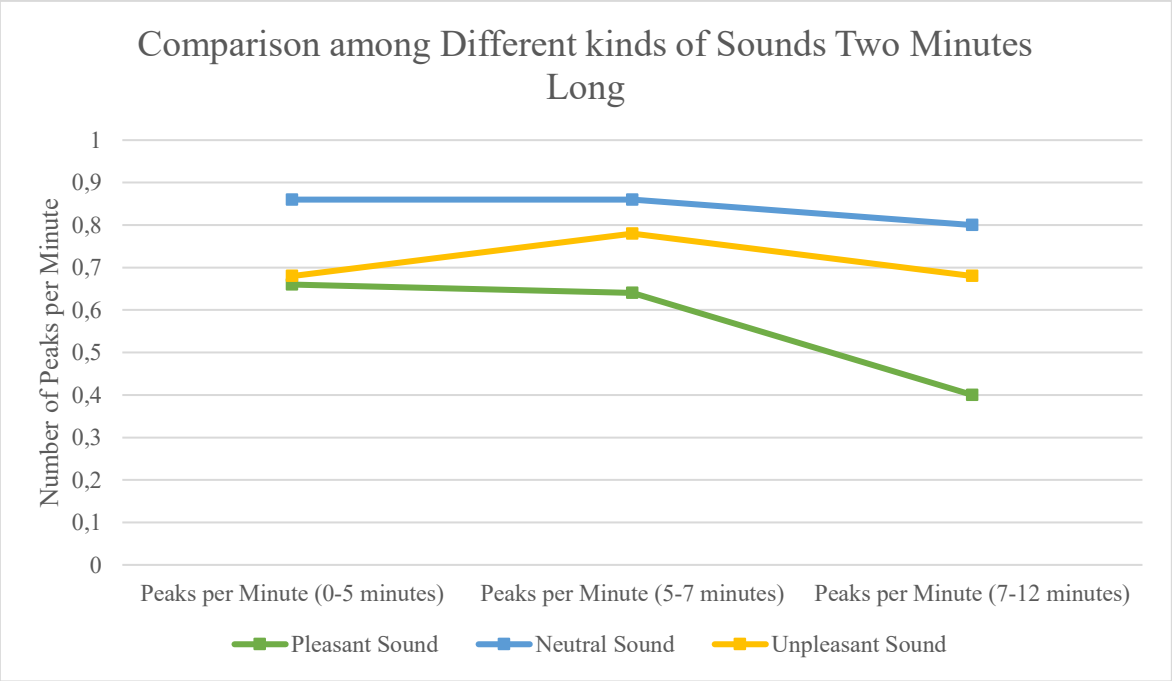

Figure 49 - Average GSR peaks rate change before, during and after the listening of pleasant, neutral and unpleasant sounds lasting two minutes, over all subjects.

Looking at the results shown in Tables and Figures above, it is possible to notice that acoustic sounds produce different effects on the GSR signals of the listeners depending on the length of the sound and its valence score. Specifically, the listening of pleasant and neutral sounds produces a different effect depending on the sound's duration. A slight increase of GSR peaks per minute is recorded during the listening of one-minute-long pleasant sound, while the same sound lasting two minutes does not. At the same time, while listening neutral sound lasting one-minute subjects have recorded a slight decrease of GSR peaks frequency, the same behavior is not recorded during the listening for two minutes of the same neutral acoustic stimulus. Conversely, results obtained from the listening of an unpleasant sound one and two minutes long have the same behavior. In both cases, an increase in the number of GSR peaks per minute is recorded during the period of unpleasant sound listening. However, this increase is much more evident in the case of a one-minute-long unpleasant audio track.

5.2 **Analysis of the SAM Scores Given by Enrolled Subjects**

In order to perform this experimental test, three sounds were selected from the IADS-2 database. This database contains a collection of acoustic stimuli rated using the three dimensions of the SAM scales [11]. Among all the stimuli collected in the IADS-2, three acoustic sounds were selected considering their valence score, in order to choose sounds assessed from the population as pleasant, neutral and unpleasant sound. However, in order to verify if the feelings evoked by the chosen sounds on our population are similar to the ones experienced by the subjects involved in the database construction, it was thought to require the participants to evaluate their feelings using the SAM scale. For this reason, at the end of each acquisition, the subjects involved in the experiment were asked to rate the feeling produced by the listened sound by using the valence, arousal and dominance dimensions of the SAM scale. The valence represents a form of pleasure level and it ranges from negative to positive [24]. The arousal ranges from low to high and it indicates the psychological and physiological level of being awake [24]. While, the dominance dimension represents changes in control with changes in manikin's size, it ranges from a small figure to a large one [24]. The subjects had to give a score ranging from 1 to 9 at each dimension of the scale.

Scores given by the enrolled individuals for each heard sound are presented in *Table 29*, in which are detailed the mean scores of valence, arousal and dominance and the related standard deviation for each type of listened sound.

Table 29 - Average scores (dimensionless values) of valence, arousal and dominance and relating standard deviation for each sound chosen.

	Valence	**Arousal**	**Dominance**
RockNRoll	7.1 ± 0.8	6.9 ± 0.7	6.5 ± 1.1
Walking	5.3 ± 0.5	4.0 ± 0.9	5.1 ± 1.5
Scream	2.3 ± 0.8	6.7 ± 0.9	3.1 ± 1.1

By analyzing the valence scores shown in Table above, it is possible to notice that the ‘RockNRoll’ sound is rated as pleasant, the sound of ‘Walking’ as neutral and the ‘Scream’ as unpleasant sound. Subjects involved in the experimental test evaluate the ‘RockNRoll’ and ‘Scream’ sounds as arousing, while the ‘Walking’ is considered a sound rather relaxing. Finally, the ‘Scream’ makes subjects feel dominated, the ‘RockNRoll’ sound produces a sensation of dominance, while the ‘Walking’ sound is rated as neutral in the dominance dimension.

Chapter 6
Conclusion

The GSR is a biometric index reflecting changes in the electrical properties of the skin produced by internal or external emotional stimuli [4].

In this work, the whole process of acquisition, elaboration and analysis of the GSR signal was presented. Specifically, some individuals were enrolled and contributed to two different experimental tests. The GSR signal was acquired by using E4 wristband and, processed in the time and frequency domain implementing two algorithms in Matlab. In the time domain, the GSR peaks number was identified and counted, while in the frequency domain the AUC of PSD curve was computed. The results were analyzed in order to understand the effect that different kinds and levels of stimuli have on the electrical properties of the skin.

In the first experimental test, the GSR data were measured after participants have performed physical efforts of different intensities. By analyzing signals in the time domain, it was found that the number of GSR peaks grows with the increase of physical activity intensity. However, this parameter has shown high intra-subject and inter-subject variability, especially when participants performed physical efforts of medium and high intensity. For this reason, GSR signals acquired during this experimental test were examined also in the frequency domain. The spectral analysis of our data has confirmed the findings of Posada-Quintero et al. [13][27]. Indeed, more than 50% of the spectral content is confined in the frequency band 0-0.25 Hz and most of it is contained in the frequency range 0.045-0.25 Hz [27]. Moreover, the amount of PSD confined in both the ranges of frequency decreases with the increase of the physical activity intensity [27].

During the second experimental test, the GSR signals were acquired while subjects listened to pleasant, neutral and unpleasant sounds selected from the IADS-2 database. GSR signals were measured before, during and after the listening, and each audio track was listened two times, for a duration of one and two minutes. Measured signals were analyzed only in the

time domain. By analyzing the results obtained, no clear conclusions could be drawn. Indeed, it was not found a common response to acoustic stimuli, especially to pleasant and neutral sounds. While, with regard to the unpleasant sound, this seems to produce the same effect (i.e. an increase of GSR peaks per minute during the listening period) in almost all individuals. However, this effect appears more evident in the shorter sound probably due to the habituation phenomenon. Moreover, at the end of each acquisition, the subjects rated the listened sound using the valence, arousal and dominance dimensions of the SAM scale. These values were found to be comparable to the scores given by the IADS-2 participants.

In conclusion, physical efforts produce evident changes in the GSR signal. In particular, these changes can be appreciated in the time and frequency domain but also performing just a visual inspection of the raw GSR data. On the contrary, the chosen acoustic stimuli do not cause consistent variations of the GSR, especially when participants were subjected to the listening of pleasant and neutral sounds.

Chapter 7

Limitations and Future Developments

Some limitations were found in this thesis work. However, these could be valued in the future as a starting point to develop an improved study of the GSR signal in response to emotional stimuli of physical and acoustic type.

Some limitations are common between the two tests, while other ones are specific to each test.

For both the experimental tests, the number of subjects enrolled is very restricted. In the future, by increasing the population involved in the experiments, more reliable and accurate results could be reached. Moreover, enrolling a more heterogeneous population in terms of gender and age, the GSR fluctuations resulting from physical and acoustic stimuli could be analyzed comparing the effect that the above stimuli produce on males and females of different ages.

The main limitation of the first experimental test was to have not established a precise protocol to define the intensity of a physical effort. Indeed, looking at the analysis of the results, it is evident that the behavior of the GSR signal recorder after physical efforts of medium intensity is ambiguous and very variable. Probably, this can be related to the difficulty to establish for each subject whether a performed physical effort may be considered of low, medium or high intensity. In the second experimental test, the main limitation encountered is related to the low number of GSR signals measured. In the future, this limitation could be overcome by performing a greater number of measurements. These could be done by using also more sounds of different duration.

Finally, since some findings presented by Chamberlin et al. show variations of the GSR signal depending on the time of the day [28], carrying out acquisitions during different periods of the day could provide interesting results.

References

[1] Kołodziej, M., et al. "Electrodermal Activity Measurements for Detection of Emotional Arousal." *Bull. Pol. Ac.: Tech*, vol 67, 2019: p. 4.

[2] Ayata, Deger, et al. "Emotion Recognition Via Galvanic Skin Response: Comparison of Machine Learning Algorithms and Feature Extraction Methods." *Istanbul University-Journal of Electrical & Electronics Engineering*, vol 17, no. 1, 2017: pp. 3147-3156.

[3] Varghese, Ashwini A., et al. "Overview on Emotion Recognition System." *2015 International Conference on Soft-Computing and Networks Security (ICSNS)*. IEEE, 2015.

[4] Cowley, Benjamin U., and Jari Torniainen. "A Short Review and Primer on Electrodermal Activity in Human Computer Interaction Applications." *arXiv preprint arXiv:1608.06986,* 2016.

[5] Topoglu, Yigit, et al. "Electrodermal Activity in Ambulatory Settings: A Narrative Review of Literature." *International Conference on Applied Human Factors and Ergonomics*. Springer, Cham, 2019.

[6] "EDA / GSR Pocket Guide - Imotions". *Imotions*, https://imotions.com/guides/eda-gsr/.

[7] Benedek, Mathias and Christian Kaernbach. "Ledalab". *Ledalab.De*, http://www.ledalab.de/.

[8] Boucsein, Wolfram. *Electrodermal Activity*. Springer Science & Business Media, 2012.

[9] Christopoulos, George I. et al. "The Body and The Brain: Measuring Skin Conductance Responses to Understand the Emotional Experience." *Organizational Research Methods*, vol 22, no. 1, 2016: pp. 394-420.

[10] Al Machot, Fadi et al. "A Deep-Learning Model for Subject-Independent Human Emotion Recognition Using Electrodermal Activity Sensors." *Sensors*, vol 19, no. 7, 2019: p. 1659.

[11] Betella, Alberto, and Paul F. M. J. Verschure. "The Affective Slider: A Digital Self-Assessment Scale for The Measurement of Human Emotions." *PloS one*, vol 11, no. 2, 2016.

[12] Bradley, Margaret M., and Peter J. Lang. "Measuring Emotion: The Self-Assessment Manikin and The Semantic Differential." *Journal of Behavior Therapy and Experimental Psychiatry*, vol 25, no. 1, 1994: pp. 49-59.

[13] Posada-Quintero, Hugo F., et al. "Electrodermal Activity Is Sensitive to Cognitive Stress Under Water." *Frontiers in Physiology*, vol 8, 2018: p. 1128.

[14] *Biopac.Com*, 2015, https://www.biopac.com/wp-content/uploads/EDA-Guide.pdf.

[15] Posada-Quintero, Hugo F., et al. "Power Spectral Density Analysis of Electrodermal Activity for Sympathetic Function Assessment." *Annals of Biomedical Engineering*, vol 4, no. 10, 2016: pp. 3124-3135.

[16] Posada-Quintero, Hugo F., et al. "Highly Sensitive Index of Sympathetic Activity Based on Time-Frequency Spectral Analysis of Electrodermal Activity." *American Journal of Physiology-Regulatory, Integrative and Comparative Physiology*, vol 311, no. 3, 2016: pp. R582-R591.

[17] Society for Psychophysiological Research Ad Hoc Committee on Electrodermal Measures, et al. "Publication Recommendations for Electrodermal Measurements." *Psychophysiology*, vol 49, no. 8, 2012: pp. 1017-1034.

[18] Alexander, David M., et al. "Separating Individual Skin Conductance Responses in a Short Interstimulus-Interval Paradigm." *Journal of Neuroscience Methods*, vol 146, no. 1, 2005: pp. 116-123.

[19] Benedek, Mathias, and Christian Kaernbach. "Decomposition of Skin Conductance Data by Means of Nonnegative Deconvolution." *Psychophysiology*, vol 47, no. 4, 2010: pp. 647-658.

[20] Benedek, Mathias, and Christian Kaernbach. "A Continuous Measure of Phasic Electrodermal Activity." *Journal of Neuroscience Methods*, vol 190, no. 1, 2010: pp. 80-91.

[21] E4 Wristband User's Manual. *Empatica*, Milano, Italy, 2015.

[22] Garbarino, Maurizio, et al. "Empatica E3 - A Wearable Wireless Multi-Sensor Device for Real-Time Computerized Biofeedback and Data Acquisition." *2014 4th International Conference on Wireless Mobile Communication and Healthcare-Transforming Healthcare Through Innovations in Mobile and Wireless Technologies (MOBIHEALTH)*. IEEE, 2014.

[23] "E4 Get Started Guide - Start Acquiring Physiological Signals". *Empatica* https://www.empatica.com/get-started-e4.

[24] Bradley, Magargaret M. and Peter J. Lang. "The International Affective Digitized Sounds (2nd Ediotion; IADS-2), Affective Ratings of Sounds and Instruction Manual." *NIMH Center for the Study of Emotion and Attention*, 2007.

[25] Yang, Wanlu, et al. "Affective Auditory Stimulus Database: An Expanded Version of The International Affective Digitized Sounds (IADS-E)." *Behavior Research Methods*, vol 50, no. 4, 2018: pp. 1415-1429.

[26] Akdemir, Saime, et al. "Investigation into the Effects of Classical Turkish Music on Galvanic Skin Response and Skin Temperature of Schizophrenic Patients." *Journal of Networking Technology*, vol 1, no. 4, 2010: pp. 181-188.

[27] Posada-Quintero, Hugo F. et al. "Time-Varying Analysis of Electrodermal Activity During Exercise". *PloS one*, vol 13, no. 6, 2018: p. e0198328.

[28] Chamberlin, Steve et al. "P02.178. Skin Conductance at 24 Source (Yuan) Acupoints in 8637 Patients: Influence of Age, Gender and Time of Day". *BMC Complementary and Alternative Medicine*, vol 12, no. S1, 2012.